AD_____

Grant Number DAMD17-94-J-4419

TITLE: Molecular Study of Interactions Between P-Glycoprotein and Anticancer Drugs

PRINCIPAL INVESTIGATOR: Jian-Ting Zhang, Ph.D.

CONTRACTING ORGANIZATION: University of Texas Medical Branch
Galveston, Texas 77555-0136

REPORT DATE: September 1996

TYPE OF REPORT: Annual

DTIC QUALITY INSPECTED 2

PREPARED FOR: U.S. Army Medical Research and Materiel Command
Fort Detrick, Maryland 21702-5012

DISTRIBUTION STATEMENT: Approved for public release;
distribution unlimited

The views, opinions and/or findings contained in this report are those of the author(s) and should not be construed as an official Department of the Army position, policy or decision unless so designated by other documentation.

19970610 030

# REPORT DOCUMENTATION PAGE

*Form Approved*
*OMB No. 0704-0188*

Public reporting burden for this collection of information is estimated to average 1 hour per response, including the time for reviewing instructions, searching existing data sources, gathering and maintaining the data needed, and completing and reviewing the collection of information. Send comments regarding this burden estimate or any other aspect of this collection of information, including suggestions for reducing this burden, to Washington Headquarters Services, Directorate for Information Operations and Reports, 1215 Jefferson Davis Highway, Suite 1204, Arlington, VA 22202-4302, and to the Office of Management and Budget, Paperwork Reduction Project (0704-0188), Washington, DC 20503.

| 1. AGENCY USE ONLY *(Leave blank)* | 2. REPORT DATE | 3. REPORT TYPE AND DATES COVERED |
|---|---|---|
| | September 1996 | Annual (1 Aug 95 - 31 Jul 96) |

**4. TITLE AND SUBTITLE**

Molecular Study of Interactions Between P-Glycoprotein and Anticancer Drugs

**5. FUNDING NUMBERS**

DAMD17-94-J-4419

**6. AUTHOR(S)**

Jian-Ting Zhang, Ph.D.

**7. PERFORMING ORGANIZATION NAME(S) AND ADDRESS(ES)**

University of Texas Medical Branch
Galveston, Texas 77555-0136

**8. PERFORMING ORGANIZATION REPORT NUMBER**

**9. SPONSORING / MONITORING AGENCY NAME(S) AND ADDRESS(ES)**

U.S. Army Medical Research Command
Fort Detrick, Maryland 21702-5012

**10. SPONSORING / MONITORING AGENCY REPORT NUMBER**

**11. SUPPLEMENTARY NOTES**

**12a. DISTRIBUTION / AVAILABILITY STATEMENT**

Approved for public release; distribution unlimited

**12b. DISTRIBUTION CODE**

**13. ABSTRACT** *(Maximum 200 words)*

P-glycoprotein is a plasma membrane protein that functions as a drug transporter and is responsible for multidrug resistance in some breast cancers. In the past one year, we have generated two site-specific antibodies and used them to determine the topologies of P-glycoprotein in multidrug resistant cancer cells. We found that P-glycoproteins in the plasma membrane of mammalian cells express at least two alternate topologies. This observation is consistent with our previous study using cell-free expression system. The more than one topology feature of P-glycoprotein may be responsible for its multifunctional nature. We have also been able to express the transmembrane domains of P-glycoprotein in bacteria. The success in this study will allow us to map the drug-binding domain in P-glycoprotein and study the drug-P-glycoprotein interactions.

**14. SUBJECT TERMS**

Breast Cancer

**15. NUMBER OF PAGES**

51

**16. PRICE CODE**

| 17. SECURITY CLASSIFICATION OF REPORT | 18. SECURITY CLASSIFICATION OF THIS PAGE | 19. SECURITY CLASSIFICATION OF ABSTRACT | 20. LIMITATION OF ABSTRACT |
|---|---|---|---|
| Unclassified | Unclassified | Unclassified | Unlimited |

# FOREWORD

Opinions, interpretations, conclusions and recommendations are those of the author and are not necessarily endorsed by the U.S. Army.

____ Where copyrighted material is quoted, permission has been obtained to use such material.

____ Where material from documents designated for limited distribution is quoted, permission has been obtained to use the material.

____ Citations of commercial organizations and trade names in this report do not constitute an official Department of Army endorsement or approval of the products or services of these organizations.

____ In conducting research using animals, the investigator(s) adhered to the "Guide for the Care and Use of Laboratory Animals," prepared by the Committee on Care and use of Laboratory Animals of the Institute of Laboratory Resources, National Research Council (NIH Publication No. 86-23, Revised 1985).

____ For the protection of human subjects, the investigator(s) adhered to policies of applicable Federal Law 45 CFR 46.

__✓__ In conducting research utilizing recombinant DNA technology, the investigator(s) adhered to current guidelines promulgated by the National Institutes of Health.

__✓__ In the conduct of research utilizing recombinant DNA, the investigator(s) adhered to the NIH Guidelines for Research Involving Recombinant DNA Molecules.

____ In the conduct of research involving hazardous organisms, the investigator(s) adhered to the CDC-NIH Guide for Biosafety in Microbiological and Biomedical Laboratories.

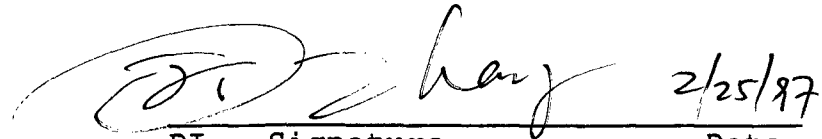

PI - Signature

2/25/87

Date

## 4. TABLE OF CONTENTS:

## 5. INTRODUCTION:

**5.1. Background and Nature of the Problem:** Despite the improvement in early detection and treatment of breast cancer, the mortality rate of women with breast cancer remained high. One major obstacle for curing breast cancer is the development of **multidrug resistance** in breast cancer cells which reduces the effectiveness of chemotherapy. Breast cancer is often intrinsically drug resistant, and sometimes acquires resistance following chemotherapy. Although there are conflicting reports, **P-glycoprotein** (Pgp)-mediated multidrug resistance seems to be the most frequent mechanism of drug resistance in breast cancer (Sugawara *et al.*, 1988; Schneider *et al.*, 1989; Ro *et al.*, 1990; Goldstein *et al.*, 1989; Keith *et al.*, 1989; Salmon *et al.*, 1989; Merkel *et al.*, 1989; Sanfilippo *et al.*, 1991; Verrelle *et al.*, 1991; Wishart and Kaye, 1991; Charpin *et al.*, 1994; Bates *et al.*, 1995).

Pgp is a plasma membrane protein which functions as an efflux pump for anticancer drugs (Gottesman and Pastan, 1993). Overexpression of Pgp reduces the accumulation of cytotoxic drugs in breast cancer cells which, therefore, will survive the chemotherapeutic treatment. Pgp has been shown to interact directly with various anticancer drugs, for example, adriamycin (Bushe *et al.*, 1989), vinblastine (Cornwell *et al.*, 1986; Safa *et al.*, 1986), and colchicine (Safa *et al.*, 1989). Pgp expressed in the plasma membrane has been covalently labeled by photosensitive drug analogues (Safa *et al.*, 1987). Greenberger *et al.* (1991) and Bruggemann *et al.* (1989, 1992) suggested that the [$^3$H]azidopine and [$^3$H]vinblastine cross-linked to fragments including TM6 and TM12 of mouse and human Pgp, respectively. Despite the success of these drug-labelling studies, it is still not known if these domains directly bind drugs or the azido groups of these drugs are simply in a close proximity to the labelled sites. The detailed interaction between Pgp and drugs is unknown.

Using a cell-free expression system, I have previously shown that Pgp has at least two distinct topological structures in microsomal membranes (Zhang and Ling, 1991; Zhang *et al.*, 1993). Pgp molecules have also been suggested to function as chloride channels as well as drug transporters and these two functions are separable (Valverde *et al.*, 1992; Gill *et al.*, 1992; Higgins, 1992; Alternberg *et al.*, 1994). Indeed, drug transport requires ATP hydrolysis whereas the channel function can be supported by non-hydrolyzable ATP analogues (Gill *et al.*,, 1992). I have previously proposed that these two functions may be carried out by the two different topological structures of the molecule; while molecules with one structure may function as a chloride channel, molecules with the other structure may function as a drug-efflux pump. However, one question remains to be answered is whether Pgp in multidrug resistant cancer cells have two alternate topologies.

**5.2. Purpose of the Present Work:** The current project is designed to (1) determine the topological structure of Pgp in multidrug-resistant mammalian cells and (2) map the drug-binding site in Pgp.

**5.3. Methods of Approaches:** To determine the topological structure of Pgp in multidrug resistant cancer cells, site-specific antibodies will be produced against relevant domains of Pgp. We will use immunocytochemistry and proteolysis/membrane protection assay to map the membrane

orientation of the relevant domains of Pgp. To map the drug-binding domain, different domains of Pgp will be expressed in bacteria in large quantity and used to study its drug binding property.

## 6. BODY:

### 6.1. Methods Used:

6.1.1. Generation and characterization of site specific antibodies:

**(a), production of fusion proteins:** cDNA fragments encoding relevant Pgp domains were generated using PCR technology and cloned into a bacterial expression vector (pGEX series, Pharmacia LKB Biotechnology). The final DNA products were sequenced to ensure the correct reading frame and to eliminate any possible mutations introduced by Taq DNA polymerase. The pGEX vectors provide all three possible reading frames in the multiple cloning site for generating fusion proteins with glutathione S-transferase at the N-terminus and inserted foreign protein at the C-terminus. All vectors also supply stop codons in all three reading frames for translation termination. Fusion protein was prepared from transformed bacteria JM109 and purified by separation through an affinity column of glutathione-conjugated Sepharose-4B (Smith and Johnson, 1988). The glutathione S-transferase can be cleaved off from the fusion protein using factor Xa or thrombin and removed by separation on a second glutathione-conjugated Sepharose-4B column. The purified Pgp peptides were used to raise antibodies.

**(b), production of polyclonal antibodies:** Rabbits were immunized subcutaneously with fusion proteins in complete Freund's adjuvant, followed by periodic boosting with peptide in incomplete Freund's adjuvant, and then bled for serum. The polyclonal antibodies were characterized against their fusion peptide antigens using ELISA or Western blot analysis (Harlow and Lane, 1988). The specificity of these antibodies for Pgp was assessed against plasma membrane fractions containing Pgp isolated from MDR cells (e.g. $CH^{r}B30$ which has 10% Pgp in its total plasma membrane proteins) using Western blot and immunofluorescence. Polyclonal antibodies were affinity-purified on a MAC-25 cartridge using purified fusion peptide as previously described (Zhang and Nicholson, 1994).

6.1.2. Proteolysis/membrane protection assay of isolated membrane vesicles: Membrane vesicles were prepared from MDR cells as previously described (Lever, 1977) and subjected to complete protease digestion using trypsin or proteinase K. The digested fragments were then separated on SDS-PAGE and detected by using site-specific polyclonal antibodies on Western blot. Size of the fragments resistant to protease digestion and detected by each specific antibody were analyzed according to the two alternative topologies (Zhang *et al.*, 1993).

To determine the potential conformational change of Pgp in its catalytic cycle, inside-out membrane vesicles containing Pgp were preincubated for 30 min at room temperature with 5 mM ATP, ADP, or its non-hydrolyzable ATP analogous (AMP-PNP) in the presence of 5 mM $MgCl_2$, followed by trypsin digestion in the presence of these ligands. The trypsin digestion was then stopped after two-hour incubation at 37°C by addition of trypsin inhibitor and PMSF. The

membrane fraction was then be separated from the soluble trypsin fraction by centrifugation at 4°C and immediately solubilized in SDS-PAGE sample buffer. The Pgp fragments containing the loop 8 was detected on Western blot using the mAb MD-7 which has an epitope in the loop 8 (Zhang *et al.*, 1996).

6.1.3. Immunocytochemistry staining: The polyclonal antibodies generated in 6.1.1. were used to label fixed or fixed and permeabilized cells. The cells were fixed with paraformaldehyde (fixed, but not permeabilized) or fixed and permeabilized with acetone/methanol as previously described (Kartner *et al.*, 1985). This method of fixation and permeabilization does not affect the antigenicity of mAb C219 epitope. The labelling was detected using secondary antibody conjugated with peroxidase and the staining was viewed under a microscope.

6.1.4. Expression of a domain including TM11-TM12 of Pgp and drug labelling: Engineering the cDNA fragments into bacterial expression vectors and preparation of fusion protein have been described in detail elsewhere (Zhang *et al.*, 1996). Briefly, cDNA fragments encoding the relevant domains of Pgp were amplified by PCR and cloned into the multiple cloning site of a bacterial expression vector (pGEX series, Pharmacia LKB Biotechnology). The pGEX vectors provide all three possible reading frames in the multiple cloning site for generating fusion proteins of glutathione S-transferase (GST) at the N-terminus and inserted foreign Pgp at the C-terminus. The vectors also supply stop codons in all three reading frames for translation termination at the C-terminus of the fusion protein. The constructs encoding fusion proteins of N-terminal GST and various C-terminal Pgp sequences were introduced into *E. coli* (e.g. JM109, BL-21) using the $CaCl_2$ transformation technique (Perbal, 1984). The transformed cells were selected by ampicillin and positive clones were screened by DNA restriction mapping and confirmed by DNA sequencing.

Expression of fusion proteins was induced by IPTG (Isopropyl b-D-Thiogalactopyranoside). Bacteria clones expressing the fusion protein were lysed using sonication and the membrane fraction of the lysate were prepared by centrifugation at 100,000 g for 1 hr. For purification, fusion proteins in the membrane were solubilized with detergent and the fusion proteins were isolated with an affinity column of glutathione-conjugated Sepharose-4B. The size and purity of the fusion protein were determined on an SDS-PAGE stained with Commassie blue.

The drug binding was performed using photoactive drug analogous [$^3$H]azidopine. The membranes containing fusion protein were incubated with photosensitive [$^3$H]azidopine in the dark, followed by UV irradiation. The drug-linked peptides were analyzed by SDS-PAGE. After separation, the gel was fixed, treated with Amplify™, and exposed to x-ray film for fluorography. To eliminate the role of GST portion of the fusion protein in binding drugs, we removed the GST from the fusion protein by thrombin digestion. For competitive inhibition of the drug binding, vinblastine was used.

To purify the expressed drug-binding domain of Pgp, the fusion protein in bacterial membranes wasill be solubilized with detergent. The detergent will then be removed by dialysis and the protein will be allowed to refold at 4°C as described previously (Fiermonte *et al.*, 1993).

Glutathione-conjugated Sepharose will then be added to precipitate the fusion protein. Alternatively, we will use classical methods, such as gel-filtration and ion-exchange chromatography to purify the fusion protein as described in D.2.D.2. Preparation of large amount of the purified Pgp domains will allow us to investigate the detailed interaction between Pgp and its substrates at 3-D level. With large amount of drug-binding domains of Pgp, we will be able to address how Pgp can interact with such a wide variety of drug substrates.

**6.2. Results Obtained:**

6.2.1. The site-specific polyclonal antibodies generated against fusion proteins detect specifically P-glycoprotein from multidrug-resistant cells We have generated site-specific polyclonal antibodies against fusion proteins containing the loop linking TM4 and TM5 (loop 4) and the loop linking TM8 and TM9 (loop 8). These antibodies are designated αPgp-L4 and αPgp-L8, respectively. Fig. 1 shows a Western blot of membranes isolated from sensitive and drug-resistant CHO cells detected by monoclonal antibody (mAb) C219 as well as polyclonal antibody (pAb) αPgp-L4 and αPgp-L8. The mAb C219 (lane 2), pAb αPgp-L4 (lane 5) and pAb αPgp-L8 (lane 8) specifically detected the 180-kDa Pgp. This protein was not detected in the sensitive Aux B1 cells (lanes 1, 4 and 7). It has been shown previously that hamster Pgp can be cleaved into two halves by mild protease digestion and both halves have a mAb C219 epitope (Georges *et al.*, 1991). As shown in lane 3, two half molecules of Pgp were produced by trypsin digestion and both react with the mAb C219. However, as expected, the pAb αPgp-L4 reacted only with the N-terminal half (lane 6), whereas the pAb αPgp-L8 reacted only with C-terminal half (lane 9) of Pgp.

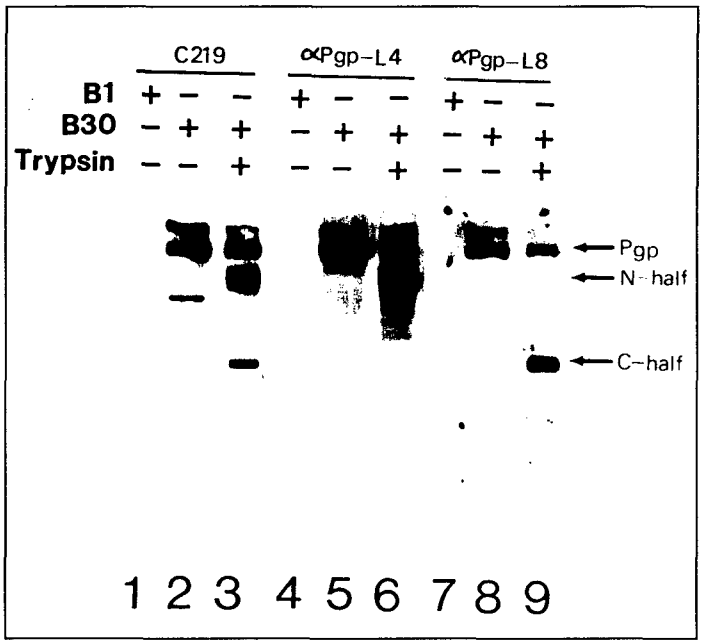


**Figure 1. Characterization of the specificity of αPgp-L4 and αPgp-L8 antibodies to P-glycoprotein of $CH^RB30$ cells. Crude membranes were isolated from parental Aux B1 (lanes 1, 4 and 7) and multidrug-resistant $CH^RB30$ cells (lane 2, 5 and 8). Monoclonal antibody C219 as well as the polyclonal antibodies αPgp-L4 and αPgp-L8 specifically detected the 180-kDa Pgp and its aggregated and degraded products (lanes 2, 5 and 8). No protein from Aux B1 cells was detected by any of these antibodies. C219 detects both N- and C-terminal half fragments (lane 3). As expected, only the N-terminal half fragment was recognized by αPgp-L4 (lane 6) whereas the C-terminal half was recognized by αPgp-L8 (lane 9).**

To confirm whether pAb αPgp-L4 and αPgp-L8 specifically detect Pgp on plasma membranes, we labelled fixed and permeablized multidrug-resistant cells with mAb C219, pAb αPgp-L4 and αPgp-L8, and detected the binding with FITC-conjugated secondary antibodies and viewed on a confocal-fluorescence microscope. As shown in Fig. 2, mAb C219 (panel A), as well as pAb αPgp-L4 (panel C) and αPgp-L8 (panel E) stained predominantly the plasma membranes. No signal was detected on plasma membranes in control experiments with either normal mouse IgG (panel B), or preimmune sera of αPgp-L4 (panel D) or αPgp-L8 (panel F).

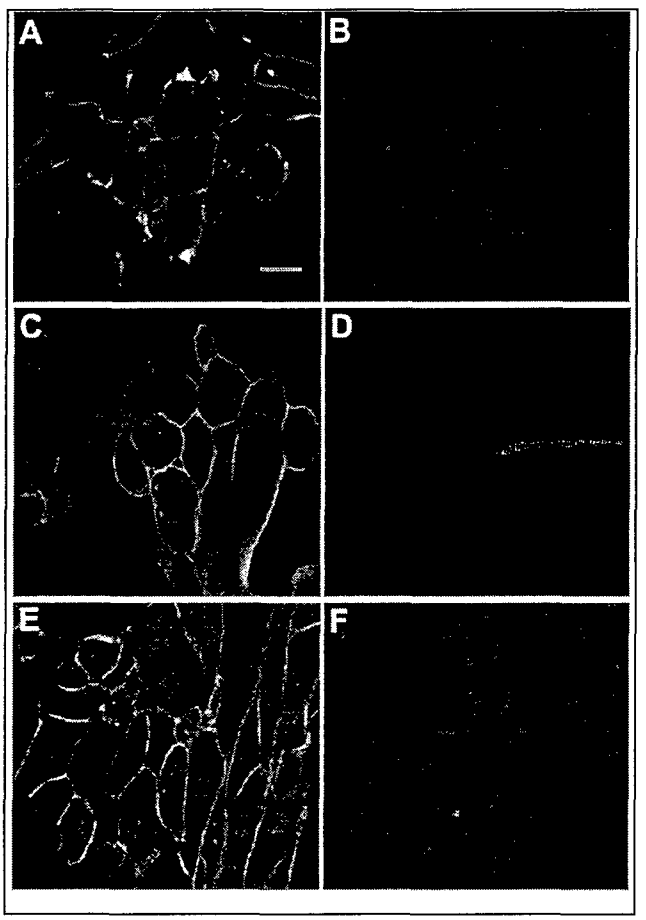


**Figure 2. Immunofluorescence labelling of $CH^RB30$ cells using αPgp-L4 and αPgp-L8. Multidrug-resistant $CH^RB30$ cells were fixed and permeabilized with acetone/methanol and labelled with mAb C219 (panel A), pAb αPgp-L4 (panel C), pAb αPgp-L8 (panel E). The labeling was detected using FITC-conjugated secondary antibodies and by confocal fluorescence microscopy. In the controls, cells were labelled using normal mouse IgG (panel B) and preimmune sera of αPgp-L4 (panel D) and αPgp-L8 (panel F). All three antibodies labelled predominantly on the plasma membranes. The bar in panel A denotes 10 μm. All photographs were taken with the same magnification.**

6.2.2. Expression of multiple topologies of Pgp in multidrug resistant cells: Two methods were used to determine the membrane orientation of Pgp in drug-resistant cells: proteolysis/membrane protection assay and immunocytochemistry as described in 6.1.2. Fig. 3 shows the results of proteolysis/membrane protection assay detected by various antibodies.

**(a), the loop 8 of Pgp in inside-out membrane vesicles is resistant to trypsin digestion:** To confirm that the loops 4 and 8 of Pgp in MDR cells were located extracellularly, we performed proteolysis/membrane protection assay and Western blot of isolated membrane vesicles. We used the human multidrug-resistant SKOV/VLB cells (Bradley et al., 1989), from which all vesicles isolated are inside-out (data not shown) as determined using acetylcholinesterase (extracellular marker). This is confirmed by another marker $Na^+/K^+$-ATPase (cytoplasmic side marker) (data not

shown). Meanwhile, we obtained a mAb MD-7 which has an epitope in the loop 8 (Shapiro et al., 1996).

Fig. 3A shows the trypsin-digestion profile of Pgp detected by the mAb MD-7. Under mild conditions, peptides indicated as C (C-half) were detected (lanes 2 and 3, Fig. 3A). More extensive trypsin digestion generated smaller fragments labeled as X, Y, and Z, respectively (lanes 4 and 5, Fig. 3A). All these fragments were presumably derived from the C-half molecule with the epitope for the mAb MD-7. The smallest trypsin-resistant fragment detected by the mAb MD-7 has an apparent molecular mass of 17 kDa (peptide Z). It is possible that the generation of these fragments represents the progressive digestion of the C-terminal half molecule of Pgp and the peptide Z represents the minimum membrane-protected fragment containing the loop 8 with the mAb MD-7 epitope.

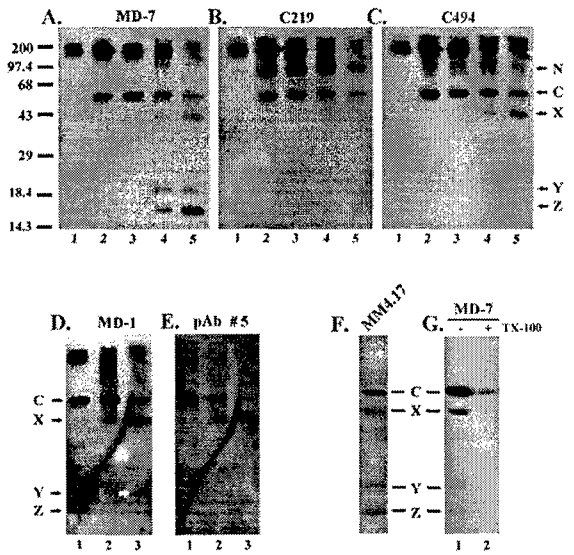


**Figure 3 Proteolysis profile of P-glycoprotein. (A-C), trypsin cleavage profile of human P-glycoprotein. 10 mg of SKOV/VLB cell membranes were incubated in the presence of 0.2 mg (lanes 2 and 3), 3 mg (lane 4), and 6 mg (lane 5) trypsin at 37°C. The reaction duration was 15 min (lane 2), 30 min (lane 3), and 2 hrs (lanes 4 and 5), respectively. Lane 1 is a control of 3 mg undigested SKOV/VLB cell membranes. Panels A-C are the same blot probed with different antibodies. A=MD-7, B=C219, C=C494. (D and E), panels D and E are the same blot as A-C, but only the corresponding lanes 3-5 were shown. D=MD-1, E=pAb #5. Separate experiments have also been performed with MD-1 and pAb #5 and the results are consistent with the data shown here. However, to be consistent with the panels A, B, C, only the stripped blot was shown. (F), 10 mg of SKOV/VLB cell membranes were incubated in the presence of 3 mg trypsin at 37°C for 2 hrs (same as lane 4, panel A). The blot was probed with MM4.17. (G), 10 mg of SKOV/VLB cell membranes were incubated in the presence of 3 mg trypsin at 37°C for 2 hrs (same as in lane 4, panel A) in the absence (lane 1) or presence (lane 2) of 1% Triton X-100. The blot was probed by MD-7.**

To determine the likelihood of the above possibility, we stripped the same blot and probed it with other mAbs or site-specific pAbs. Fig. 3B shows the same blot from Fig. 3A probed with the mAb C219. Only two peptide fragments indicated as N and C were detected by C219 (lanes 2-5, Fig. 3B). The peptide N did not react with the mAb MD-7 and represents the N-terminal half molecule (lane 2-5, Fig. 3A). The mAb C494, on the other hand, detected the peptide C, (lanes 2-5, Fig. 3C). Together, these results suggest that the peptides N and C represent the N- and C-terminal half molecules, respectively. These results are consistent with the previous studies which showed

that the mAb C219 has two epitopes, one in each ATP-binding domain, and the mAb C494 has only one epitope in the C-terminal half molecule (Georges et al., 1990; see also Fig. 1) and Pgp can be cleaved into two halves by trypsin (Georges et al., 1991).

In addition to the peptide C, the mAb C494 also reacted with the peptide X (lanes 4 and 5, Fig. 3C) which was not detected by the mAb C219 (lanes 4 and 5, Fig. 3B). This peptide is likely a further degradation product from the peptide C. Thus, after Pgp was cleaved into two halves, the C-terminal half molecule was further digested and the ATP-binding domain containing the mAb C219 epitope was removed, resulting in peptide X. However, the C494 epitope is still attached to the truncated C-terminal half molecule (peptide X). Both the mAb C219 and C494 did not react with peptides Y and Z, suggesting that these two peptides are further degradation products and have lost epitopes for both C219 and C494.

To determine whether the peptide Z contains the linker region and the loop 10, we probed the same stripped blot again with a mAb MD-1 (Shapiro et al., 1996) and a site-specific pAb #5 (Greenberger et al., 1991). The mAb MD-1 is specific to the minilinker region whereas the epitope for the pAb #5 is in the loop 10. Both antibodies are specific to the C-terminal half molecule as shown by their reactivity with the peptide C, but not the peptide N (lanes 1 and 2 in Fig. 3D and Fig. 3E). Both antibodies also reacted with the peptide X (lanes 2 and 3 in Fig. 3D and Fig. 3E), suggesting that the peptide X still contains the epitope for both antibodies. The mAb MD-1 detected, in addition, the peptide Y (lane 3, Fig. 3D) which, however, was not detected by the pAb #5 (lane 3, Fig. 3E). Therefore, the peptide Y lost the epitope for the pAb #5, but still retains the epitope for the mAb MD-1. The mAb MD-1, however, did not detect the peptide Z albeit the amount of peptide Z is higher than the peptide Y (compare lane 5 in Fig. 3A with lane 3 in Fig. 3D). The peptides Y and Z are still on membrane after stripping as determined using MD-7 (data not shown). These results suggest that the peptide Z is a final trypsin-resistant fragment which only retains the epitope for the mAb MD-7 and does not contain the epitopes for the mAbs C219, C494, MD-1, nor the site-specific pAb #5.

To prove that the peptide Z also contains the loop 7 (linking TM7 and TM8) in addition to the loop 8 (linking TM8 and TM9), we probed the digested products with another mAb MM4.17 of which the epitope is in the loop 7 (Cianfriglia et al., 1994). As expected, the mAb MM4.17 reacted with all the peptides C, X, Y, and Z (Fig. 3F). To confirm that the trypsin resistance of the peptide Z was due to membrane protection, we performed a digestion in the presence of Triton X-100 to permeabilize the membrane. As shown in Fig. 3G, the trypsin-resistant peptide Z was produced in the absence of Triton X-100 (lane 1, Fig. 3G), but was completely digested in the presence of Triton X-100 (lane 2, Fig. 3G). The above results showed that the domain containing loop 7 and loop 8 (with mAb MM4.17 and MD-7 epitopes) in inside-out vesicles is resistant to trypsin digestion whereas the loop 10 (linking TM10 and TM11 with pAb #5 epitope) and the C-terminal ATP-binding domain (containing mAb C219 and C494 epitopes) are sensitive to trypsin digestion. Thus, the segment containing both the loop 7 and loop 8 is likely located in the lumen of the isolated inside-out membrane vesicles (extracellular location), consistent with the alternative topology.

**(b), the loop 4 of human Pgp in inside-out membrane vesicles is protected from trypsin digestion** To determine whether the loop linking the putative TM4 and TM5 (loop 4) is also resistant to trypsin digestion in inside-out vesicles of MDR cells (SKOV/VLB), we again stripped the blot shown in Fig. 3A and probed it with the pAb aPgp-L4. This antibody specifically detected the peptide N (lanes 2-5, Fig. 4). In addition, further digested products X', X", Y' (a doublet), and Z' were also detected (lanes 4 and 5, Fig. 4). The peptide Z', with an apparent molecular mass of 14.5 kDa, is the smallest trypsin-resistant fragment from the N-terminal half molecule. It presumably represents the membrane-protected fragment containing the loop 4 with the epitope for the pAb aPgp-L4 whereas the peptides X', X", and Y' are incompletely digested products of the peptide Z'. In the presence of Triton X-100, these peptides were also completely digested (data not shown). Therefore, by analogy to the study of loop 8 in the C-terminal half, it is likely that the loop 4 of Pgp is also located in the lumen of the inside-out membrane vesicles (extracellular location).

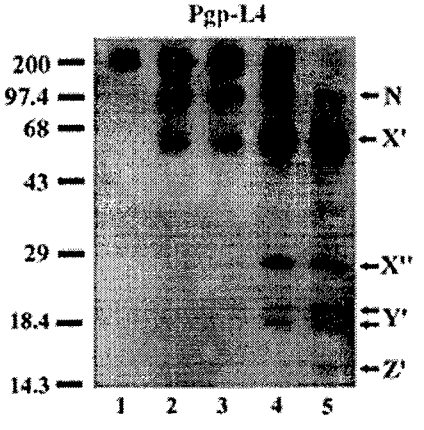


**Figure 4. Membrane protection of loop 4. The same blot from Fig. 3A-3C (membranes from the SKOV/VLB cells) was stripped and probed with the pAb αPgp-L4. The minimum peptide fragment Z' is the protected loop 4 of Pgp.**

6.2.3. Conformational changes of Pgp in its catalytic cycle.

**(a), MgATP and its nonhydrolyzable analogous affect the generation of the membrane protected TM7-loop7-TM8-loop8-TM9 of Pgp in inside-out vesicles:** To determine whether the binding of MgATP to Pgp causes any structural change, we used trypsin sensitivity of the loop 8 as an indicator and the change of trypsin sensitivity was determined using the mAb MD-7 on Western blot. If there is any structural change of Pgp, the loop 8 of Pgp may become either more or less sensitive to trypsin due to the change in topological structure. As shown in Fig. 5A, the peptide Y was generated in large quantity relative to the peptide Z in the presence of MgATP (lane 3) as compared with the control digestion (lane 2, Fig. 5A).

To determine whether $Mg^{++}$ is required for ATP to stimulate the generation of the peptide Y, we performed a trypsin digestion of Pgp in the presence of ATP without $Mg^{++}$. As shown in Fig. 5B, ATP without $Mg^{++}$ stimulated little the generation of the peptide Y (lane 1, Fig. 5B). $Mg^{++}$ alone did not stimulate the generation of the peptide Y (lane 2, Fig. 5B). Therefore, the complex of $Mg^{++}$ with ATP is apparently required to stimulate the generation of the peptide Y. The non-hydrolyzable analogues MgATPgS (lane 4, Fig. 5B) and MgAMP-PNP (lane 5, Fig. 5B) did not stimulate the generation of the peptide Y. However, more peptide C was observed in the presence

of MgATPgS and MgAMP-PNP. These results suggest that different conformational states of Pgp may exist and can be generated by the binding and/or hydrolysis of MgATP.

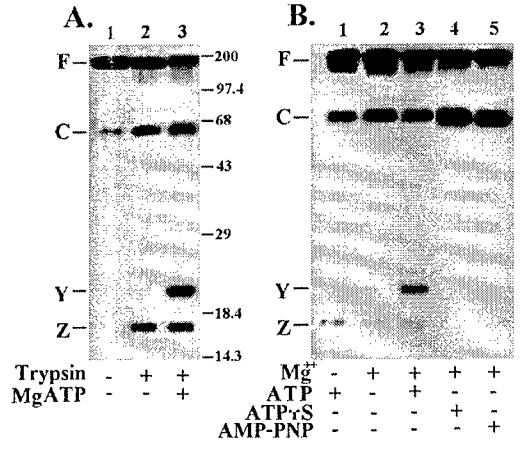


**Figure 5. Trypsin digestion of Pgp in inside-out membrane vesicles and MgATP effects. (A), effects of MgATP on trypsin digestion of Pgp. 30 mg of membrane proteins were pre-treated without (lane 2) or with 5 mM MgATP (lane 3) for 30 min at room temperature, followed by digestion with 6 mg trypsin at 37°C for 2 hrs. The reaction was stopped by using PMSF and soybean trypsin inhibitor. The membrane fraction was pelleted by centrifugation, separated by SDS-PAGE and transferred onto a PVDF membrane. Pgp and its fragments were detected by the mAb MD-7. Lane 1 is control membranes not digested by trypsin. (B), requirement of $Mg^{++}$ for ATP-induced digestion of Pgp. 30 mg of membrane proteins were pre-treated for 30 min at room temperature with 5 mM ATP (lane 1), 5 mM $MgCl_2$ (lane 2), or in the presence of 5 mM each MgATP (lane 3), MgATPgS (lane 4), and MgAMP-PNP (lane 5). 6 mg trypsin was then added and the digestion was performed for 2 hrs at 37°C. Pgp and its fragments were detected using the mAb MD-7. F=full length. C=carboxyl half. Y=peptide Y. Z=peptide Z.**

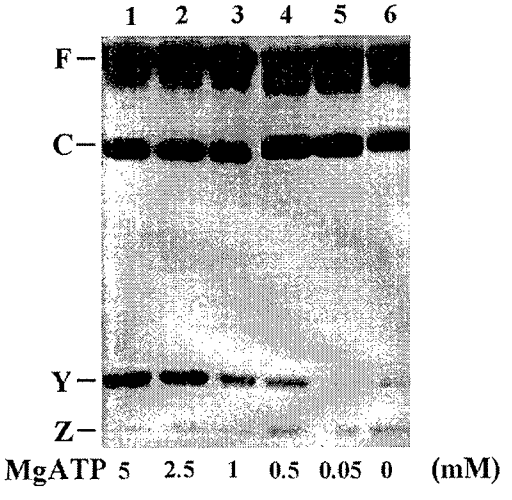


**Figure 6. Concentration dependence of MgATP effects. 30 mg of membrane proteins were pre-treated for 30 min at room temperature with MgATP at 5 mM (lane 1), 2.5 mM (lane 2), 1 mM (lane 3), 0.5 mM (lane 4), or 0.05 mM (lane 5). Lane 6 is a control reaction pre-treated without any nucleotides. Trypsin digestion, SDS-PAGE, and Western blot were performed as described in Fig. 5.**

**(b), concentration dependence of MgATP effects on trypsin digestion of Pgp:** As shown in Fig. 6, 1 mM MgATP was sufficient to stimulate the generation of the peptide Y (compare lanes 1-5 with lane 6, Fig. 6). This value corresponds nicely to the estimated $K_m$ (MgATP) value of 0.6-1.4 mM (Doige *et al.*, 1992; Al-Shawi *et al.*, 1993; Shapiro and Ling, 1994; Rao, 1995).

**(c), the trypsin digestion profile of Pgp is also altered by vinblastine, but not by methotrexate:** Limited trypsin digestion of inside-out vesicles from human SKOV/VLB cells was

performed in the absence (lane 1, Fig. 7) or presence of 5 mM (lane 2), 50 mM (lane 3), and 100 mM (lane 4) methotrexate (MTX) or 5 mM (lane 5), 50 mM (lane 6), and 100 mM (lane 7) vinblastine (VLB). It is clear that more peptide Z was produced in the presence of vinblastine whereas no change was observed in the presence of MTX. The fact that 5 mM VLB enhanced the proteolysis of Pgp to generate the peptide Z is consistent with the Kd(VLB) of ~2 mM (Cornwell *et al.*, 1986). It is also interesting to note that the generation of the peptide Y was enhanced by MgATP whereas the generation of the peptide Z was enhanced by VLB. This suggests that different structural changes may be elicited by MgATP and VLB respectively

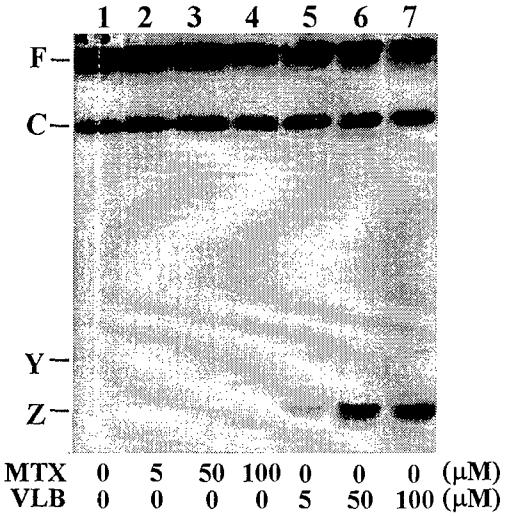


**Figure 7. Effects of drug substrates on trypsin digestion of Pgp. 30 min at room temperature with methotrexate (MTX, lanes 2-4) or vinblastine (VLB, lanes 5-7) at various concentrations as indicated. Lane 1 is 30 mg of membrane proteins were pre-treated for a control reaction pre-treated without drugs. Trypsin digestion, SDS-PAGE, and Western blot were performed as described in Fig. 5.**

6.2.4. Expression of a drug-binding domain of Pgp

**(a), expression and drug binding of Pgp fragment as a fusion protein in bacterial membranes:** It has been shown previously that a domain including TM11-TM12 of Pgp binds photoactive drug analogous (Safa *et al.*, 1987; Greenberger *et al.*, 1991; Bruggemann *et al.*, 1989; 1992). We have engineered a Pgp cDNA fragment encoding the TM11-TM12 with the C-terminal ATP-binding domain into the GST fusion protein expression vector pGEX-2T. The expression of a 65-kDa fusion protein in bacterial BL-21 membranes was induced by IPTG and was detected by commassie blue staining (lane 2, Fig. 8A) and by monoclonal antibody C219 (lane 1, Fig. 8C). Thrombin digestion cleaved off the GST portion from the fusion protein and the Pgp portion of ~40 kDa was detected (lane 3, Fig. 8A and lane 2, Fig. 8C).

To determine if the fusion protein binds drugs, we incubated the bacterial membranes with photoactive [$^3$H]azidopine and the crosslinking was activated by exposing the reaction mixture to UV light. The labeled proteins were then separated on an SDS-PAGE which was then fixed in acetic acid/methanol, treated with amplify$^{TM}$, and dried before exposing to an x-ray film for fluorography. As shown in lane 1 (Fig. 8B), the fusion protein was apparently crosslinked to [$^3$H]azidopine. Using thrombin digestion, it was also shown that the Pgp portion of fusion protein can bind [$^3$H]azidopine (lane 2, Fig. 8B). The binding of azidopine to the fusion protein was inhibited by the competition with vinblastine (Fig. 9). Therefore, it is likely that the Pgp fragment

alone containing TM11, TM12, and the C-terminal ATP-binding domain can bind drugs. This study shows that the drug binding to Pgp does not require the full-length Pgp molecule and that the fusion protein expression system can be used to investigate molecular interaction between drug substrates and Pgp.

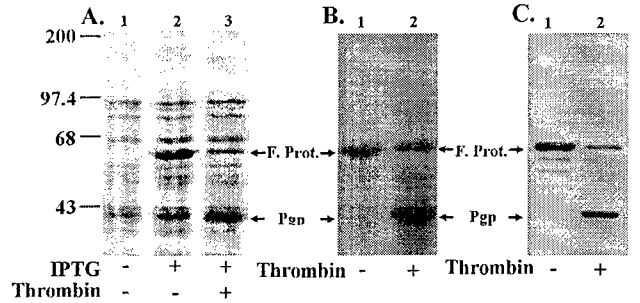


**Figure 8. Binding of [$^3$H]azidopine to Pgp fragments expressed in bacteria membranes. (A), expression of TM11,TM12-NBD. The cDNA encoding the TM11,TM12-NBD of human MDR1 Pgp was cloned into the pGEX-2T expression vector, and transformed into bacteria BL-21. The expression of the fusion protein was induced by IPTG (lane 2). Thrombin digestion cleaved the GST off the fusion protein and the Pgp portion remained with the membrane (lane 3). Lane 1 is a control membrane prepared from cells that were not induced by IPTG. The proteins were detected by commassie blue staining. (B), [$^3$H]azidopine binding to the fusion protein. Membranes containing fusion protein (lane 1) or Pgp portion (lane 2) were incubated with [$^3$H]azidopine at room temperature for 30 min and the labeling was activated using a UV Stratalinker (Stratagene). The proteins were then fractionated on an SDS-PAGE and the labeled proteins were recorded on an x-ray film. (C), Western blot of the fusion protein. Membrane preparations containing fusion protein or Pgp portion were separated on an SDS-PAGE, and transferred onto a PVDF membrane. The blot was probed with the Pgp-specific monoclonal antibody C219.**

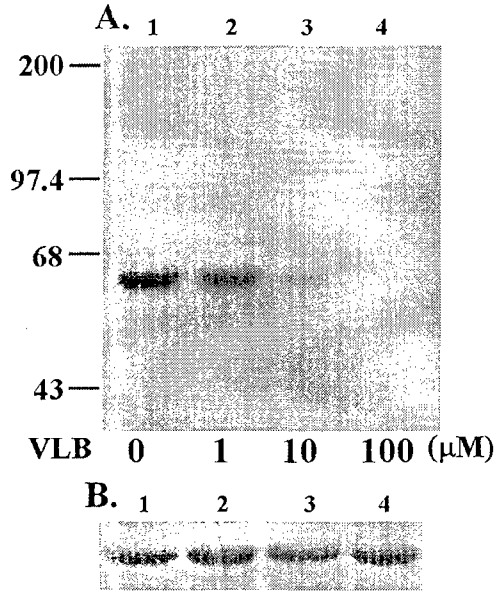


**Figure 9. Vinblastine competition of the azidopine binding to the fusion protein. (A), equal amount of fusion proteins in membranes were pretreated with 0 (lane 1), 1 (lane 2), 10 (lane 3), or 100 (lane 4) mM vinblastine, followed by addition of 0.25 mM [$^3$H]azidopine and incubation for 30 min at room temperature. The crosslinking was then activated by UV light. The proteins were separated on an SDS-PAGE, dried, and the labeled proteins were recorded on an x-ray film. (B), after recording the signal of labeled proteins on x-ray film, the gel in panel A was rehydrated and stained with commassie blue. The results confirmed the equal amount of fusion protein used in each reaction.**

**(b), solubilization of the fusion protein including TM11, TM12 and the nucleotide-binding domain:** We have attempted to solubilize the fusion protein of Pgp expressed in bacterial membranes using various detergents and

chaeotropic reagents. We have worked out a method to purify the fusion protein partially. As shown in Fig. 10, membranes containing the fusion protein was treated with 1% b-D-maltoside to remove most membrane proteins. The pellet was then treated with 0.4% N-lauroylsarcosine including 25 mM DTT to solubilize the fusion protein. In the second step, at least 50% of the solubilized proteins are the fusion protein.

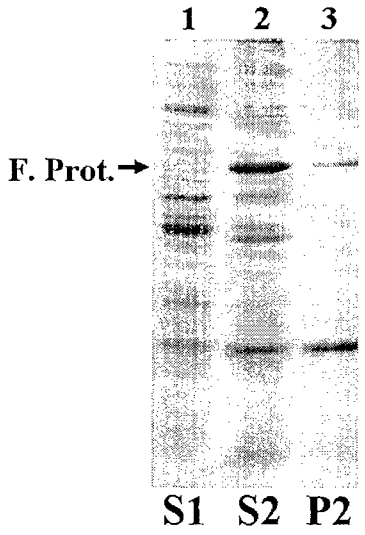


**Figure 10. Solubilization of fusion proteins containing TM11, TM12, and their following sequences of Pgp. 15 mg of membranes containing the fusion protein of GST and Pgp fragment were first treated with 1% b-D-maltoside in PBS for 30 min on ice. The soluble and insoluble fractions were separated by centrifugation. The soluble (S1) fraction was used for SDS-PAGE (lane 1) and the pellet was resuspended in 0.4% N-lauroylsarcosine in PBS containing 25 mM DTT and treated for 30 min on ice. The soluble (S2) lane 2) and insoluble (P2) (lane 3) fractions were separated again by centrifugation and were analyzed on SDS-PAGE. It is clear that the fusion protein was insoluble in 1% b-D-maltoside, but soluble in 0.4% N-lauroylsarcosine. Majority of other proteins were removed by the first treatment with b-D-maltoside.**

## 7. CONCLUSIONS:

In the two and half years, we have determined the topologies of P-glycoprotein in multidrug resistant cells using site-specific antibodies. We found that P-glycoproteins in the plasma membrane of mammalian cells express at least two alternate topologies. This observation is consistent with our previous study using cell-free expression system. The more than one topology feature of Pgp may be responsible for its multifunctional nature.

We have also determined the potential conformation changes of Pgp in its catalytic cycle. Pgp is an ATPase that hydrolyzes ATP even in the absence of drug substrates. We showed that the trypsin digestion profile of Pgp was altered in the presence of ribonucleotide ligands. This suggests that the conformation of Pgp was altered by the binding of various nucleotides.

Furthermore, we were able to express the transmembrane domain of Pgp in bacteria for drug binding studies. The putative TM11 and TM12 have been suggested to be drug-binding site (Zhang *et al.*, 1995b). By expressing the drug-binding domain alone in bacterial will provide an opportunity to prepare large quantity for further structure and function studies. For example, the 3-dimensional (3-D) fold of the drug-binding peptides can be analyzed using x-ray crystallography and NMR technology. Studies of 3-D structure will help define the group(s) of drugs that interact

with the drug binding peptides. Alteration of the groups of these drugs may lead to a design of new agents that will overcome the MDR, but still have therapeutic effects.

## 8. REFERENCES:


Al-Shawi, M.K., and Senior, A.E. (1993) J. Biol. Chem. 268:4197-4206.

Altenberg, G.A., Vanoye, C.G., Han, E.S., Deitmer, J.W. and Reuss, L. (1994) J. Biol. Chem. 269:7145-7149.

Bates, S.E., Meadows, B., Goldspiel, B.R., Denicoff, A., Le, T.B., Tucker, E., Steinberg, S.M., Elwood, L.J. (1995) Pharma. 35:457-463.

Bradley, G., Naik, M. and Ling, V. (1989) Cancer Res. 49:2790-2796.

Bruggemann, E.P., Germann, U.A., Gottesman, M.M. and Pastan, I. (1989) J. Biol. Chem. 264:15483-15488.

Bruggemann, E.P., Currier, S.J., Gottesman, M.M. and Pastan, I. (1992) J. Biol. Chem. 267:21020-21026.

Busche, R., Tummler, B., Cano-Gauci, D.F. and Riordan, J.R. (1989) Eur. J. Biochem. 183:189-197.

Charpin, C., Vielh, P., Duffaud, F., Devictor, B., Andrac, L., Lavaut, M.N., Allasia, C., Horschowski, N., Piana, L. (1994) J. Natl. Cancer Inst., 86:1539-1545.

Cianfriglia, M., Willingham, M.C., Tombesi, M., Scagliotti, G.V., Frasca, G. and Cherst, A. (1994) *Int. J. Cancer* 56:153-160.

Cornwell. MM., Safa, A.R., Felsted, R.L., Gottesman, M.M. and Pastan, I. (1986) Proc. Natl. Acad. Sci. USA 83:3847-3850.

Doige, C.A., Yu, X. and Sharom, F.J. (1992) Biochim. Biophys. Acta 1109:149-160.

Georges, E., Bradley, G., Gariepy, J., and Ling, V. (1990). Proc. Natl. Acad. Sci. USA 87:152-156.

Georges, E., Zhang, J.T., and Ling, V. (1991) J. Cell. Physiol. 148:479-484.

Goldstein, L., Galski, H., Fojo, A., Willingham, M., Lai, S-L., Gazdar, A., Pirker, R., Green, A., Crist, W., Brodeur, G., Lieber, M., Cossman, J., Cottesman, M. and Pastan, I. (1989) J. Natl. Cancer Inst. 81:116-124.

Gill, D.R., Hyde, S.C., Higgins, C.F., Valverde, M.A., Mintenig, G.M., and Sepulveda, F.V. (1992) Cell 71:23-32.

Gottesman, M.M. and Pastan, I. (1993) Annu. Rev. Biochem. 62:385-427.

Greenberger, L.M. Lisanti, C.J., Silva, J.T. and Horwitz, S.B. (1991) J. Biol. Chem. 266:20744-20751.

Harlow, E. and Lane, D. (1988) Antibodies, a laboratory manual. Cold Spring Harbor Lab.

Higgins, C. (1992) Annu. Rev. Cell Biol. 8:67-

Kadle, R., Zhang, J.T. and Nicholson, B. (1991) Mol. Cell. Biol. 11:363-369.

Kartner, N., Evernden-Porelle, D., Bradley, G., and Ling, V. (1985) Nature 316:820-823.

Keith, W.N., Stallard, S. and Brown, R. (1989) Br. J. Cancer 61:712-716.

Lever, J. E. (1977) J. Biol. Chem. 252:1990-1997.

Merkel, D.E., Fuqua, S.A.W., Tandon, A.K., Hill, S.M., Buzdar, A.U. and McGuire, W.L. (1989) J. Clinical Oncology 7:1129-1136.

Rao, U.S. (1995) J. Biol. Chem., 270:6686-6690.

Ro, J., Sahin, A., Ro, J.Y., Fritsche, H., Hortobagyi, G. and Blick, M. (1990) Human Path. 21:787-791.

Safa, A.R., Glover, C.J., Meyers, M.B., Biedler, J.L. and Felsted, R.L. (1986) J. Biol. Chem. 261:6137-6140.

Safa, A.R., Mehta, N.D. and Agresti, M. (1989) Biochem. Biophys. Res. Commun. 162:1402-1408.
Safa, A.R., Glover, C.J., Sewell, J.L., Meyers, M.B., Biedler, J.L. and Felsted, R.L. (1987) J. Biol. Chem. 262:7884-7888.
Shapiro, A. and Ling, V. (1994) J. Biol. Chem. 269:3745-3754.
Shapiro, A., Duthie, M., Childs, S., Okubo, T., and Ling, V. (1996) Int. J. Cancer 67:256-263.
Salmon, S., Grogan, T., Miller, T., Scheper, R. and Dalton, W. (1989) J. Natl. Cancer Inst 81:696-701.
Sanfilippo, O., Ronchi, E., De Marco, C., Di Fronzo, G. and Silvestrini, R. (1991) Eur. J. Cancer 27:155-158.
Schneider, J. Bak, M., Efferth, T., Kaufmann, M., Mattern, J. Volm, M. (1989) Br. J. Cancer 60:815-818.
Smith, D. and Johnson, K. (1988) Gene 67:31-40.
Sugawara, I., Kataoka, I., Morishita, Y., Hamada, H., Tsuruo, T., Itoyama, S and Mori, S. (1988) Cancer Res. 48:1926-1929.
Valverde, M.A., Diaz, M., Sepulveda, F.V., Gill, D.R., Hyde, S.C. and Higgins, C.F. (1992) Nature 355:830-833.
Verrelle, P., Meissonnier, F., Fonck, Y., Feillel, V., Dionet, C., Kwiatkowski, F., Plagne, R. and Chassagne, J. (1991) J. Natl. Cancer Inst. 83:111-116.
Wishart, G.C. and Kaye, S.B. (1991) Eur. J. Surg. Oncol. 17:485-488.
Zhang, J.T. and Ling, V. (1991) J. Biol. Chem. 266:18224-18232.
Zhang, J.T., Duthie, M. and Ling, V. (1993) J. Biol. Chem. 268:15101-15110.
Zhang, J.T. and Nicholson, B.J. (1994) J. Memb. Biol. 139:15-29.
Zhang, J.T., Lee, Zhang, J.T., Lee, C.-H., Duthie, M., and Ling, V. (1995a) J. Biol. Chem. 270:1742-1746.
Zhang, X., Collins, K.I., Greenberger, L.M. (1995b) J. Biol. Chem. 270:5441-5448.

## 9. PUBLICATIONS:

### Full Articles:

Zhang, J.T. and Chong, C.H. (1996) Co-transltional effects of temperature on membrane insertion and orientation of P-glycoprotein sequences. *Mol. Cell. Biochem.* 159:25-31.

Zhang, M., Wang, G., Shapiro, A., and Zhang, J.T. (1996) Topological folding and proteolysis profile of P-glycoprotein molecules in membranes of multidrug-resistant cells: implications for the drug transport mechanism. *Biochemistry* 35:9728-9736; 1996.

Zhang, J.T. (1996) Sequence requirements for membrane assembly of polytopic membrane proteins: molecular dissection of the membrane insertion process and topogenesis of the human MDR3 P-glycoprotein *Mol. Biol. Cell* 7:1709-1721; 1996.

Zhang, J.T. (1997) Use of cell-free expression systems to determine P-glycoprotein topology. *Methods Enzymol.* (in press).

Wang, G.C., Zhang, M., Pincheira, R., and Zhang, J.T. (1997) Molecular dissection of conformational changes of P-glycoprotein in its catalytic cycle. (manuscript submitted for publication).

Wang, C.S., Chen, M.A., and Zhang, J.T. (1997) Role of ribosomes in regulating membrane protein folding during translation (manuscript submitted for publication).

Han, E.S., Chong, C., and Zhang, J.T. (1997) Identification of topology regulatory elements of the C-half of P-glycoprotein, a polytopic membrane protein (manuscript submitted for publication).

Chen, M.A., Wang, C.S., and Zhang, J.T. (1997) Analysis of *de novo* membrane targeting and insertion activities of internal transmembrane segments of ABC transporters (manuscript in preparation).

### Abstracts:

Zhang, M. and Zhang, J.T. Evidence for the expression of multiple topologies of P-glycoprotein in $CH^{r}B30$ cells. Proceedings of American Association for Cancer Research 36:337a; 1995

Zhang, J.T. and Zhang, M. Topology of P-glycoprotein and multidrug resistance. The 6th international SCBA symposium and workshop, Vancouver, Canada, 1995 (invited presentation).

Han, E.S. and Zhang, J.T. Alternate membrane topology for the C-terminal half of hamster P-glycoprotein differs from human P-glycoprotein. UTMB medical student research presentation, Galveston, TX, June, 1995 (Best Basic Sciences Award-winning poster).

Zhang, M., Wang, G.C., Shapiro, A., and Zhang, J.T. P-glycoprotein: proteolysis profile, topology, and conformational changes induced by drug binding. Proceedings of American Association for Cancer Research 37:328a; 1996.

Zhang, J.T., Wang, C.S. and Chen, M. Role of ribosomes in regulating topogenesis of P-glycoprotein. Keystone Symposia on Molecular and Cellular Biology, Taos, NM, 1997.

Han, E. Zhang, J.T. Identification of topology regulatory elements of the C-half of P-glycoprotein, a polytopic membrane protein. Keystone Symposia on Molecular and Cellular Biology, Taos, NM, 1997.

Wang, G., Pincheira, R., Zhang, M., Zhang, J.T. Molecular dissection of conformational changes of P-glycoprotein in its catalytic cycle. American Association for Cancer Research, 1997.

## 10. APPENDIX

Reprints of the published articles were appended.

*Molecular and Cellular Biochemistry* **159:** 25–31, 1996.
© 1996 *Kluwer Academic Publishers. Printed in the Netherlands.*

# Co-translational effects of temperature on membrane insertion and orientation of P-glycoprotein sequences

Jian-Ting Zhang and Crispina H. Chong

*Department of Physiology and Biophysics, University of Texas Medical Branch, Galveston, Texas 77555-0641, USA*

Received 30 October 1995; accepted 16 January 1996

## Abstract

P-glycoprotein (pgp) is a membrane transport protein that causes multidrug resistance (MDR) by actively extruding a wide variety of cytotoxic agents out of cells. It may also function as a peptide transporter, a volume-regulated chloride channel, and an ATP channel. Previously, it has been shown that hamster *pgp1* Pgp is expressed in more than one topological form and that the generation of these structures is modulated by charged amino acids flanking the predicted transmembrane (TM) segments 3 and 4 and by soluble cytoplasmic factors. Different topological structures of Pgp may be related to its different functions. In this study, we examined the effects of translation temperature on the membrane insertion process and the topologies of Pgp. Using the rabbit reticulocyte lysate expression system, we showed that translation at different temperatures affects the membrane insertion and orientation of the putative TM3 and TM4 of hamster *pgp1* Pgp in a co-translational manner. This observation suggests that the membrane insertion process of TM3 and TM4 of Pgp molecules may involve a protein conducting channel and/or the interaction between TM3 and TM4, which act in a temperature sensitive manner. We speculate that manipulating temperature may provide a way to understand the structure-function relationship of Pgp and help overcome Pgp-related multidrug resistance of cancer cells. (Mol Cell Biochem **159:** 25–31, 1996)

*Key words*: multidrug resistance, *in vitro* translation, thermal therapy, P-glycoprotein, topology, CFTR

*Abbreviations*: Pgp – P-glycoprotein; MDR – multidrug resistance; ABC – ATP-binding cassette; RRL – rabbit reticulocyte lysate; TM – transmembrane; RM – rough microsomes; ER – endoplasmic reticulum

## Introduction

P-glycoprotein (Pgp) is a member of the ATP-binding cassette (ABC) membrane transporter superfamily which transports a wide variety of substrates [1–4]. Pgp molecules not only cause multidrug resistance (MDR) in cancer cells by extruding chemotherapeutic drugs, they also transport peptides [5] and may also be associated with a cell-swelling activated $Cl^-$ channel [6–8] or the regulator of a $Cl^-$ channel [9], and an ATP-channel [10].

Hydropathy analyses of deduced protein sequences suggest that Pgp has 12 predicted transmembrane (TM) segments. However, alternate topologies of Pgp have been identified in recent studies using rabbit reticulocyte lysate (RRL) [11–12], *Xenopus* oocytes [13], and bacteria [14] as expression systems. In addition to the predicted 12-TM structure, alternate structures of Pgp containing only 8 [12] or 10 [15] TM segments have been identified. It has been postulated that the different topological structures of Pgp may be involved in the multiplicity of functions attributed to this protein [11–12]. Recently, it has been shown that the generation of the alternate topology in RRL is dependent on charged amino acids flanking some internal predicted TM segments [16] and that the soluble cytoplasmic factors may involve the regulation of membrane inser-

*Address for offprints*: J.-Ting Zhang, Dept. of Physiology and Biophysics, University of Texas Medical Branch, Galveston, Texas 77555-0641, USA

tion and orientation of the internal Pgp TM segments [17].

In the present study, we tested the possibility that translation temperature affected the membrane insertion and orientation of Pgp sequences. We discovered that the membrane insertion of putative TM3 and TM4 of hamster *pgp1* Pgp decreases when the incubation temperature is increased. These results suggest that the membrane insertion and orientation of some internal TM segments of Pgp are temperature dependent. This observation may have significant implication for the use of thermal therapy to overcome the Pgp-related MDR phenotype of cancer cells.

## Materials and methods

### *Materials*

SP6 RNA polymerase, RNasin, ribonucleotides, RQ1 DNase, rabbit reticulocyte lysate, and dog pancreatic microsomal membranes were obtained from Promega. [$^{35}$S]methionine and Amplify were purchased from New England Nuclear and Amersham Corp, respectively. m$^7$G(5')ppp(5')G cap analog was obtained from Pharmacia LKB Biotechnology Inc. Peptide N-glycosidase F (PNGase F) and restriction enzymes were obtained from Boehringer Mannheim, New England Biolabs, or Promega. All other chemicals were obtained from Sigma or Fisher Scientific.

### In vitro *transcription and translation*

About 6 μg of recombinant DNA linearized with *Hind* III was transcribed in the presence of 5 $A_{260}$ units/ml cap analog m$^7$G(5')ppp(5')G as described previously [11]. Removal of DNA templates with RQI DNase after transcription and purification of RNA transcripts was carried out according to Zhang and Ling [11]. Cell-free translations using rabbit reticulocyte lysate were performed as described previously [11]). For pulse-chase experiment, the translation reaction was first incubated at indicated temperatures for 45 min. The reaction was then either chilled on ice or incubated for 45 min at indicated temperatures, respectively. The membrane fraction of translation products was then isolated by centrifugation and analyzed using SDS-PAGE and fluorography as described previously [11].

## Results

Previously, it has been shown that hamster *pgp1* Pgp sequences in microsomal membranes have two alternative topologies [11–12]. The variable topologies were generated by the altered membrane insertion pattern of the internal putative TM segments, such as TM3 and TM4. Fig. 1A shows the example of alternate topologies of truncated Pgp sequences. In both model I and II structures, the putative TM1 and TM2 are in the membrane. However, the putative TM3 and TM4 inserts into membranes differently, generating the two alternate topologies of truncated Pgp molecules.

In this study, we used the previously constructed pGPGP-N3 and pGPGP-N4 plasmid DNA [12] to study whether the membrane insertion and orientation of the internal putative TM segments are affected by the incubation temperature. These two plasmids encode truncated Pgp with the N-terminal 3 or 4 putative TM segments linked to a C-terminal ATP-binding domain. Two populations of truncated Pgp were generated from both pGPGP-N3 and pGPGP-N4 DNA in a rabbit reticulocyte lysate expression system [12; see also Fig. IA]. The C-terminal tails of the nascent molecules can be on the either side of the microsomal membranes (RM) depending on the membrane insertion pattern of the putative TM3 and TM4. Any molecule with the C-terminal tail in the RM lumen has an extra oligosaccharide chain attached and will have a slower mobility on SDS-PAGE than the molecules with their C-terminal tail on the outside of RM [12]. The proportion of the two populations of proteins with different mobility on SDS-PAGE will serve as a convenient indication for the relative amounts of model I and II molecules [12, 16].

Figure 1B shows an example of the translation product of PGP-N3 (lanes 1–5) and PGPN4 (lanes 6–10). Two products of 54 and 57 kDa for PGP-N3 (lane 1) and two products of 59 and 62 kDa for PGP-N4 (lane 6) were generated in rabbit reticulocyte lysate translation system in the presence of RM. The 57-kDa peptide of PGP-N3 and the 62-kDa peptide of PGP-N4 contains 4 oligosaccharide chains and represent the molecules with their C-terminal reporter in the RM lumen (Fig. 1A) [12]. In contrast, the 54-kDa and 59-kDa peptides contain only 3 oligosaccharide chains and represent the molecules with their C-terminal reporter on the outside of RM (Fig. 1A) [12]. This is demonstrated by limited endoglycosidase treatment which produced the peptide intermediates containing 1 and 2 oligosaccharide chains (see the indications by arrow in lanes 2–4 for PGP-N3 and lanes 7–9 for PGP-N4). The fully deglycosylated PGP-N3 and PGP-N4 peptides are shown in lanes 5 and 10, respectively. These results are consistent with our previous studies [12].

At 30°C, about 45% model I (57-kDa peptide) and 55% model II (54-kDa peptide) of the total membrane-associated PGP-N3 molecules were generated (lane 1, Fig. 2A), consistent with the previous study [12]. However, as the incubation temperature increases, generation of the model I PGP-N3 molecules decreases at a faster rate than the model II molecules (compare lanes 2–4 with lane 1, Fig. 2A) and does not appear to be generated at 42°C. Similar observation was made with the

translation of pGPGP-N4 transcript. This is shown in Fig. 2B. Two populations of microsome-associated peptides of 62 kDa (model II) and 59 kDa (model I) were produced from the PGP-N4 transcript. At 30°C, about 75% of model II and 25% of model I PGP-N4 molecules were produced (lane 1, Fig. 2B). However, as the incubation temperature increases, the proportion of the 62-kDa PGP-N4 molecules (model II) decreases whereas the model I molecules did not change significantly (compare lanes 2–4 with lane 1, Fig. 2B). It should also be noted that the total amount of microsome-associated nascent molecules also decreased with the increase of the incubation temperature. This is probably due to the decreased translation rate at higher temperatures as shown in Fig. 2C. When the translation of PGP-N4 transcript was performed at different temperatures without membrane, the total amount of PGP-N4 precursor molecules (~51 kDa) decreased as the incubation temperature increased.

The above results showed that the relative proportion of nascent protein products with an extra glycosylation (model I of PGP-N3 and model II of PGP-N4) was decreased with the increase of incubation temperature. This observation is probably due to (1) the putative TM3 and TM4 are less able to insert into the membrane individually at elevated temperatures, (2) the glycosylation was decreased by the elevated incubation temperature, or (3) the change in translation rate results in the change in membrane insertion. Both the second and the third possibilities are unlikely as we will show below, suggesting that elevated temperature decreased the individual membrane insertion of the putative TM3 and TM4 to generate the further glycosylated protein species, respectively.

To determine whether or not the glycosylation was affected by temperature, we translated prepro-α-factor at different temperatures to test the effects of incubation temperature on glycosylation. Prepro-α-factor is an 18.5-kDa peptide which has three potential glycosylation sites [18] and all three sites were glycosylated when RM was supplemented in the trans-

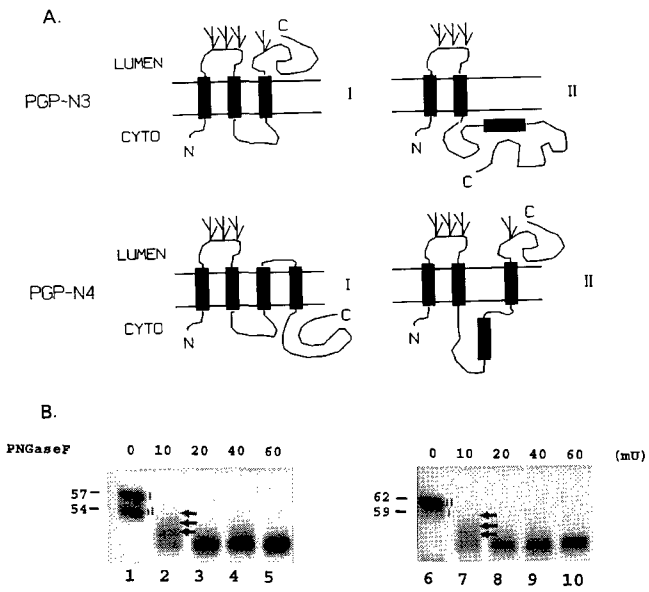


*Fig. 1.* A, membrane orientations of truncated Chinese hamster *pgp1* Pgp (PGP-N3 and PGP-N4). Two different topologies of PGP-N3 and PGP-N4 are shown as model I and II. Translocation of the C-terminal reporter peptide into the RM lumen will generate a molecule with an extra oligosaccharide chain attached (model I for PGP-N3 and model II for PGP-N4). The branched symbols represent the oligosaccharide chains. The filled bars represent the putative TM segments. B, *in vitro* translation and limited endoglycosidase treatment. Two mature translation products (indicated by I and II) were generated from PGP-N3 (lane 1) and PGP-N4 (lane 6), respectively in rabbit reticulocyte lysate supplemented with RM. They presumably represent the two different orientations shown in panel A. Lanes 2–4 and 7–9 show limited endoglycosidase PNGase F treatment. Enzyme concentration is given in milliunits (mU). The partially deglycosylated peptides are indicated by *arrows*. The fully deglycosylated PGP-N3 and PGP-N4 peptides are shown in lanes 5 and 10, respectively.

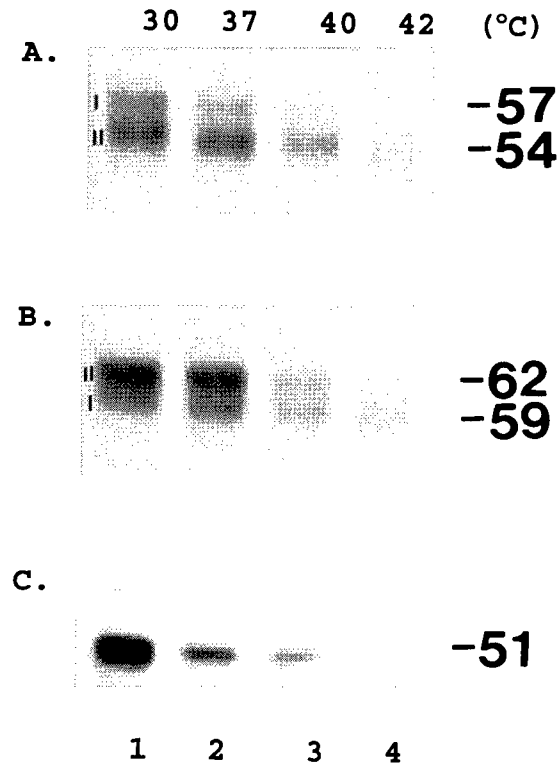


*Fig. 2.* Increased incubation temperature decreases the membrane insertion of the putative TM3 and TM4. Translation of PGP-N3 (panel A) and PGP-N4 (panel B) was performed in rabbit reticulocyte lysate in the presence of RM at 30°C (lane 1), 37°C (lane 2), 40°C (lane 3), and 42°C (lane 4) and the membrane fraction was isolated and separated on an SDS-PAGE. It is clear that the top band for both PGP-N3 and PGP-N4 molecules decreases with the increase of incubation temperature. Longer exposure of the gel did not show any significant change. Panel C shows the translation of PGP-N4 in the absence of RM performed at different temperatures. It shows that the increased incubation temperature decreases the translation rate.

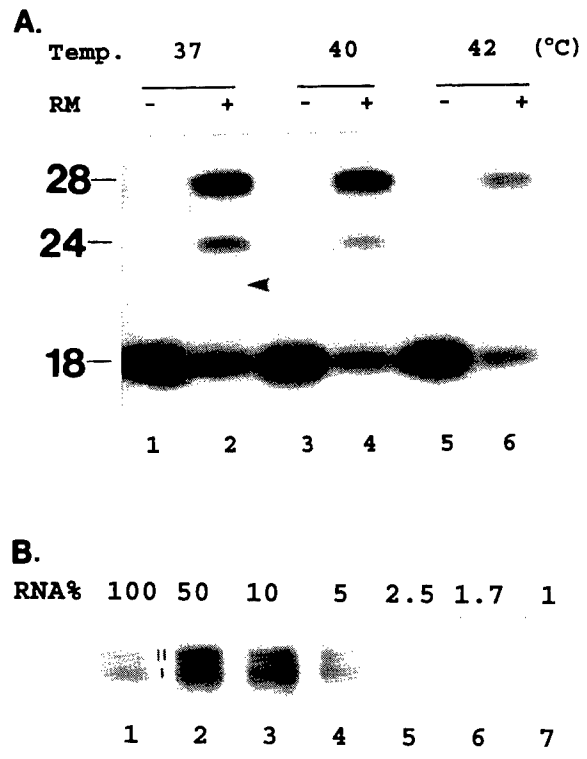


*Fig. 3.* A, *In vitro* translation of prepro-α-factor. Translation of prepro-α-factor in rabbit reticulocyte lysate in the absence (lanes 1, 3, and 5) or presence (lanes 2, 4, and 6) of RM was performed at different temperatures as indicated. An 18-kDa protein was produced in the absence of RM whereas peptides containing two (24 kDa) and three (28 kDa) oligosaccharide chains were also generated in the presence of RM. The total translation rate in the presence of RM decreases at higher incubation temperatures (compare lanes 2, 4, and 6). A shorter exposure of the same gel shows that the translation rate in the absence of RM also decreases (data not shown). B, reduced translation rate does not alter the generation of the model II topology of PGP-N4 molecules. Translations were directed by different amount of PGP-N4 RNA templates. The amount of RNA in each reaction was normalized against that in the translation shown in lane 1. The reduced amount of RNA templates significantly reduced the translation rate in the RRL system (lanes 1–5). However, both model I and II topologies of PGP-N4 molecules were produced in a similar proportion in all the reactions (lanes 1–5).

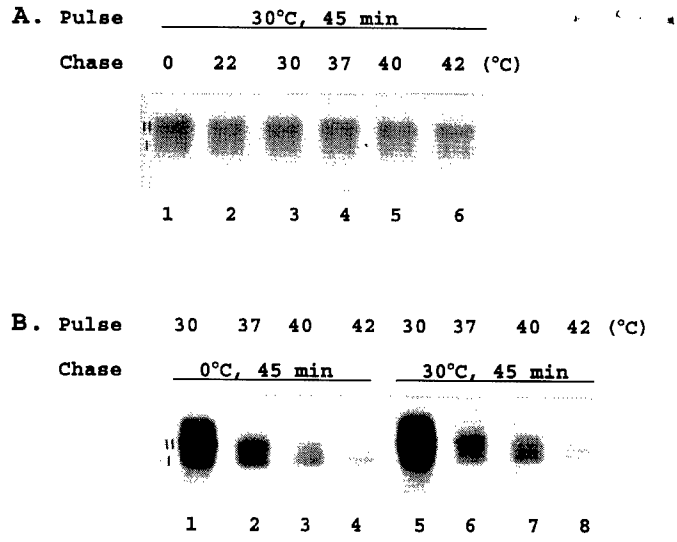


*Fig. 4.* Pulse-chase studies of PGP-N4 membrane insertion. A, pulse translation at 30°C with a chase at various temperatures. Translation of PGP-N4 in the presence of RM was performed as described in Materials and methods at 30°C for 45 min. Each reaction was then chased for 45 min at different temperatures as indicated. B, pulse translation at various temperatures with a chase at 30°C. Translation of PGP-N4 in the presence of RM was performed at various temperatures as indicated for 45 min. Then, half of each reaction was chased at 30°C for 45 min (lanes 5–8) whereas the other half was kept on ice as a control (lanes 1–4). No change in the proportion of the two populations of the PGP-N4 molecules was observed by chasing the translation at temperatures different from that for the pulse of translation.

lation [18–21]. In the present study, an 18-kDa precursor peptide was produced from the prepro-α-factor RNA in the absence of RM (lane 1, 3, and 5, Fig. 3A). In the presence of RM, peptides with two (24 kDa), and three (28 kDa) oligosaccharide chains attached were produced (lanes 2, 4, and 6, Fig. 3A). If the elevated incubation temperature decreases the glycosylation, we would expect that the amount of unglycosylated precursor of 18 kDa or partially glycosylated peptides of 24 kDa will increase as the amount of fully-glycosylated peptide of 28 kDa decreases at higher temperatures. However, the glycosylation pattern did not change with the temperature, i.e. the proportion between glycosylated peptides, partially glycosylated peptides, and the unglycosylated peptides at different temperatures did not vary significantly (compare lanes 2, 4, and 6 in Fig. 3A). Therefore, we conclude that the incubation temperature does not affect the enzymatic reaction of core-sugar transfer. However, our control experiments using a secretory protein could not rule out the possibility that some unknown and more complex effect of folding confers temperature sensitive glycosylation of a membrane protein such as Pgp.

To rule out the possibility that reduced translation rate alters the membrane insertion, we performed an experiment to reduce the translation rate by decreasing the PGP-N4 RNA template concentration in the reaction and to determine the topologies of Pgp sequences under these conditions. The results are shown in Fig. 3B. As the concentration of RNA templates changes, the translation rate changes (compare lanes 1–7, Fig. 3B) with a maximum rate when 50% of RNA was included (lane 2, Fig. 3B). However, the ratio between model I and II molecules were not altered in these reactions. This observation suggests that the change in translation rate does not cause the change in membrane insertion and folding of Pgp sequences.

To determine whether or not elevating temperature after the completion of translation will change the topology of Pgp sequences, we performed a pulse chase experiment. The translation of PGP-N4 was performed at 30°C for 45 min, treated

with RNase A to stop further initiation of translation, then followed by incubation at different temperatures for additional 45 min. Membrane-associated proteins were then isolated and used for SDS-PAGE. As shown in Fig. 4A, when the chase experiment was performed at lower (lanes 1 and 2, Fig. 4A) or higher (lanes 4–6, Fig. 4A) temperatures, the proportion of the model I and II PGP-N4 molecules did not change as compared with the chase reaction at 30°C (lane 3, Fig. 4A). Therefore, altering temperature after translation does not change the model II PGP-N4 molecules to the model I structure.

To determine whether the effect of temperature on the individual membrane insertion of the putative TM4 is cotranslational, we performed a similar pulse chase experiment as described in Fig. 4A. Translations of PGP-N4 molecules were first performed at 30°C, 37°C, 40°C, or 42°C for 45 min, treated with RNase A to stop further initiation of translation, then half of each reaction was immediately chilled on ice (lanes 1–4, Fig. 4B) whereas the other half was incubated at 30°C (lanes 5–8, Fig. 4B) for 45 min. The membrane-associated proteins were then isolated and analyzed on SDS-PAGE. The proportion of the model II products decreased with the elevated temperature (lanes 1–4, Fig. 4B). Chasing all reactions at 30°C after translation did not increase the proportion of the model II molecules of PGP-N4 (lanes 5–8, Fig. 4B). We therefore conclude that the effect of temperature on the individual membrane insertion of the putative TM4 is likely a co-translational process.

## Discussion

P-glycoprotein has been found to have multiple topologies which may be responsible for its multiple functions (11–15). The generation of these topologies are regulated by the charged amino acids surrounding the putative TM3 and TM4 [16] and by cytoplasmic protein factors [17]. In this study, we showed that in a cell-free system the incubation temperature also regulates the membrane insertion and orientation of Pgp sequences. Increasing incubation temperature above 30°C decreases the individual membrane insertion ability of the internal putative TM segments in a co-translational manner. Once a topology of the protein is formed, changing temperature does not alter that topology.

We also showed that increasing the translation temperature decreases the translation rate. However, the alteration in translation rate does not alter the individual membrane insertion of the putative TM3 and TM4 (Fig. 3B). Recently, it has been proposed that a protein conducting channel in the ER membrane plays an important role in the membrane translocation of membrane and secretory proteins [22]. Effects on membrane insertion and orientation of Pgp sequences by internal charged amino acids and incubation temperature are presumably due to the interaction between the charged amino acids in the nascent peptide and the protein components in the protein conducting channel. Increasing temperature may alter the enthalpies of different folded states as a consequence of the interaction between charged amino acids of the nascent peptides and the components in the protein conducting channel. We note that van der Waals forces, hydrogen bonds, and ionic bonds have positive enthalpies, whereas hydrophobic interactions have negative enthalpies [32]. It is also noteworthy that elevated temperature decreased the individual membrane insertion of both TM3 and TM4, suggesting that, at higher temperatures, paired membrane insertion of TM3 and TM4 is favored. This is possibly due to the increased hydrophobic interaction between TM3 and TM4 at higher temperatures. However, it is premature to correlate much regarding the thermodynamics of the membrane insertion and folding of Pgp until we have a better understanding of the actual chemical interaction.

Although altered topologies of Pgp molecules have been observed using bacteria [14], frog oocytes [13], and mammalian cell-free [11–12] expression systems, recent studies by Loo and Clarke [23] suggest that mutant human Pgp expresses only the predicted topology in the membrane. The discrepancy between these studies is not known, but may be due to alteration of the cDNA sequence by mutation or truncation, or due to the different expression systems used. In our recent studies, we showed that alteration of charged amino acids surrounding TM4 changed the membrane insertion process of TM4 [16] and expression of hamster Pgp in the wheat germ extract expression system resulted in only the predicted topology [17]. However, a recent study by Zhang and Zhang [24] using site-specific antibodies to label Pgp in multidrug resistant cells ($CH^RB30$) suggests that both the predicted and the alternate topologies shown previously [12] are expressed.

Previously, it has been shown that a deletion mutant ΔF508 of CFTR, a homologous protein of Pgp, was not expressed on the cell surface and, therefore, causes cystic fibrosis [25]. It was thought that this deletion mutant was misfolded and was retained in the endoplasmic reticulum (25–26). However, growing the cells at lower temperature allows the mutant CFTR protein to traffic to the plasma membrane (27–29). In light of our findings from the current study, it is tempting to speculate that the deletion of Phe-508 altered membrane insertion and orientation of CFTR which cannot traffic to the cell surface. However, lowering the incubation temperature may have reversed the effect of deletion on the membrane insertion and thus corrected the membrane orientation of the mutant CFTR.

The observation that elevated temperature alters the membrane insertion and orientation of Pgp sequences may provide a way to understand structure-function relationships of Pgp. If Pgp molecules with different topologies have different functions, functional studies at different temperatures may elucidate the correlation between topology and function of Pgp. If Pgp molecules with the model II topology involve drug efflux in MDR cells, temperature effects on the genera-

tion of this structure may help to overcome the Pgp-related MDR of cancer cells. Previously, Bates and Mackillop [30] have shown that a 20 min exposure to elevated temperature increases the cytotoxicity of adriamycin to the drug sensitive Aux B1 cells, but not to the multidrug resistant $CH^RC5$ cells. This observation may be due to the fact that a brief exposure of elevated temperature does not change the topological structure of the existing Pgp molecules and therefore their drug transport function. Because the half life of Pgp is ~50 h [31], the MDR cells may need to be exposed to higher temperature for extended period before the hyperthermia takes effect. We speculate that a proper combination of hyperthermia and chemotherapy will have a significant impact on overcoming the Pgp-related MDR phenotype in cancer cells. Since the current study involved only truncated Pgp sequences with reporter peptides, it is not known whether the temperature effects on the membrane insertion and orientation of Pgp sequences will be the same in the context of full-length protein without any reporter. However, studies using full-length Pgp without any reporter will require development of reliable approaches to differentiate the different topologies of the full-length Pgp generated at different temperatures.

## Acknowledgements

This work was supported by a grant CA-64539 from the National Institutes of Health and by a grant from the U.S. Army Research and Development Command. The authors would like to thank Dr. Victor Ling for providing the hamster cDNA and Drs. Malcolm Brodwick and Karl Karnaky Jr. at UTMB for their critical comments and valuable suggestions on this manuscript.

## References

1. Endicott J A, Ling V: The biochemistry of P-glycoprotein-mediated multidrug resistance. Annu Rev Biochem 58:137–171, 1989
2. Gottesman MM, Pastan I: Biochemistry of multidrug resistance mediated by the multidrug transporter. Annu Rev Biochem 62: 385–427, 1993
3. Higgins CF: ABC transporters from microorganisms to man. Annu Rev Cell Biol 8: 67–113, 1992
4. Childs S, Ling V: The MDR superfamily of genes and its biological implications. In: V. T. DeVita, S. Hellman and S.A. Rosenberg (eds). Important Advances in Oncology. J.B. Lippincott Company, Philadelphia, 1994, pp 21–36
5. Sharma RC, Inuoe S, Roitelman J: Peptide transport by the multidrug resistance pump. J Biol Chem 267: 5731–5734, 1992
6. Valverde MA, Díaz M, Sepúlveda FV, Gill DR, Hyde SC, Higgins CF: Volume-regulated chloride channels associated with the human multidrug-resistance P-glycoprotein. Nature 355: 830–833, 1992
7. Altenberg GA, Vanoye CG, Han ES, Deitmer JW, Reuss L: Relationship between rhodamine 123 transport, cell volume, and ion-channel function of P-glycoprotein. J Biol Chem 269: 7145–7149, 1994
8. Bear CE: Drug transported by P-glycoprotein inhibits a 40pS outwardly rectifying chloride channel. Biochem Biophys Res Comm 200: 513–521, 1994
9. Hardy SP, Goodfellow HR, Valverde MA, Gill DR, Sepulveda FV, Higgins CF: Protein kinase C-mediated phosphorylation of the human multidrug resistance P-glycoprotein regulates cell volume-activated chloride channels. EMBO J 14: 68–75, 1995
10. Abraham EH, Prat AG, Gerweck L, Seneveratne T, Arceci R, Kramer R, Guidotti G, Cantiello HF: The multidrug resistance (mdrl) gene product functions as an ATP channel. Proc Natl Acad Sci USA 90: 312–316, 1993
11. Zhang JT, Ling, V: Study of membrane orientation and glycosylated extracellular loops of mouse P-glycoprotein by *in vitro* translation. J Biol Chem 266: 18224–18232, 1991
12. Zhang JT, Duthie M, Ling V: Membrane topology of the N-terminal half of the hamster P-glycoprotein molecule. J Biol Chem 268: 15101–15110, 1993
13. Skach WR, Calayag MC, Lingappa VR: Evidence for an alternate model of human P-glycoprotein structure and biogenesis. J Biol Chem 268: 6903–6908, 1993
14. Bibi E, Béjà O: Membrane topology of multidrug resistance protein expressed in *Escherichia coli*. J Biol Chem 269: 19910–19915, 1994
15. Skach, WR, Lingappa, VR: Transmembrane orientation and topogenesis of the third and fourth membrane-spanning regions of human P-glycoprotein (*MDR1*). Cancer Res 54: 3202–3209, 1994
16. Zhang JT, Lee CH, Duthie M, Ling V: Topological determinants of internal transmembrane segments in P-glycoprotein sequences. J Biol Chem 270: 1742–1746, 1995
17. Zhang JT, Ling V: Involvement of cytoplasmic factors regulating the membrane orientation of P-glycoprotein sequences. Biochemistry 34: 9159–9165, 1995
18. Kurjan J, Herskowitz I: Structure of a yeast pheromone gene (MFa): a putative α-factor precursor contains four tandem copies of mature α-factor. Cell 30: 933–943, 1982
19. Waters M.G, Blobel G: Secretory protein translocation in a yeast cell-free system can occur posttranslationally and requires ATP hydrolysis. J Cell Biol 102: 1543–1550, 1986
20. Rothblatt JA, Meyer DI: Secretion in yeast: translocation and glycosylation of prepro-α-factor *in vitro* can occur via an ATP-dependent post-translational mechanism. EMBO J 5: 1031–1036, 1986
21. Hansen W, Garcia PD, Walter P: *In vitro* protein translocation across the yeast endoplasmic reticulum: ATP-dependent post-translational translocation of the prepro-α-factor. Cell 45: 397–406, 1986
22. Simon SM, Blobel G: A protein-conducting channel in the endoplasmic reticulum. Cell 65: 371–380, 1991
23. Loo TW, Clarke DM: Membrane topology of a cysteine-less mutant of human P-glycoprotein. J Biol Chem 270: 843–848, 1995
24. Zhang M, Zhang JT: Evidence for the expression of multiple topologies of P-glycoprotein in multidrug resistant $CH^RB30$ cells. Proceedings of American Association for Cancer Research 36: 337a, 1995
25. Cheng SH, Gregory RJ, Marshall J, Paul S, Souza DW, White GA, O'Riordan CR, Smith AE: Defective intracellular transport and processing of CFTR is the molecular basis of most cystic fibrosis. Cell 63: 827–834, 1990
26. Thomas PJ, Shenbagamurthi P, Sondek J, Hullihen JM, Pedersen PL: The cystic fibrosis transmembrane conductance regulator: effects of the most common cystic fibrosis-causing mutation on the secondary structure and stability of a synthetic peptide. J Biol

Chem 267: 5727–5730, 1992
27. Dalemans W, Barbry P, Champigny G, Jallat S, Dott K, Dreyer D, Crystal RG, Pavirani A, Lecocq JP, Lazdunski M: Altered chloride ion channel kinetics associated with ΔF508 cystic fibrosis mutation. Nature 354: 526–528, 1991
28. Denning GM, Anderson MP, Amara JF, Marshall J, Smith AE, Welsh JJ: Processing of mutant CFTR (ΔF508) is temperature sensitive. Nature 358: 761–764, 1992
29. Drumm ML, Wilkinson DJ, Smit LS, Worrell RT, Strong TV, Frizzell RA, Dawson DC, Collins FS: Chloride conductance expressed by ΔF508 and other mutant CFTRs in *Xenopus* oocytes. Science 254: 1797–1799, 1991
30. Bates DA, Mackillop WJ: Hyperthermia, adriamycin transport, and cytotoxicity in drug-sensitive and -resistant Chinese hamster ovary cells. Cancer Res 46: 5477–5481, 1986
31. Loo TW, Clarke DM: Prolonged association of temperature-sensitive mutants of human P-glycoprotein with calnexin during biogenesis. J Biol Chem 269: 28683–28689, 1994
32. Hochachka PW, Somero GN: Strategies of biochemical adaptation. W.B. Saunders, Philadelphia, 1973, pp 180–181

# Topological Folding and Proteolysis Profile of P-glycoprotein in Membranes of Multidrug-Resistant Cells: Implications for the Drug-Transport Mechanism

**Mei Zhang, Guichun Wang, Adam Shapiro, and Jian-Ting Zhang**

Department of Physiology and Biophysics,
University of Texas Medical Branch, Galveston, Texas 77555-0641,
and British Columbia Cancer Center, 601 West 10th Avenue,
Vancouver, Canada V5Z 1L3

Biochemistry®

Reprinted from
Volume 35, Number 30, Pages 9728–9736

# Topological Folding and Proteolysis Profile of P-glycoprotein in Membranes of Multidrug-Resistant Cells: Implications for the Drug-Transport Mechanism†

Mei Zhang,‡ Guichun Wang,‡ Adam Shapiro,§ and Jian-Ting Zhang*,‡

*Department of Physiology and Biophysics, University of Texas Medical Branch, Galveston, Texas 77555-0641, and British Columbia Cancer Center, 601 West 10th Avenue, Vancouver, Canada V5Z 1L3*

*Received February 20, 1996; Revised Manuscript Received May 7, 1996*⊗

ABSTRACT: P-glycoprotein (Pgp)[1] is a polytopic membrane protein and functions as an energy-dependent drug efflux pump. It is responsible for multidrug resistance (MDR) in cancer cell lines. Recently, the topological structure of Pgp has been investigated. However, the results are in dispute. A major question concerning the Pgp topology is the membrane orientation of the loop linking TM4 and TM5 (loop 4) and the loop linking TM8 and TM9 (loop 8). In this study, we generated polyclonal antibodies specific to these two loops. In combination with a panel of other well-characterized site-specific polyclonal and monoclonal antibodies of Pgp, we tested the membrane orientation of these two loops of Pgp in multidrug-resistant cells using immunocytochemistry and proteolysis/membrane protection assay. Our results showed that (1) both loops 4 and 8 are located extracellularly whereas other domains, such as the ATP-binding sites, are in the cytoplasm and (2) proteolysis of Pgp is not a random event and the trypsin-sensitive sites are cleaved in orders. Since the Pgp was not genetically manipulated in this study, in contrast to previous studies, we believe that naturally expressed Pgp molecules have an unconventional topology. We speculate that this alternate topology of Pgp may represent a different functional state of the protein. Further detailed analysis of Pgp topology will help to understand the fundamental mechanism of drug transport by Pgp.

P-glycoprotein (Pgp)[1] is a polytopic plasma membrane protein with a molecular weight of 130−180 kDa (Gottesman & Pastan, 1993; Borst et al., 1993; Childs & Ling, 1994). Overexpression of Pgp causes multidrug resistance (MDR) which may be responsible for the failure of cancer chemotherapy. Pgp belongs to a superfamily of ATP-binding cassette (ABC) transporter (Higgins, 1992) or traffic ATPases (Doige & Ames, 1993) and is thought to function as a drug efflux pump supported by energy from ATP hydrolysis. Pgp has a broad spectrum of drug substrates including vinca alkaloids, anthracyclines, epidophyllotoxins, and antimicrotubule drugs.

Pgp consists of two homologous halves with each containing six putative transmembrane (TM) segments linked by loops of various lengths and a hydrophilic ATP-binding domain (Gottesman & Pastan, 1993; Childs & Ling, 1994). Epitope mapping and immunocytochemistry studies using monoclonal antibodies MRK16 (Georges et al., 1993), C219 (Kartner et al., 1985), and MM4.17 (Cianfriglia et al., 1994) have confirmed the cytoplasmic location of the ATP-binding domains and the extracellular location of the loop linking the putative TM1 and TM2 and the loop linking the putative TM7 and TM8. The extracellular location of the loop linking the putative TM1 and TM2 is also supported by studies using cell-free and frog oocyte expression systems (Zhang & Ling, 1991; Zhang et al., 1993; Skach & Lingappa, 1993). However, topologies of Pgp different from prediction have been observed in cell-free (Zhang & Ling, 1991; Zhang et al., 1993; Skach et al., 1993), *Xenopus* oocyte (Skach et al., 1993), and bacteria (Bibi & Béjà, 1994; Béjà & Bibi, 1995) expression systems. The major difference between the conventional and unconventional models is the membrane sidedness of loop 4 (between TM4 and TM5) and loop 8 (between TM8 and TM9).

In this study, we generated and used a panel of site-specific polyclonal and monoclonal antibodies to approach the topology of Pgp naturally expressed in MDR cells in an attempt to determine the membrane orientation of loop 4 and loop 8. Our results indicate that both loops 4 and 8 are detected on the outside of cells and, therefore, the unconventional topology of Pgp exists in the MDR cells.

## MATERIALS AND METHODS

*Materials.* Plasmid pGEM-4z and restriction enzymes were obtained from Promega and New England Biolabs. pGEX-3X, pGEX-2T, and glutathione-conjugated Sepharose 4B were purchased from Pharmacia. The ImmunoPure Ag/Ab immobilization kit was obtained from Pierce. Avidin, biotin, biotinylated anti-mouse IgG, biotinylated anti-rabbit IgG, and ExtrAvidin peroxidase were purchased from Vector. Thrombin, trypsin, 3,3′-diaminobenzidine tetrahydrochloride (DAB), Freund's adjuvant, FITC-conjugated anti-mouse and anti-rabbit IgG, normal mouse IgG, normal goat serum, and other chemicals were from Sigma Chemical Co.

*Cell Lines.* CHO cell line Aux B1, colchicine-selected multidrug-resistant subclone $CH^RB30$, and the vinblastine-selected multidrug-resistant human ovarian cancer cell line SKOV/VLB were gifts from Dr. Victor Ling. The CHO cell

† This work was supported by National Institutes of Health Grant CA 64539 and by a grant from the U.S. Army Research and Development Command.

* Corresponding author. Tel 409-772-3434; Fax 409-772-3381.
‡ University of Texas Medical Branch.
§ B.C. Cancer Center.

⊗ Abstract published in *Advance ACS Abstracts,* July 15, 1996.

[1] Abbreviations: Pgp, P-glycoprotein; MDR, multidrug resistance; ABC, ATP-binding cassette; mAb, monoclonal antibody; pAb, polyclonal antibody; TM, transmembrane; GST, glutathione *S*-transferase; A/M, acetone/methanol; PF, paraformaldehyde; Ag, antigen.

S0006-2960(96)00400-X CCC: $12.00 © 1996 American Chemical Society

lines were maintained in α-MEM medium containing 10% FCS. Colchicine was added to the media for the maintenance of drug-resistant $CH^RB30$ cells at a final concentration of 30 μg/mL. The SKOV/VLB cell line was maintained in α-MEM medium containing 15% FCS and 1 μg/mL vinblastine.

*Antibodies.* Monoclonal antibodies C219 and C494 were gifts from Dr. Victor Ling. The epitopes of these two antibodies have been mapped (Georges et al., 1990; also see Figure 1). Polyclonal antibody 5 from Dr. Susan B. Horwitz was generated against a synthetic peptide of loop 8 of mouse Pgp (Greenberger et al., 1991). Only 2 of the 19 amino acids in the synthetic peptides are different between mouse and human Pgp and apparently the pAb 5 reacts also with human Pgp. The mAb MM4.17 was a gift from Dr. Maurizio Cianfriglia, and its epitope has been mapped to loop 7 of Pgp (Cianfriglia et al., 1994). Monoclonal antibodies MD-1 and MD-7 were generated against purified hamster Pgp, and their epitopes have been mapped to 22 and 11 amino acid residues in the linker region and loop 8, respectively (Shapiro et al., 1996). These two mAbs have been shown to react with human Pgp.

*Construction of Fusion Protein Expression Plasmids.* A 200 bp *Nde*I−*Nde*I cDNA fragment was released from a full-length Chinese hamster *pgp1* cDNA (Endicott et al., 1991). It was separated and purified by electrophoresis on a 2% agarose gel and was then subcloned into the *Hin*cII site of pGEM-4z. By a sequential treatment of this recombinant DNA with *Nco*I, Klenow polymerase, and *Bam*HI, a cDNA fragment encoding loop 4 (the loop linking putative TM4 and TM5, amino acids 241−289) of Pgp was isolated and ligated between the *Bam*HI and *Sma*I sites of the pGEX-2T vector containing the GST (glutathione *S*-transferase) gene. The resultant plasmid was named pGST-PgpL4.

A cDNA fragment encoding loop 8 (the loop linking putative TM8 and TM9) of Pgp was made by the polymerase chain reaction (PCR) using oligonucleotides 5′-TGGAGAGATCCTCAC-3′ (from the Pgp sequence) and 5′-TAATACGACTCACTATAGGG-3′ (T7 promoter sequence) as sense and antisense primers, respectively, and Chinese hamster *pgp1* cDNA as template. The PCR product was treated with T4 DNA polymerase to blunt each end and purified before ligation into the *Hin*cII site of pGEM-4z. By digestion of this recombinant DNA with *Hin*dIII and *Hin*cII, a 200 bp cDNA fragment was isolated and treated with *Tru*9I and Klenow polymerase. The final *Hin*dIII-*Tru*9I cDNA fragment encoding amino acids 778−822 of Pgp was subcloned into the *Sma*I site of pGEX-3X to generate the plasmid pGST-PgpL8. Both pGST-PgpL4 and pGST-PgpL8 were sequenced to confirm the correct reading frame and to eliminate any potential mutations introduced by PCR.

*Generation and Purification of Fusion Proteins.* Two hundred milliliters of overnight cultures of *Escherichia coli* transformed with pGEX (−2T or −3X), pGST-PgpL4, or pGST-PgpL8 plasmids was added to 2 L of YT medium containing 2% glucose and 100 μg/mL ampicillin and grown at 37 °C to an $OD_{600}$ of 1−2. IPTG was then added to a final concentration of 0.1 mM, and the cells were allowed to grow for an additional 3 h at 37 °C before harvest by centrifugation (5600*g*) for 10 min at 4 °C. The cell pellet was resuspended in 100 mL of ice-cold PBS, and cells were then disrupted by sonication. Triton X-100 was added to cells harboring pGEX or pGST-PgpL4 plasmid to a final concentration of 1%, and the cell lysate was centrifuged (12000*g*) for 10 min at 4 °C. The supernatant was mixed with 2 mL of 50% glutathione-conjugated Sepharose 4B and incubated for 30 min at room temperature with shaking. The GST from the pGEX plasmid and the GST-L4 fusion protein from the pGST-PgpL4 were isolated by centrifugation at 500*g* for 30 s. The Sepharose pellet was washed 3 times with 15 mL of PBS each time before resuspension in 2 mL of PBS. To isolate the Pgp portion (Pgp-L4) from the GST-L4 fusion protein, the glutathione-conjugated Sepharose-absorbed fusion proteins were digested with 50 units of thrombin for 4 h while being shaken at room temperature. The Sepharose beads containing GST and the supernatant containing the released Pgp-L4 peptide were separated by centrifugation at 500*g* for 30 s. Because of formation of inclusion bodies in cells harboring pGST-PgpL8 plasmid, the disrupted cells after sonication were dissolved in sample buffer and subjected to a 12.5% SDS−PAGE. Fusion protein GST-L8 was visualized by Coomassie blue staining, excised, and purified by electroelution (Harlow & Lane, 1988).

*Generation and Purification of Antibodies.* Approximately 500 μg each of the purified Pgp-L4 peptide and GST-L8 fusion protein in complete Freund's adjuvant was injected subcutaneously into New Zealand white rabbits. One hundred fifty micrograms of purified proteins in incomplete Freund's adjuvant was injected as first boost 30 days after the initial injection, and sera were collected 2−4 times in 1 month 7 days after each boost. These antisera were named αPgp-L4 and αPgp-L8, respectively. Preimmune sera were collected as control before all above steps were taken.

Affinity purification of the antisera was performed using an ImmunoPure Ag/Ab immobilization kit from Pierce following the supplier's instructions. Briefly, 2 mg of Pgp-L4 peptide or GST-L8 fusion protein was added to an Ag immobilization column and conjugated to an activated affinity chromatography gel after incubation at room temperature for 8 h. The column was then washed excessively with PBS before 1 mL of relevant crude antiserum was applied to the column and maintained at room temperature for 1 h. The affinity-bound antibodies were eluted with 0.1 M glycine (pH 2.8), immediately neutralized with 1 M Tris-HCl (pH 9.5), and concentrated by using a Centricon filtration unit (Amicon).

*Confocal Fluorescence Microscopy.* Parental Aux B1 and MDR $CH^RB30$ cells grown on a cover glass for 2 days were washed in TBS (10 mM Tris-HCl, pH 7.4, 0.9% NaCl) and fixed/permeabilized in acetone/methanol (50:50) for 5 min at room temperature. Following three washes with TBS, the cells were blocked by 10% skim milk in TBS for 2 h and then incubated with mAb C219 (1 μg/mL), affinity-purified αPgp-L4 (1:2000 dilution) or affinity-purified αPgp-L8 (1:1000 dilution) in TBS containing 1% skim milk for 2 h at room temperature. After three washes with TBS, the cells were incubated with either FITC-conjugated anti-mouse IgG (for mAb C219) or anti-rabbit IgG (for αPgp-L4 or αPgp-L8) for 30 min at room temperature. The fluorescence was detected with an Odyssey digital video confocal laser imaging system (Noram Instruments) coupled to a Nikon inverted microscope. Fluorescence was detected at 515 nm using an excitation of 488 nm.

*Immunocytochemical Staining.* $CH^RB30$ cells were grown overnight or for 2 days on a cover glass and were then fixed

and permeabilized with acetone/methanol (50:50) at 4 °C for 10 min or only fixed with 4% paraformaldehyde. After several washes with PBS, endogenous peroxidase and biotin-like activities were blocked by pretreatment with $H_2O_2$ and avidin/biotin, respectively. The fixed cells were then labeled with primary antibodies C219, affinity-purified αPgp-L4, or affinity-purified αPgp-L8, followed by biotinylated anti-mouse IgG or anti-rabbit IgG. The final staining with ExtrAvidin peroxidase and DAB was performed as described by Georges et al. (1990). For competition studies, the primary antibodies were incubated for 2 h with an excess amount of the C219 epitope peptide, purified Pgp-L4 peptide, or GST-PgpL4 fusion protein before being used for labeling cells. The labeled cells were counterstained with hematoxylin and mounted with Permount for visualization.

*Proteolysis/Membrane Protection Assay.* Membranes were isolated from $CH^RB30$, SKOV/VLB, and BC19/3 cells according to the method described previously by Riordan and Ling (1979). Sealed inside-out vesicles were prepared according to the procedure by Steck and Kant (1974). Briefly, 1 mg of crude membranes was diluted into 10 mL of 0.5 mM sodium phosphate buffer, pH 8.2 (PB). After 3 h of incubation on ice, the membranes were pelleted at 28000*g* for 30 min. The membrane pellet was then resuspended in 1 mL of PB buffer by using a 25 gauge needle and a 1 mL syringe. The membrane orientation was determined as described previously (Bender et al., 1971). Using this procedure, the sealed membrane vesicles isolated from both SKOV/VLB and BC19/3 cells are all inside out.

Trypsin digestion of 10 μg of inside-out membrane vesicles was performed at different conditions. After incubation of membrane with 0.2 μg (for 15 min), 0.2 μg (for 30 min), 3 μg (for 2 h), or 6 μg (for 2 h) of trypsin at 37 °C, the reaction was stopped by addition of PMSF to a final concentration of 10 mM and the membrane fraction was separated from trypsin by microcentrifugation at 4 °C. The final membrane pellet was immediately solubilized in SDS−PAGE sample buffer and used for electrophoresis.

*Characterization of the Orientation of Membrane Vesicles.* The membrane vesicle orientation was determined using marker enzyme acetylcholinesterase and $Na^+/K^+$-ATPase as described previously (Bender et al., 1971; Chifflet et al., 1988; Doige et al., 1992). Briefly, acetylcholinesterase activity was determined by incubating the sealed membrane vesicles (50 μg of protein) in the absence or presence of 0.1% Triton X-100 with 0.78 μM acetylthiocholine chloride and 0.625 mM DTNB [5,5′-dithiobis(2-nitrobenzoic acid)] in TBS containing 0.25 M sucrose. The reaction was performed at 37 °C for 20 min and stopped by addition of 10% SDS. Absorption at 412 nm wavelength was measured on a Shimatzu UV-160 spectrophotometer. The activity was calculated using purified acetylcholinesterase (Sigma) as standard. The $Na^+/K^+$-ATPase activity was determined by incubating 12 μg of membrane proteins in the absence or presence of 1 mM ouabain in the assay buffer (10 mM Tris-HCl, pH 7.4, 100 mM NaCl, 10 mM KCl, 3 mM $MgCl_2$, 0.02% $NaN_3$, 2 mM ATP). After 20 min of incubation at 37 °C, the reaction was stopped by addition of an equal volume of 6% SDS/3% ascorbate/0.5% ammonium molybdate in 0.5 M HCl. Products were stabilized by addition of the same volume of 2% sodium citrate/2% sodium arsenite/2% acetic acid. The absorption at 850 nm was measured on a Shimatzu UV-160 spectrophotometer. The activity was calculated according to Chifflet et al. (1988). The ouabain-sensitive ATPase activity reflects the $Na^+/K^+$-ATPase activity.

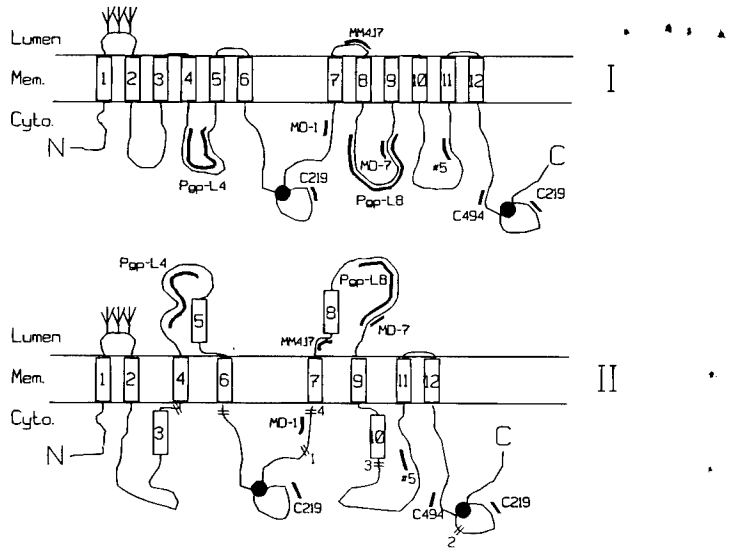


FIGURE 1: Topology of P-glycoprotein and positions of antibody epitopes. The model I structure is predicted on the basis of the hydropathy plot analysis of the amino acid sequence. The model II structure is one example of the alternate topologies observed with Pgp expressed in a heterologous expression system. The branched symbols indicate oligosaccharide chains. The solid circle represents the ATP-binding domain. The thick lines denote the relative positions of antibody epitopes. The symbol (=) indicates the trypsin cleavage sites deduced from Figure 5.

*Western Blot Analysis.* Purified fusion proteins or Pgp-L4 peptides and crude membranes isolated from MDR cells were subjected to SDS−PAGE. The fractionated proteins were then transferred to a PVDF membrane and probed with primary antibodies (mAb C219, C494, MD-1, and MD-7 at 1 μg/mL, MM4.17 at 2 μg/mL, pAb αPgp-L4 at 1:2000 dilution, αPgp-L8 at 1:1000 dilution, and antibody 5 at 1:1000) followed by a secondary antibody (peroxidase-conjugated anti-mouse IgG or anti-rabbit IgG at 1:2500 dilution) and detected by enhanced chemiluminescence using an ECL detection kit (Amersham). To strip the blot for reprobing, the blot was incubated at 50 °C in stripping buffer (62.5 mM Tris-HCl, pH 6.7, 100 mM β-mercaptoethanol, 2% SDS) for 25 min and washed in TBS 2 × 10 min at room temperature. The blot was then used for reprobing.

## RESULTS

*Both Polyclonal Antibodies αPgp-L4 and αPgp-L8 React with Pgp on Western Blot.* In the unconventional topology of Pgp, the loop linking TM4 and TM5 (loop 4) and the loop linking TM8 and TM9 (loop 8) are extracellular (model II, Figure 1). However, these two loops are intracellular in the conventional or predicted topology (model I, Figure 1). To determine the membrane orientation of these two loops in MDR cells, we generated site-specific polyclonal antibodies to these loops using fusion proteins as immunogens (see Materials and Methods). These two pAbs were named αPgp-L4 and αPgp-L8. Using Western blot analysis, both antibodies specifically reacted with their immunogen and no cross-reaction was detected (data not shown). To determine the specificity of αPgp-L4 and αPgp-L8 to Pgp, crude membranes were isolated from parental Aux B1 and multidrug-resistant $CH^RB30$ cells, and Pgp was separated on an SDS−PAGE. Figure 2 shows a Western blot of crude

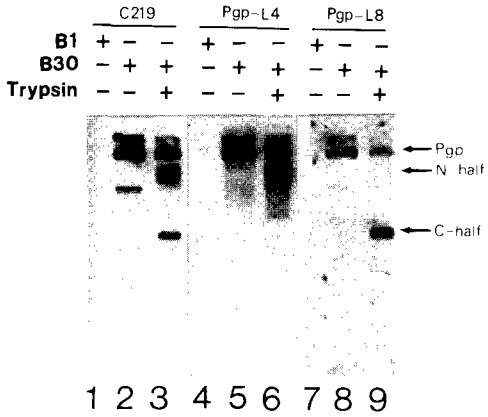


FIGURE 2: Characterization of the specificity of αPGp-L4 and αPgp-L8 antibodies to P-glycoprotein on CH$^R$B30 cells. Crude membranes were isolated from parental Aux B1 (lanes 1, 4, and 7) and multidrug resistant CH$^R$B30 cells (lanes 2, 5, and 8) and were used for Western blot analysis (10 μg of proteins in each lane). Monoclonal antibody C219 as well as the polyclonal antibodies αPgp-L4 and αPgp-L8 specifically detected the 180 kDa Pgp and its aggregated and degraded products (lanes 2, 5, and 8). No protein from Aux B1 cells was detected by any of these antibodies. After limited trypsin digestion (10 μg of protein was digested using 0.2 μg of trypsin for 30 min at 37 °C), Pgp from CH$^R$30 cells was cleaved into N- and C-terminal half fragments as detected by C219 (lane 3). As expected, only the N-half fragment was recognized by αPgp-L4 (lane 6) whereas the C-half was recognized by αPgp-L8 (lane 9). Lanes 3, 6, and 9 contains 6 μg of proteins.

membranes detected by monoclonal antibody (mAb) C219 as well as pAb αPgp-L4 and αPgp-L8. The mAb C219 (lane 2, Figure 2), pAb αPgp-L4 (lane 5, Figure 2), and pAb αPgp-L8 (lane 8, Figure 2) specifically detected a 180 kDa protein. This protein was not detected in the sensitive Aux B1 cells (lanes 1, 4, and 7, Figure 2). Endoglycosidase treatment reduced the size of the protein detected by these antibodies (data not shown), indicating that it is a glycoprotein. Additional bands of higher and lower molecular weight detected by these antibodies represent the aggregated and degraded products of Pgp.

*αPgp-L4 and αPgp-L8 React with N- and C-Terminal Half Molecules of Pgp, Respectively.* Previously, it has been shown that Pgp isolated from multidrug-resistant CH$^R$B30 cells can be cleaved into two halves with limited proteolysis using trypsin, and both halves react with the mAb C219 (Georges et al., 1991). To determine whether pAb αPgp-L4 and αPgp-L8 specifically react with N- and C-terminal halves of Pgp, respectively, we performed a limited trypsin digestion to cleave Pgp into two separate halves. As shown in Figure 2, both halves of Pgp react with the mAb C219 (lane 3, Figure 2). However, as expected, the pAb αPgp-L4 reacted only with the N-terminal half (lane 6, Figure 2), while the pAb αPgp-L8 reacted only with the C-terminal half (lane 9, Figure 2) of Pgp. Therefore, we conclude that we have generated site-specific pAb to putative loops 4 and 8 of Pgp.

*Both αPgp-L4 and αPgp-L8 React Predominantly with the Plasma Membranes of CH$^R$B30 Cells.* To confirm whether pAb αPgp-L4 and αPgp-L8 specifically detect Pgp on plasma membranes, we labeled fixed and permeabilized CH$^R$B30 cells with mAb C219, pAb αPgp-L4, and αPgp-L8. The binding was detected with FITC-conjugated secondary antibodies using confocal fluorescence microscopy (see Materials and Methods). As shown in Figure 3, mAb C219 (panel A), as well as pAb αPgp-L4 (panel C) and

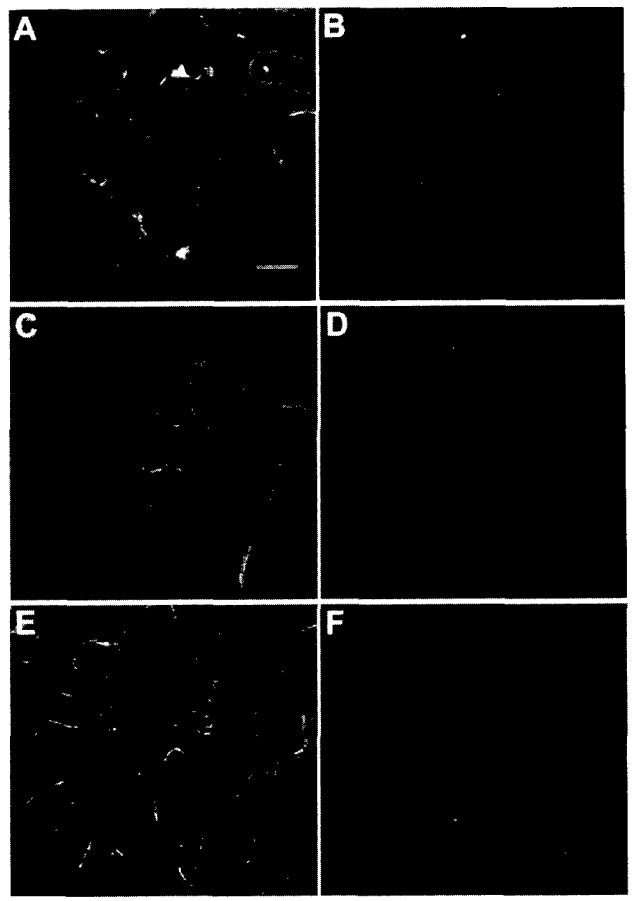


FIGURE 3: Immunofluorescence labeling of CH$^R$B30 cells using αPgp-L4 and αPgp-L8. Multidrug-resistant CH$^R$B30 cells were fixed and permeabilized with acetone/methanol and labeled with mAb C219 (panel A), pAb αPgp-L4 (panel C), or pAb αPgp-L8 (panel E). The labeling was detected using FITC-conjugated secondary antibodies and observed by confocal fluorescence microscopy. In the controls, cells were labeled using normal mouse IgG (panel B) and preimmune sera of αPgp-L4 (panel D) and αPgp-L8 (panel F). All three antibodies labeled predominantly on the plasma membranes. The bar in panel A denotes 10 μm. All photographs were taken with the same magnification.

αPgp-L8 (panel E) stained predominantly the plasma membrane of CH$^R$B30 cells. No signal was detected on plasma membranes in control experiments with either normal mouse IgG (panel B) or preimmune sera of αPgp-L4 (panel D) or αPgp-L8 (panel F). Under the same condition, no staining was observed with the parental Aux B1 cells (data not shown), consistent with the results on Western blot shown in Figure 2. These results indicate that the pAb αPgp-L4 and αPgp-L8 specifically react with Pgp both on Western blot and in plasma membranes of whole cells.

*Immunocytochemical Staining.* To investigate the membrane sidedness of loops 4 and 8 of Pgp in plasma membranes, we performed indirect whole-cell staining with the pAb αPgp-L4, αPgp-L8, and mAb C219 in permeabilized and nonpermeabilized conditions (see Materials and Methods). CH$^R$B30 cells were first fixed and permeabilized with acetone/methanol (A/M) or only fixed with paraformaldehyde (PF) and then probed with C219, αPgp-L4, or αPgp-L8. The secondary antibodies were biotinylated goat anti-mouse or goat anti-rabbit IgG. The staining was performed using ExtrAvidin peroxidase and DAB. As shown in Figure 4, specific staining of fixed and permeabilized (A/M) CH$^R$B30 cells was observed with mAb C219 (panel D), as well as

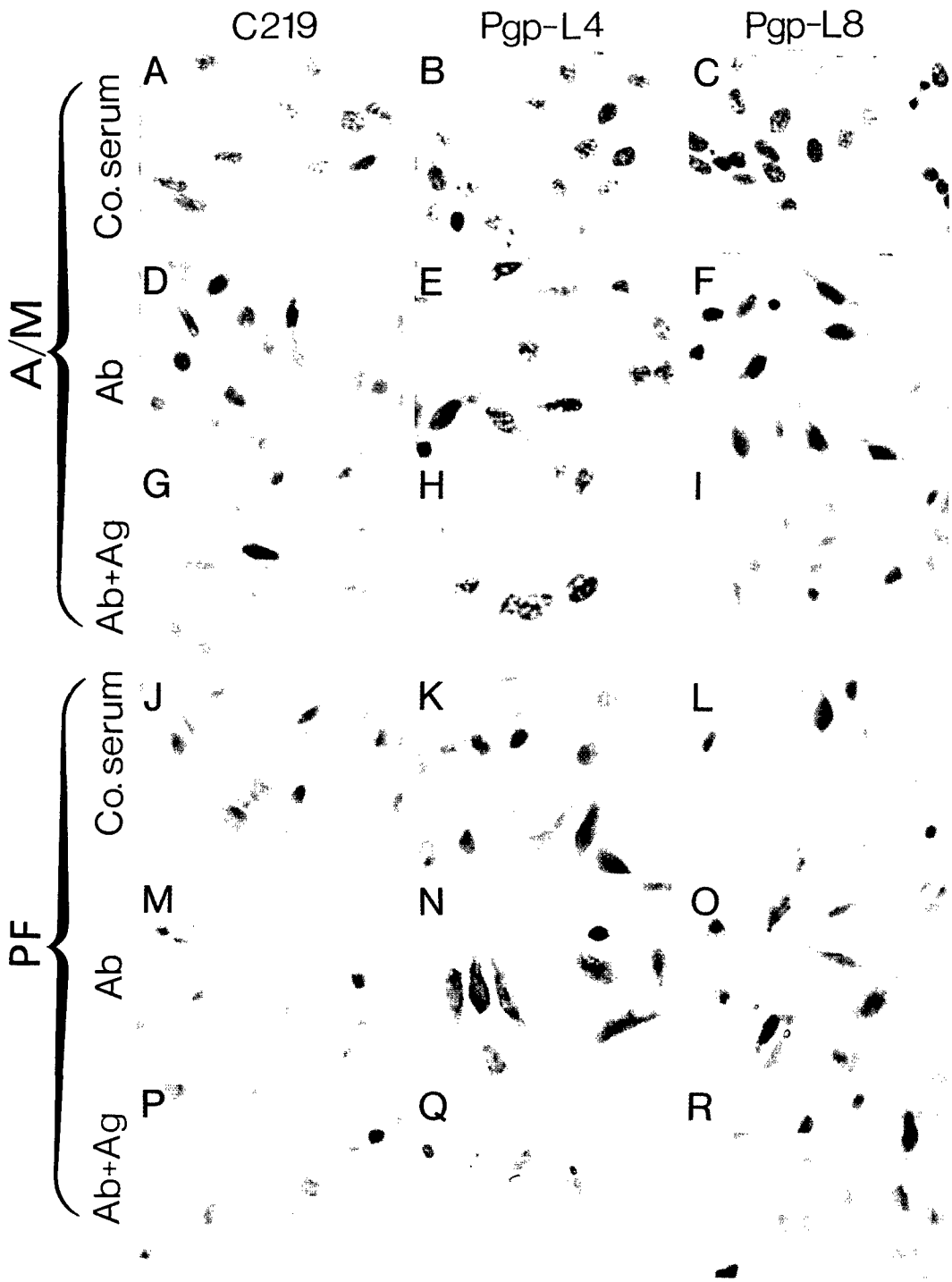


FIGURE 4: Immunocytochemistry staining of multidrug-resistant $CH^RB30$ cells with αPgp-L4 and αPgp-L8. $CH^RB30$ cells were grown on a cover glass and fixed and permeabilized with acetone/methanol (panels A–I) or only fixed with paraformaldehyde (panels J–R). The fixed cells were probed with either C219 (panels D, G, M, P), αPgp-L4 (panels E, H, N, Q), or αPgp-L8 (panels F, I, O, R). Normal mouse IgG (panels A and J), preimmune sera of αPgp-L4 (panels B and K), and αPgp-L8 (panels C and I) were used as controls at the same concentration as the antibodies. C219-epitope peptide analog (panels G and P), purified Pgp-L4 peptide (panels H and Q), or GST-L8 fusion proteins (panels I and R) were used to compete the Pgp-specific bindings of mAb C219, pAb αPgp-L4, and pAb αPgp-L8, respectively. Nuclei were stained using hematoxylin. A/M = acetone/methanol fixed; PF = paraformaldehyde fixed; Ab = antibodies; Ab + Ag = antibody preincubated with antigen; Co. serum = control IgG or preimmune serum.

pAb αPgp-L4 (panel E) and αPgp-L8 (panel F). The pAb αPgp-L4 and αPgp-L8 were also able to stain the nonpermeabilized (PF) cells (panels N and O). Monoclonal antibody C219, on the other hand, did not stain the nonpermeabilized cells (panel M), consistent with the intracellular location of the C219 epitope. This is further supported by the observation that mAb C219 stained the paraformaldehyde-fixed cells after permeabilization with Triton X-100 (data not shown). Normal mouse IgG (panels A and J), preimmune sera of pAb αPgp-L4 (panels B and K), and pAb αPgp-L8 (panels C and L) did not stain the cells fixed with acetone/methanol (panels A–C) or with paraformaldehyde (panels J–L). It should be noted that the staining of intact cells with pAb αPgp-L8 (panel O) was lower than that of the permeabilized cells. This suggests that loop 8 may be partially buried in the plasma membrane or it may exist in both extracellular and cytoplasmic locations (see Discussion).

Table 1: Activity of Marker Enzymes in Membrane Vesicles of SKOV/VLB Cells

| | enzyme activity (nmol $mg^{-1}$ $min^{-1}$) | |
|---|---|---|
| detergent[a] | − | + |
| acetylcholinesterase | 0.00 (3) | 2.07 ± 0.29 (3) |
| $Na^+/K^+$-ATPase | 10.4 ± 0.88 (3) | 11 ± 2.5 (3) |

[a] 0.1% Triton X-100 was used for the assay of total acetylcholinesterase activity (extracellular marker), and 0.8 mM CHAPS was used for the assay of total $Na^+/K^+$-ATPase activity (cytoplasmic marker). Activity measured in the presence of detergent represents the total activity derived from both inside-out and outside-out vesicles. Acetylcholinesterase was detected only when the vesicles were permeabilized whereas the $Na^+/K^+$-ATPase activity was detected in the intact vesicles. $n = 3$.

To determine the cell-labeling specificity to Pgp with mAb C219, pAb αPgp-L4, and αPgp-L8, we stained cells with these antibodies in the presence of excess amounts of the C219 epitope peptide (panels G and P), purified PgpL4 peptide (panels H and Q), and GST-PgpL8 fusion proteins (panels I and R), respectively (Ab + Ag). As shown in Figure 4, the preincubation prevented the staining of $CH^R$-B30 cells, suggesting that the staining is specific for Pgp. However, the nonrelevant peptide antigens did not block the antibody binding (data not shown). Together, the above immunocytochemical results suggest that the epitopes for mAb C219 are located inside cells whereas the epitopes for pAb αPgp-L4 and αPgp-L8 can be detected extracellularly.

*Loop 8 of Pgp in Inside-Out Membrane Vesicles Is Resistant to Trypsin Digestion.* To confirm that loops 4 and 8 of Pgp in MDR cells were located extracellularly, we performed proteolysis/membrane protection assay and Western blot of isolated membrane vesicles. We used the human multidrug-resistant SKOV/VLB cells (Bradley et al., 1989), from which all vesicles isolated are inside out (Table 1) as determined using acetylcholinesterase (extracellular marker). This is confirmed by another marker $Na^+/K^+$-ATPase (cytoplasmic side marker) (Table 1). Meanwhile, we obtained a mAb MD-7 which has an epitope in loop 8 (Shapiro et al., 1996). Furthermore, an advantage for using human MDR cells is that more site-specific antibodies are available and they can be used as controls in the proteolysis study (see Figure 1 for locations in Pgp of each antibody epitope used in this study).

Figure 5A shows the trypsin digestion profile of Pgp detected by the mAb MD-7. Under mild conditions, peptides indicated as C (C-half) were detected (lanes 2 and 3, Figure 5A). More extensive trypsin digestion generated smaller fragments labeled as X, Y, and Z, respectively (lanes 4 and 5, Figure 5A). All these fragments were presumably derived from the C-half molecule with the epitope for the mAb MD-7. The smallest trypsin-resistant fragment detected by the mAb MD-7 has an apparent molecular mass of 17 kDa (peptide Z). It is possible that the generation of these fragments represents the progressive digestion of the C-terminal half molecule of Pgp and peptide Z represents the minimum membrane-protected fragment containing loop 8 with the mAb MD-7 epitope.

To determine the likelihood of the above possibility, we stripped the same blot and probed it with other mAbs or site-specific pAbs. Figure 5B shows the same blot from Figure 5A probed with the mAb C219. Only two peptide fragments indicated as N and C were detected by C219 (lanes 2−5, Figure 5B). Peptide N did not react with the mAb MD-7 and represents the N-terminal half molecule (lanes 2−5, Figure 5A; see also Figure 2). The mAb C494, on the other hand, detected peptide C (lanes 2−5, Figure 5C). Together, these results suggest that peptides N and C represent the N- and C-terminal half molecules, respectively. These results are consistent with the previous studies which showed that the mAb C219 has two epitopes, one in each ATP-binding domain, and the mAb C494 has only one epitope in the C-terminal half molecule (Georges et al., 1990) and Pgp can be cleaved into two halves by trypsin (Georges et al., 1991; see Figure 1 for cleavage site 1).

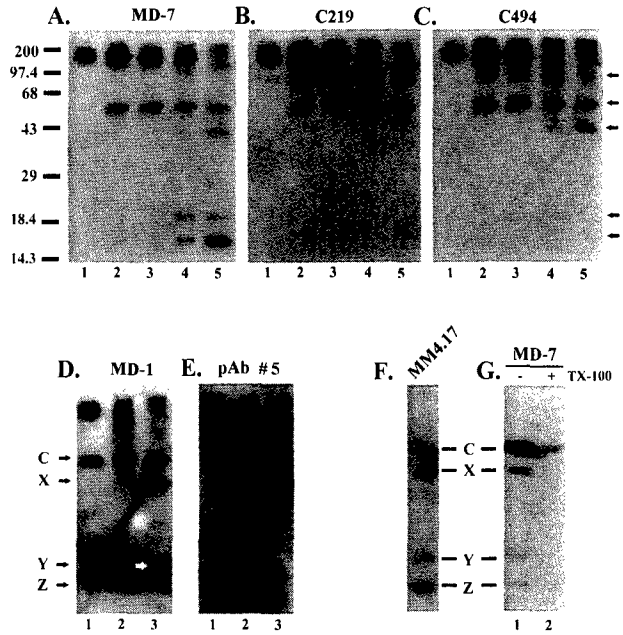


FIGURE 5: Proteolysis profile of P-glycoprotein. (A−C) Trypsin cleavage profile of human P-glycoprotein. 10 μg of SKOV/VLB cell membranes was incubated in the presence of 0.2 μg (lanes 2 and 3), 3 μg (lane 4), and 6 μg (lane 5) of trypsin at 37 °C. The reaction duration was 15 min (lane 2), 30 min (lane 3), and 2 h (lanes 4 and 5), respectively. Lane 1 is a control of 3 μg of undigested SKOV/VLB cell membranes. Panels A−C are the same blot probed with different antibodies. A = MD-7, B = C219, and C = C494. (D and E) Panels D and E are the same blot as in panels A−C, but only the corresponding lanes 3−5 were shown. D = MD-1 and E = pAb 5. Separate experiments have also been performed with MD-1 and pAb 5, and the results are consistent with the data shown here. However, to be consistent with the panels A, B, and C, only the stripped blot was shown. (F) 10 μg of SKOV/VLB cell membranes was incubated in the presence of 3 μg of trypsin at 37 °C for 2 h (same as lane 4, panel A). The blot was probed with MM4.17. (G) 10 μg of SKOV/VLB cell membranes was incubated in the presence of 3 μg of trypsin at 37 °C for 2 h (same as in lane 4, panel A) in the absence (lane 1) or presence (lane 2) of 1% Triton X-100. The blot was probed by MD-7.

In addition to peptide C, the mAb C494 also reacted with peptide X (lanes 4 and 5, Figure 5C) which was not detected by the mAb C219 (lanes 4 and 5, Figure 5B). This peptide is likely a further degradation product from peptide C. Thus, after Pgp was cleaved into two halves, the C-terminal half molecule was further digested and the ATP-binding domain containing the mAb C219 epitope was removed, resulting in peptide X (see Figure 1 for cleavage site 2). However, the C494 epitope is still attached to the truncated C-terminal half molecule (peptide X). Both the mAb C219 and C494 did not react with peptides Y and Z, suggesting that these two peptides are further degradation products and have lost epitopes for both C219 and C494.

To determine whether peptide Z contains the linker region and loop 10, we probed the same stripped blot again with a mAb MD-1 (Shapiro et al., 1996) and a site-specific pAb 5 (Greenberger et al., 1991). As shown in Figure 1, the mAb MD-1 is specific to the linker region whereas the epitope for the pAb 5 is in loop 10. Both antibodies are specific to the C-terminal half molecule as shown by their reactivity with peptide C but not peptide N (lanes 1 and 2 in Figure 5D,E). Both antibodies also reacted with peptide X (lanes 2 and 3 in Figure 5D,E), suggesting that peptide X still contains the epitope for both antibodies. The mAb MD-1 detected, in addition, peptide Y (lane 3, Figure 5D) which, however, was not detected by the pAb 5 (lane 3, Figure 5E). Therefore, peptide Y lost the epitope for the pAb 5 but still retains the epitope for the mAb MD-1. The mAb MD-1, however, did not detect peptide Z, albeit the amount of peptide Z is higher than peptide Y (compare lane 5 in Figure 5A with lane 3 in Figure 5D). Peptides Y and Z are still on the membrane after stripping as determined using MD-7 (data not shown). These results suggest that peptide Z is a final trypsin-resistant fragment which only retains the epitope for the mAb MD-7 and does not contain the epitopes for the mAbs C219, C494, and MD-1 nor the site-specific pAb 5 (see model II in Figure 1).

To prove that peptide Z also contains loop 7 (linking TM7 and TM8) in addition to loop 8 (linking TM8 and TM9), we probed the digested products with another mAb MM4.17 of which the epitope is in loop 7 (Cianfriglia et al., 1994). As expected, the mAb MM4.17 reacted with all the peptides C, X, Y, and Z (Figure 5F). To confirm that the trypsin resistance of peptide Z was due to membrane protection, we performed a digestion in the presence of Triton X-100 to permeabilize the membrane. As shown in Figure 5G, the trypsin-resistant peptide Z was produced in the absence of Triton X-100 (lane 1, Figure 5G) but was completely digested in the presence of Triton X-100 (lane 2, Figure 5G). The above results showed that the domain containing loop 7 and loop 8 (with mAb MM4.17 and MD-7 epitopes) in inside-out vesicles is resistant to trypsin digestion whereas loop 10 (linking TM10 and TM11 with pAb 5 epitope) and the C-terminal ATP-binding domain (containing mAb C219 and C494 epitopes) are sensitive to trypsin digestion. Thus, the segment containing both loop 7 and loop 8 is likely located in the lumen of the isolated inside-out membrane vesicles (extracellular location), consistent with the model II structure in Figure 1.

*The Trypsin-Resistant Fragment Z Is Also Observed from a Cell Transfected with Human MDR1 cDNA.* To determine whether the trypsin-resistant fragment Z was due to the overexpression of Pgp in the multidrug-resistant SKOV/VLB cells, we took use of cells transfected with the human *MDR1* Pgp cDNA (BC19/3 cells). The Pgp level expressed in BC19/3 cells is less than 10% of Pgp expressed in the SKOV/VLB cells (unpublished observation). Using the same procedure, the vesicles isolated from BC19/3 cells are also all inside out as determined using acetylcholinesterase (data not shown). Trypsin digestion of the inside-out membrane vesicles from BC19/3 cells was performed. The digested fragments were subjected to a Western blot and probed with the mAb MD-7. As shown in Figure 6A, peptides C, X, Y, and Z were all detected. Therefore, generation of the trypsin-resistant fragment Z of Pgp in MDR cells is not related to the high expression levels of Pgp. Peptides C, X, Y, and Z were not detected when membranes from sensitive parental cell lines were digested by trypsin (data not shown). This result rules out the possibility that these peptides were generated from digestion of non-Pgp proteins.

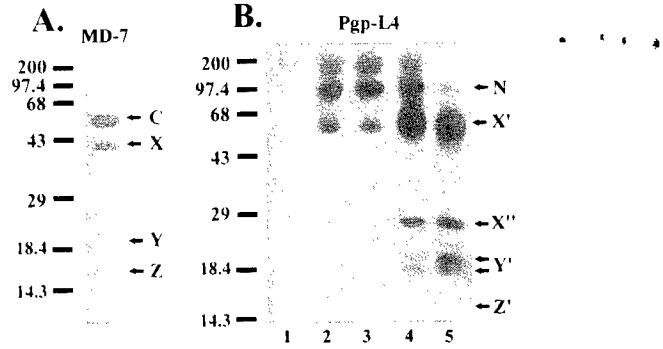


FIGURE 6: (A) Trypsin digestion of BC19/3 cell membranes. 20 $\mu$g of BC19/3 cell membranes was digested with 3 $\mu$g of trypsin at 37 °C for 2 h (same condition as in lane 4, Figure 5A). The blot was probed with the mAb MD-7. (B) Membrane protection of loop 4. The same blot from Figure 5A–C (membranes from the SKOV/VLB cells) was stripped and probed with the pAb αPgp-L4. The minimum peptide fragment Z′ is the protected loop 4 of Pgp.

*Loop 4 of Human Pgp in Inside-Out Membrane Vesicles Is Protected from Trypsin Digestion.* To determine whether the loop linking the putative TM4 and TM5 (loop 4) is also resistant to trypsin digestion in inside-out vesicles of MDR cells (SKOV/VLB), we again stripped the blot shown in Figure 5A and probed it with the pAb αPgp-L4. This antibody specifically detected peptide N (lanes 2–5, Figure 6B; see also Figure 2). In addition, further digested products X′, X″, Y′ (a doublet), and Z′ were also detected (lanes 4 and 5, Figure 6B). Peptide Z′, with an apparent molecular mass of 14.5 kDa, is the smallest trypsin-resistant fragment from the N-terminal half molecule. It presumably represents the membrane-protected fragment containing loop 4 with the epitope for the pAb αPgp-L4 whereas peptides X′, X″, and Y′ are incompletely digested products of peptide Z′. In the presence of Triton X-100, these peptides were also completely digested (data not shown). Therefore, by analogy to the study of loop 8 in the C-terminal half, it is likely that loop 4 of Pgp is also located in the lumen of the inside-out membrane vesicles (extracellular location) as shown in the model II structure in Figure 1.

## DISCUSSION

In this study, two site-specific polyclonal antibodies were produced and were used in combination with a panel of other site-specific pAbs and mAbs to show that Pgp molecules in MDR cells have the unconventional topology. Using immunocytochemistry and proteolysis/membrane protection assay, we were able to show that both loops 4 and 8 of Pgp in MDR cells can be detected extracellularly. Our results are consistent with the expression of an unconventional topology of Pgp (see Figure 1). In this study, the Pgp sequence was not altered by cDNA manipulation. We, therefore, believe that the naturally expressed Pgp has an unconventional topology. Loops 3 and 9 of Pgp are also on different sides of the membrane in the model I and model II topology of Pgp, respectively (see Figure 1). However, antibodies against these two loops were not produced to analyze their membrane sidedness due to their short length (2–6 amino acids).

We also showed that Pgp has specific trypsin-sensitive sites. That the Pgp molecule was first cleaved into two halves suggests that a domain prior to amino acid residues 669−690 (MD-1 epitope in human Pgp) linking the N- and C-terminal half Pgp is exposed and its access to trypsin is not hindered by the two bulky cytoplasmic ATP-binding domains (Figure 1). However, other trypsin-sensitive sites in the cytoplasmic loops (e.g., loop 10) are presumably buried and accessible to trypsin only when the ATP-binding domains are removed by digestion. As shown in Figure 1, other detectable trypsin cleavage sites in the C-terminal half molecule are at the ATP-binding domain and loop 10. Further work is required to identify each trypsin cleavage site. Although it is possible that loop 8 linking TM8 and TM9 is intrinsically resistant to proteolysis, we think this possibility is highly unlikely. First, loop 8 of human Pgp contains 10 Arg or Lys residues in the loop of 55 amino acids. It is unlikely that all the Arg and Lys residues are buried by the folding of this relatively small loop. Second, other predicted cytoplasmic domains including loop 10 containing the pAb 5 epitope and the large cytoplasmic ATP-binding domain are both completely digested by trypsin. Third, loop 8 was colocalized with loop 7 in the same trypsin-resistant peptide fragment and was detectable on the extracellular surface.

Different unconventional topologies have been described by Zhang and Ling (1991), Skach et al. (1993), and Bibi and Béjà (1994), respectively. However, the common feature between all the unconventional topologies is that the loop linking TM8 and TM9 is extracellular, different from the predicted conventional topology. In this study, we have shown that loop 8 can be detected on the outside of cells, consistent with the previous studies using heterologous expression systems. The estimated size of the trypsin-resistant fragments is consistent with one of the unconventional model (Figure 1) proposed previously (Zhang et al., 1993). However, from this study, we cannot rule out the possibility that the predicted topology (model I, Figure 1) is also expressed in the MDR cells. In fact, more staining using pAb αPgp-L8 was observed when cells were permeabilized (Figure 4), suggesting that loop 8 is also located intracellularly. It is worth noting that expression of more than one topology has been observed with prion protein (Lopez et al., 1990), ductin (Alves et al., 1993), bile acid transporter (Dunlop et al., 1995), and hepatitis B virus envelope proteins (Prange & Streeck, 1995).

The estimated molecular masses of the protease-resistant fragments Z (17 kDa) and Z′ (14.5 kDa) are 2 kDa smaller than the ones (19 and 16.5 kDa, respectively) predicted on the basis of amino acid sequence and the unconventional topology in inside-out vesicles shown in Figure 1. This is probably due to the high hydrophobicity of these peptides each containing three to four putative transmembrane segments. High hydrophobicity will cause more binding of SDS and therefore results in a faster mobility on SDS−PAGE. However, due to the anonymous mobility of peptide fragments on SDS−PAGE, the unconventional topologies of Pgp as proposed by Skach et al. (1993) and by Béjà and Bibi (1995) cannot be ruled out.

Recently, Kast et al. (1995) examined the topology of mouse *mdr3* Pgp using epitope insertion and confirmed the extracellular location of putative loops 1 and 5 and the intracellular location of putative loops 2 and 6. This is consistent with both model I and model II structures shown in Figure 1. Unfortunately, the membrane sidedness of the loop linking putative TM3 and TM4 and the loop linking putative TM4 and TM5 was not examined by these authors (see discussion below). The topology of human *MDR1* Pgp has also been examined by expression of cysteine-less mutant Pgp in mammalian cells, and only the predicted topology (model I, Figure 1) was detected (Loo & Clarke, 1995). The discrepancy between these studies is currently not known. However, it may be due to the different expression systems used. It has been observed that cytoplasmic proteins expressed in different systems are involved in the regulation of topology formation of hamster Pgp (Zhang & Ling, 1995). Expression of the homologous cytoplasmic proteins in different mammalian cells may make a difference in the topological formation of Pgp. It is also possible that both the conventional and unconventional topologies of Pgp exist and interchange during drug transport (see discussion below).

It is interesting to note that the hydrophobic segments TM3 and TM5 in the N-terminal half and TM8 and TM10 in the C-terminal half of the unconventional topology of Pgp are not in the membrane. These hydrophobic segments may participate in binding and transporting lipophilic chemotherapeutic drugs. Recently, it has been shown that mutation of the proline residues in the putative TM10 of human *MDR1* Pgp drastically altered the resistance profile of the cells carrying the mutant Pgp (Loo & Clarke, 1993). This observation suggests that the putative TM10 may be involved in recognizing, binding, or transporting the cytotoxic drugs. Insertion of an epitope into the loop linking putative TM3 and TM4 and the loop linking putative TM4 and TM5 disrupted the function of mouse *mdr3* Pgp (Kast et al., 1995), suggesting that these regions are important for the drug transport function.

It is therefore tempting to propose that the unconventional topology of Pgp represents a different functional state of the molecule. The cytoplasmically located hydrophobic segments TM3 and TM10 and their flanking sequences may be involved in binding drugs in cytoplasm. By conformational change, the TM3 and TM10 may help translocate the drug substrate from the cytoplasm to the outside of cells where the extracellularly located hydrophobic segments TM5 and TM8 and their flanking sequences are involved in releasing drugs. It is also possible that this drug transport process involves the conversion of the two different topologies of Pgp supported by the energy obtained from ATP hydrolysis. Recently, the gating of colicin Ia, a voltage-sensitive channel, has been shown to involve a massive change in membrane topology between the opening and closed states (Slatin et al., 1995). At least 31 amino acids of the colicin Ia located in the *cis* side of the membrane appear to be translocated to the *trans* side of the membrane when the channel changes from the closed state to the open state. Further study of the relationship between topology and function of Pgp will elucidate the underlying drug transport mechanism.

## ACKNOWLEDGMENT

The authors thank Dr. Victor Ling for providing Aux B1, $CH^RB30$, and SKOV/VLB cell lines, mAbs C219 and C494, the C219 epitope peptide analog, and hamster *pgp1* cDNA; Dr. Susan Horwitz for pAb 5; Dr. Maurizio Cianfriglia for mAb MM4.17; and Dr. Guillermo Altenberg for BC19/3 cells

and for the assistance in use of the confocal fluorescence microscope. We also thank Drs. Guillermo Altenberg, Karl Karnaky, Jr., and Luis Reuss for their critical comments on the manuscript.

## REFERENCES

Alves, C., von Dippe, P., Amoui, M., & Levy, D. (1993) *J. Biol. Chem. 268*, 20148−20155.
Béjà, O., & Bibi, E. (1995) *J. Biol. Chem. 270*, 12351−12354.
Bender, W. W., Garan, H., Berg, H. C. (1971) *J. Mol. Biol. 58*, 783−797.
Bibi, E., & Béjà, O. (1994) *J. Biol. Chem. 269*, 19910−19915.
Borst, P., Schinkel, A. H., Smit, J. J., Wagenaar, E., van Deemter, L., Smith, A. J., Eijdems, E. W., Baas, F., & Zaman, G. J. (1993) *Pharmacol. Ther. 60*, 289−299.
Bradley, G., Naik, M., & Ling, V. (1989) *Cancer Res. 49*, 2790−2796.
Chifflet, S., Torriglia, A., Chiesa, R., & Tolosa, S. (1988) *Anal. Biochem. 168*, 1−4.
Childs, S., & Ling, V. (1994) in *Important Advances in Oncology* (DeVita, V. T., Hellman, S., & Rosenberg, S. A., Eds.) pp 21−36, Lippincott Co., Philadelphia, PA.
Cianfriglia, M., Willingham, M. C., Tombesi, M., Scagliotti, G. V., Frasca, G., & Cherst, A. (1994) *Int. J. Cancer 56*, 153−160.
Doige, C. A., & Ames, G. F.-L. (1993) *Annu. Rev. Microbiol. 47*, 291−319.
Doige, C. A., Yu, X., & Sharom, F. J. (1992) *Biochim. Biophys. Acta 1109*, 149−160.
Dunlop, J., Jones, P., & Finbow, M. E. (1995) *EMBO J. 14*, 3609−3616.
Endicott, J. A., Sarangi, F., & Ling, V. (1991) *DNA Sequence 2*, 89−101.
Georges, E., Bradley, G., Gariepy, J., & Ling, V. (1990) *Proc. Natl. Acad. Sci. U.S.A. 87*, 152−156.
Georges, E., Zhang, J. T., & Ling, V. (1991) *J. Cell. Physiol. 148*, 479−484.
Georges, E., Tsuruo, T., & Ling, V. (1993) *J. Biol. Chem. 268*, 1792−1998.
Gottesman, M. M., & Pastan, I. (1993) *Annu. Rev. Biochem. 62*, 385−427.
Greenberger, L. M., Lisanti, C. J., Silva, J. T., & Horwitz, S. B. (1991) *J. Biol. Chem. 266*, 20744−20751.
Harlow, E., & Lane, D. (1988) *Antibodies, a laboratory manual*, Cold Spring Harbor Laboratory, Cold Spring Harbor, NY.
Higgins, C. (1992) *Annu. Rev. Cell Biol. 8*, 67→113.
Kartner, N., Evernden-Porelle, D., Bradley, G., & Ling, V. (1985) *Nature 316*, 820−823.
Kast, C., Canfield, V., Levenson, R., & Gros, P. (1995) *Biochemistry 34*, 4402−4411.
Loo, T. W., & Clarke, D. M. (1993) *J. Biol. Chem. 268*, 3143−3149.
Loo, T. W., & Clarke, D. M. (1995) *J. Biol. Chem. 270*, 843−848.
Lopez, C. D., Yost, C. S., Prusinger, S. B., Myers, R. M., & Lingappa, V. R. (1990) *Science 248*, 226−229.
Prange, R., & Streeck, R. E. (1995) *EMBO J. 14*, 247−256.
Riordan, J. R., & Ling, V. (1979) *J. Biol. Chem. 254*, 12701−12705.
Shapiro, A. B., Duthie, M., Childs, S., Okubo, T., & Ling, V. (1996) *Int. J. Cancer* (in press).
Skach, W. R., & Lingappa, V. R. (1993) *J. Biol. Chem. 268*, 23552−23561.
Skach, W. R., Calayag, M. C., & Lingappa, V. R. (1993) *J. Biol. Chem. 268*, 6903−6908.
Slatin, S. L., Qiu, X.-Q., Jakes, K. S., & Finkelstein, A. (1995) *Nature 371*, 158−161.
Steck, T. L., & Kant, J. A. (1974) *Methods Enzymol. 31*, 172−180.
Zhang, J. T., & Ling, V. (1991) *J. Biol. Chem. 266*, 18224−18232.
Zhang, J. T., & Ling, V. (1995) *Biochemistry 34*, 9159−9165.
Zhang, J. T., Duthie, M., & Ling, V. (1993) *J. Biol. Chem. 268*, 15101−15110.
Zhang, J. T., Lee, C.-H., Duthie, M., & Ling, V. (1995) *J. Biol. Chem. 270*, 1742−1746.
Zhang, M., & Zhang, J. T. (1995) *Proc. Am. Assoc. Cancer Res. 36*, 337a.

BI960400S

Molecular Biology of the Cell
Vol. 7, 1709–1721, November 1996

# Sequence Requirements for Membrane Assembly of Polytopic Membrane Proteins: Molecular Dissection of the Membrane Insertion Process and Topogenesis of the Human *MDR3* P-Glycoprotein

**Jian-Ting Zhang**

Department of Physiology and Biophysics, University of Texas Medical Branch, Galveston, Texas 77555-0641

Submitted July 9, 1996; Accepted August 22, 1996
Monitoring Editor: Randy W. Schekman

The biogenesis of membrane proteins with a single transmembrane (TM) segment is well understood. However, understanding the biogenesis and membrane assembly of membrane proteins with multiple TM segments is still incomplete because of the complexity and diversity of polytopic membrane proteins. In an attempt to investigate further the biogenesis of polytopic membrane proteins, I used the human *MDR3* P-glycoprotein (Pgp) as a model polytopic membrane protein and expressed it in a coupled cell-free translation/translocation system. I showed that the topogenesis of the C-terminal half *MDR3* Pgp molecule is different from that of the N-terminal half. This observation is similar to that of the human *MDR1* Pgp. The membrane insertion properties of the TM1 and TM2 in the N-terminal half molecule are different. The proper membrane anchorage of both TM1 and TM2 of the *MDR3* Pgp is affected by their C-terminal amino acid sequences, whereas only the membrane insertion of the TM1 is dependent on the N-terminal amino acid sequences. The efficient membrane insertion of TM3 and TM5 of *MDR3* Pgp, on the other hand, requires the presence of the putative TM4 and TM6, respectively. The TM8 in the C-terminal half does not contain an efficient stop–transfer activity. These observations suggest that the membrane insertion of putative TM segments in the human *MDR3* Pgp does not simply follow the prevailing sequential event of the membrane insertion by signal–anchor and stop–transfer sequences. These results, together with my previous findings, suggest that different isoforms of Pgp can be used in comparison as a model system to understand the molecular mechanism of topogenesis of polytopic membrane proteins.

## INTRODUCTION

The early steps of biogenesis of membrane proteins closely resemble the biogenesis of secretory proteins in the endoplasmic reticulum (ER).[1] A signal sequence in membrane proteins, as in secretory proteins, is responsible for the membrane targeting to the ER, whereas topogenic sequences (including the signal sequence) determine how the protein is folded in the membrane (Blobel, 1980). Additionally, it has been shown that N-linked glycosylation of a glycoprotein is also important for the membrane protein folding in the ER (reviewed, Helenius, 1994). Membrane insertion and translocation of a nascent membrane protein also involves many translocation–machinery proteins on the ER (reviewed, Schekman, 1994).

Most polytopic (spanning the membrane twice or more) transmembrane proteins in eukaryotic cells are thought to acquire their final membrane orientations during or immediately after synthesis on the rough ER, like the monotopic (spanning the membrane once)

[1] Abbreviations used: ER, endoplasmic reticulum; MDR, multidrug resistance; Pgp, P-glycoprotein; PNGase F, peptide N-glycosidase F; RM, rough microsomes; RRL, rabbit reticulocyte lysate; TM, transmembrane.

© 1996 by The American Society for Cell Biology

membrane proteins (Goldman and Blobel, 1981; Braell and Lodish, 1982; Brown and Simoni, 1984; Wessels and Spiess, 1988). Topogenic sequences involved in signal, signal–anchorage, and stop–transfer activities have been identified in eukaryotic polytopic membrane proteins (Friedlander and Blobel, 1985; Audigier *et al.*, 1987; Lipp *et al.*, 1989; Chavez and Hall, 1991; Silve *et al.*, 1991). It is thought that a polytopic topology is generated by the sequential translocation and membrane integration of independent topogenic sequences (Blobel, 1980; Wessels and Spiess, 1988; Hartmann *et al.*, 1989; Lipp *et al.*, 1989; Skach and Lingappa, 1993a). To test this hypothesis, I used the human multidrug resistance (MDR) *MDR3* P-glycoprotein (Pgp) as a model polytopic membrane protein to investigate the topogenesis and membrane assembly process.

The results obtained suggest that the membrane topogenesis of the C-terminal half of the human *MDR3* Pgp is different from the N-terminal half molecule. This observation is similar to studies of the human *MDR1* Pgp (Skach *et al.*, 1993). The proper membrane anchorage of both transmembrane (TM)1 and TM2 of *MDR3* Pgp is affected by their C-terminal amino acid sequences. However, the membrane insertion of the TM1 is also dependent on the N-terminal amino acid sequences. The membrane insertion of TM3 and TM5, on the other hand, requires the presence of the putative TM4 and TM6, respectively. TM8 does not contain an efficient stop–transfer activity. These observations suggest that the membrane insertion of putative TM segments in the human *MDR3* Pgp does not follow the sequential event of the membrane insertion by signal–anchor and stop–transfer sequences.

## MATERIALS AND METHODS

### *Materials*

pGEM-4z plasmid, SP6 and T7 RNA polymerase, RNasin, ribonucleotides, RQ1 DNase, rabbit reticulocyte lysate, and dog pancreatic microsomal membranes were obtained from Promega (Madison, WI). [$^{35}$S]methionine and Amplify were purchased from New England Nuclear (Boston, MA) and Amersham (Arlington Heights, IL), respectively. m$^7$G(5′)ppp(5′)G cap analogue was obtained from Pharmacia LKB Biotechnology (Piscataway, NJ). Peptide *N*-glycosidase F (PNGase F) and restriction enzymes were obtained from Boehringer Mannheim (Indianapolis, IN), New England Biolabs (Beverly, MA), or Promega. All other chemicals were obtained from Sigma (St. Louis, MO) or Fisher Scientific (Pittsburgh, PA).

### *Construction of Fusion DNA between Human MDR3 cDNA and the Reporter Gene*

To study the relative orientation of the various predicted TM segments of human *MDR3* Pgp, I linked a cDNA fragment encoding the first ATP-binding domain of the hamster *pgp1* Pgp to different sites of the human *MDR3* Pgp cDNA and used it as a reporter. This reporter has been used successfully to study the membrane orientation of the Chinese hamster *pgp1* Pgp (Zhang *et al.*, 1993) and human CFTR (Chen and Zhang, 1996). It has a potential glycosylation site that can be used as an indicator of the membrane sidedness of the site to which the reporter is attached and does not have any hydrophobic sequences that will potentially act as a TM segment. The fusion between the two genes does not create any potential glycosylation sites.

The reporter cDNA fragment was released by digestion with *Hin*dIII combined with *Eco*RI, *Rsa*I, *Ssp*I, or *Bgl*II for fusion to TM2, TM3, TM4, and TM6 of human *MDR3*, respectively. Different enzymes were chosen to keep sequences in frame in the fusion constructs. The longest reporter gene was generated by digestion with *Rsa*I, and the shortest one was generated by *Bgl*II digestion. There is a difference of 25 amino acids in length between these two reporters, which has been shown not to affect the membrane translocation process of the reporter (Zhang *et al.*, 1993; Chen and Zhang, 1996). The *Eco*RI end was blunted with Klenow polymerase. Fragments of human *MDR3* Pgp cDNA encoding the N-terminal transmembrane domain were released by digesting the cDNA with *Eco*RI combined with *Hin*cII (amino acids 1–143, including TM1–TM2), *Msl*I (amino acids 1–217, including TM1–TM3), *Nco*I (amino acids 1–301, including TM1–TM4), or *Bgl*II (amino acids 1–411, including TM1–TM6). The *Msl*I, *Nco*I, and *Bam*HI ends were blunted by treatment with Klenow polymerase or T4 DNA polymerase. Different restriction endonucleases were used to create a correct reading frame of the fusion cDNAs. All DNA fragments were separated on 1% agarose gel by electrophoresis and purified as described previously (Zhang and Ling, 1991). The cDNA fragments encoding the various N-terminal transmembrane domains of the human *MDR3* Pgp were ligated to the corresponding reporter cDNA of hamster *pgp1* Pgp and cloned into pGEM-4z vector. The resulting DNA constructs were named 3-N2R, 3-N3R, 3-N4R, and 3-N6R, respectively. The 3-N5R construct was made from the 3-N6R DNA by deleting the TM6 segment and its surrounding sequences with *Bam*HI and *Xho*I. The DNA was treated with Klenow polymerase and then self-ligated to produce the 3-N5R DNA. The cDNA inserts in the 3-N2R, 3-N3R, 3-N4R, 3-N5R, and 3-N6R constructs are in the orientation such that the SP6 RNA polymerase can be used to produce sense RNA transcript. For making 3-N2 RNA transcript, the 3-N2R DNA was linearized at *Xmn*I site in the reporter sequence. Thus, the potential glycosylation site in the reporter sequence of 3-N2R was deleted. The 3-C6 DNA was constructed by cloning the 1.55-kb *Acc*I–*Sac*I fragment (encoding amino acids 618–1110) into the pGEM-4z. The orientation of cDNA insert in the 3-C6 construct required the use of T7 RNA polymerase to produce sense RNA transcript. All constructs were confirmed by DNA sequencing.

### *Construction of Mutant DNAs*

To remove the potential N-linked glycosylation sites in the human *MDR3* Pgp, I performed site-directed mutagenesis by polymerase chain reaction (PCR) as previously described (Zhang *et al.*, 1995). The *Eco*RI–*Hin*cII, *Pst*I–*Pst*I, and the *Hin*cII–*Hin*cII fragments containing mutations of glycosylation sites in the N-terminal end (Asn-8→Gln-8), in the loop linking TM2 and TM3 (Thr-170→Ala-170), and in the loop linking TM8 and TM9 (Thr-810→Ala-810), respectively, were cloned and sequenced. These fragments were then used to replace the wild-type cassette in the corresponding DNA constructs. The final mutant DNAs were confirmed by DNA sequencing. The primers carrying mutations were 5′-GTTCCTTGCTTTGCC (Asn-8→Gln-8), 5′-GAGTTCAGATGCATCATTG-3′ (Thr-170→Ala-170), and 5′-GCACCAGCACTGTTTTTA-3′ (Thr-810→Ala-810). To replace the amino terminus in 3-N2R and 3-N3RTA with the corresponding sequence of the *MDR1* Pgp, I replaced the *Eco*RI–*Bsp* HI cDNA fragment in the 3-N2R and 3-N3RTA DNA by the corresponding *Eco*RI–*Bsp* HI fragment of the human *MDR1* Pgp cDNA to generate 1/3-N2R and 1/3-N3RTA. The 1/3-N3RTA2 was generated by creating a *Kpn*I site at amino acid 53 of the *MDR1* Pgp, and the *Eco*RI–*Kpn*I fragment was used to replace the *Eco*RI–*Kpn*I fragment in the 3-N3RTA.

### *In Vitro Transcription and Translation*

Approximately 6 μg of recombinant DNA linearized with *Hin*dIII was transcribed in the presence of 5 $A_{260}$ units/ml cap analogue $m^7G(5')ppp(5')G$ as described previously (Zhang and Ling, 1991). Removal of DNA templates with RQ1 DNase after transcription and purification of RNA transcripts was performed according to Zhang and Ling (1991). Cell-free translations in rabbit reticulocyte lysate (RRL), proteolysis/membrane protection assay, limited endoglycosidase treatment, isolation of membrane fractions by centrifugation, as well as analysis with SDS-PAGE and fluorography, were performed as previously described (Zhang *et al.*, 1993). At the end of each translation, puromycin was added to a final concentration of 10 μM to terminate the translation reaction.

## RESULTS

### *Membrane Topogenesis of the C-Terminal Half Sequences of Human MDR3 Pgp*

Pgp consists of two homologous halves (Figure 1) and possibly originated from fusion of genes for two related, but independently evolved, proteins (Chen *et al.*, 1990). It has been shown that both the N- and the C-terminal halves contain independent signal sequences to target and insert into microsomal membranes via the SRP-dependent pathway (Zhang and Ling, 1991). To investigate the membrane insertion process and topogenesis of the C-terminal half of the human *MDR3* Pgp, I engineered a cDNA fragment encoding only the C-terminal half Pgp molecule into the pGEM-4z vector (Figure 2E). It has all six C-terminal half TM segments and three potential N-linked glycosylation sites. It was predicted that all of the potential glycosylation sites are in the cytoplasm and are not glycosylated (Figure 2D, model I).

When the 3-C6 in vitro transcript was used to direct translation in RRL in the absence of rough microsomes (RM), a 47-kDa protein was produced (Figure 2A, lane 1). In the presence of RM, an additional protein of 50 kDa was generated (Figure 2A, lane 2). Alkaline treatment and separation of membranes from the soluble fraction suggest that the 50-kDa protein was integrated into the RM membrane, whereas the 47-kDa protein was not (Figure 2A, compare lanes 3 and 5 with lanes 4 and 6, respectively). It is worth noting that, unlike other Pgp molecules (Zhang and Ling, 1991; Zhang *et al.*, 1993), <50% of the *MDR3* translation products was associated with membranes. This is consistent with observation of a previous study on membrane insertion properties of Pgp molecules (Zhang and Ling, 1993). Schinkel *et al.* (1991) also showed that the human *MDR3* Pgp was detected mainly in cytoplasm, whereas the *MDR1* Pgp was found in plasma membranes.

Treatment of membrane-associated proteins with endoglycosidase PNGase F, which removes the N-linked oligosaccharide chains at the innermost residue, reduced the 50-kDa protein to 47 kDa (Figure 2B, compare lanes 1 and 2). This indicates that the 50-kDa protein is a membrane-associated and glycosylated form of the 47-kDa protein. Proteinase K digestion of the membrane-associated proteins generated an 18-kDa protease-resistant fragment (Figure 2C, lane 1). However, no proteinase K-resistant fragment was produced if the RM was permeabilized with Triton X-100 (Figure 2C, lane 3). Further treatment of the protease-resistant 18-kDa fragment with PNGase F reduced its size to ~15 kDa (Figure 2C, lane 2). These results indicate that a fragment containing an oligosaccharide chain is located in the RM lumen. It presumably represents the fragment consisting of TM7-loop-TM8-loop-TM9 with an oligosaccharide chain (see below).

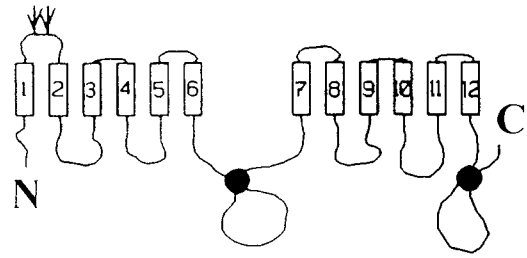


**Figure 1.** Predicted topology of human *MDR3* Pgp. The human *MDR3* Pgp is predicted to have 12 TM segments (indicated by numbered bars), and both N (N) and C termini (C) are located cytoplasmically. The loop linking TM1 and TM2 is predicted to contain two oligosaccharide chains (indicated by branched symbols). The solid circles represent the putative ATP-binding sites.

To determine whether the potential glycosylation site between the TM8 and TM9 of the *MDR3* Pgp was used, I silenced this glycosylation site by mutation in the 3-C6 DNA (Figure 2E, 3-C6TA construct). When the mutant transcript was used to direct translation in the presence of RM, only the unglycosylated protein was produced (Figure 2B, lane 3), whereas the glycosylated 50-kDa peptide was produced from the wild-type transcript (Figure 2B, lane 1). Therefore, the loop linking the TM8 and TM9 was located in the RM lumen and was glycosylated (Figure 2D, model II). This is consistent with the study of a truncated 3-C4 transcript, which encodes a peptide that lacks the potential glycosylation site at the C terminus of TM12 (Figure 2E). Proteinase K digestion of the 3-C4 translation product also generated a PNGase F-sensitive and protease-resistant 18-kDa fragment (Figure 2C, lanes 4–6).

### *In Vitro Translation of the N-Terminal Half Sequences of Human MDR3 Pgp*

A 3-N6R DNA, which encodes a protein with all six N-terminal TM segments and a C-terminal reporter, was constructed to study the membrane integration and assembly of the N-terminal half human *MDR3* Pgp (Figure 3C). If the N-terminal half molecules integrate into RM as predicted (Figure 3B), the reporter

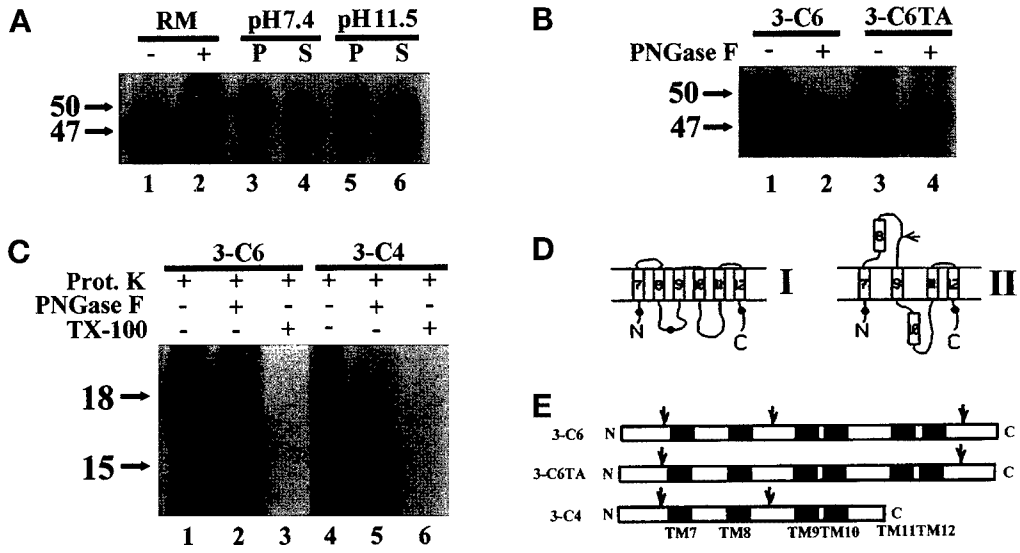


**Figure 2.** In vitro translation and post-translational treatment of wild-type and mutant 3-C6. (A) Translation and post-translational treatment of 3-C6. The translation was performed in the absence (lane 1) or presence (lane 2) of RM. Alkaline treatment with $Na_2CO_3$, pH 11.5, was used to separate the integral membrane proteins (compare lanes 5 and 6). In the control treatment, Tris-buffered saline, pH 7.4, containing 0.25 mM sucrose was used to separate membrane (lane 3) and soluble (lane 4) fractions by centrifugation; p, pellet, S, supernatant. (B) PNGase F treatment of 3-C6 and 3-C6TA. The membrane-associated translation products of 3-C6 and 3-C6TA were digested with (lanes 2 and 4) or without (lanes 1 and 3) PNGase F, and the samples were used for SDS-PAGE analysis. (C) Proteinase K treatment of 3-C6 and 3-C4. The membrane-associated 3-C6 (lanes 1–3) and 3-C4 (lanes 4–6) translation products were digested by proteinase K in the absence (lanes 1 and 4) or presence (lane 3 and 6) of Triton X-100. PNGase F treatment after proteinase K digestion is shown in lanes 2 and 5. (D) Topologies of 3-C6. The numbered bars represent the putative TM segments. The branched symbols are oligosaccharide chains. The unglycosylated potential sites in cytoplasm are indicated by solid circles. (E) Schematic drawing of linear structure of the truncated C-terminal half Pgp. The solid and open bars indicate the TM segments and their linking loops of Pgp, respectively. The branched symbols indicate the potential glycosylation sites.

peptide will have a cytoplasmic location. Thus, the nascent molecules will likely be modified by addition of only two N-linked oligosaccharide chains in the loop linking the TM1 and TM2. As shown in Figure 3A, the 3-N6R in vitro transcript directed translation of a 68-kDa protein in the absence of RM (Figure 3A, lane 1) and an additional protein of 76 kDa in the presence of RM (Figure 3A, lane 2). Limited endoglycosidase digestion of the membrane-associated products shows that the 76-kDa peptide contains two oligosaccharide chains (Figure 3A, lanes 3–5). Proteinase K digestion of the membrane fraction generated a glycosylated peptide of ~18 kDa, similar in size to the fragment from the C-terminal half molecules (Figure 2C), which presumably represents the TM1-loop-TM2 fragments. No other higher molecular weight protease-resistant fragments were observed.

### *The Loop Linking TM1 and TM2 Is Glycosylated*

To investigate whether the two potential glycosylation sites in the loop linking TM1 and TM2 were used, I generated the 3-N2 in vitro transcript and used it to direct translation in RRL. The 3-N2 transcript encodes a peptide that has the first two TM segments, three potential N-linked glycosylation sites (one at the N-terminal end and two in the loop linking the TM1 and TM2), and a shortened C-terminal reporter peptide (Figure 4D). In the absence of RM, a 24-kDa peptide was translated from the 3-N2 transcript (Figure 4A, lane 1). In the presence of RM, an additional membrane-associated product of 32 kDa was produced (Figure 4A, lane 2).

To investigate how many oligosaccharide chains were associated with the nascent 32-kDa peptide, I performed limited endoglycosidase treatment of the 32-kDa peptide. Under this condition, a partially deglycosylated intermediate of 28 kDa was detected (Fig-

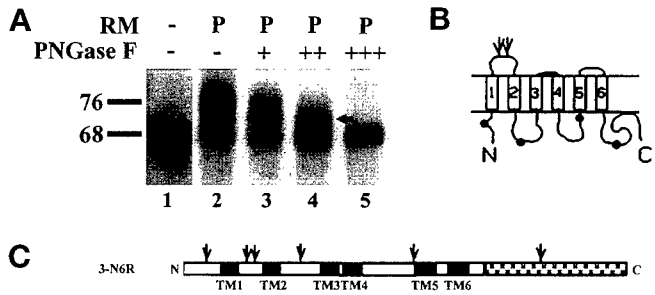


**Figure 3.** In vitro translation and post-translational treatment of 3-N6R. (A) Translation and post-translational treatment of 3-N6R. Membrane-associated translation products (p, pellet) were treated with different amounts of PNGase F (lanes 3–5) or without PNGase F as a control (lane 2). Lane 1 is a translation of 3-N6R in the absence of RM. The arrow in lane 4 indicates the deglycosylated intermediate product. (B) Topologies of 3-N6R. See Figure 2D, legend, for details. (C) Schematic drawing of the 3-N6R linear structure. See Figure 2E, legend, for details. Note that the stippled bars represent reporter peptides.

ure 4B, lane 3), confirming that the 32-kDa peptide has only two oligosaccharide chains. With proteinase K treatment of the membrane-associated 32-kDa peptide, a protease-resistant fragment of ~18 kDa was observed, which was reduced to ~10 kDa by endoglycosidase PNGase F (Figure 4E, lanes 2–3). This result suggests that the protease-resistant 18-kDa peptide contains both oligosaccharide chains and likely represents the fragment of TM1-loop-TM2 with two sugar chains, as predicted (Figure 4C). Analysis of the amino acid sequence suggests that the predicted size of the TM1-loop-TM2 is consistent with the apparent size of the protected fragment, as shown in Figure 4E. Complete removal of these fragments by proteinase K in the presence of Triton X-100 confirms that they were protected by the membrane (Figure 4E, lane 4). Minor fragments with higher molecular weight were also observed after proteinase K digestion (Figure 4E, lane 2). Their origin is not known. However, they probably represent the protected fragments of some peptides that have their C-terminal domain located in the RM lumen (see discussion of Figure 5).

### *The C-Terminal Reporter of the 3-N2R Peptide Is Exposed to the RM Lumen*

According to the "signal–stop transfer" theory (Blobel, 1980), the TM1 of 3-N2 proteins functions as a signal–anchor sequence to initiate membrane targeting and translocation, whereas the TM2 stops the translocation event. To test whether this theory applies to human *MDR3* Pgp, I performed a translation directed by the 3-N2R transcript. The difference between the 3-N2 and the 3-N2R transcripts is that the latter encodes a larger reporter with an additional glycosylation site (compare Figure 4D with Figure 5F). If TM2 stops the membrane translocation event completely, the C-terminal reporter domain will remain in the cytoplasm, and the potential glycosylation site in the reporter domain will not be exposed to the RM lumen. Thus, only two sugar chains will be added to the nascent peptides, as observed with the products of 3-N2 transcript. Surprisingly, two additional peptides of 51 and 55 kDa were generated in the presence of RM (Figure 5A, lane 2), compared with only one translation product of 43 kDa in the absence of RM (Figure 5A, lane 1). These two peptides represent proteins with two and three oligosaccharide chains, as demonstrated by limited endoglycosidase treatment (Figure 5B). The 51-kDa peptide may represent the membrane-integrated peptide with the reporter in the cytoplasm (Figure 5D, model I). The 54-kDa peptide presumably has its C-terminal reporter located in the RM lumen and therefore has an extra oligosaccharide chain attached (Figure 5D, model II, and Table 1).

To determine whether the model II structure exists, I performed a proteolysis/membrane protection as-

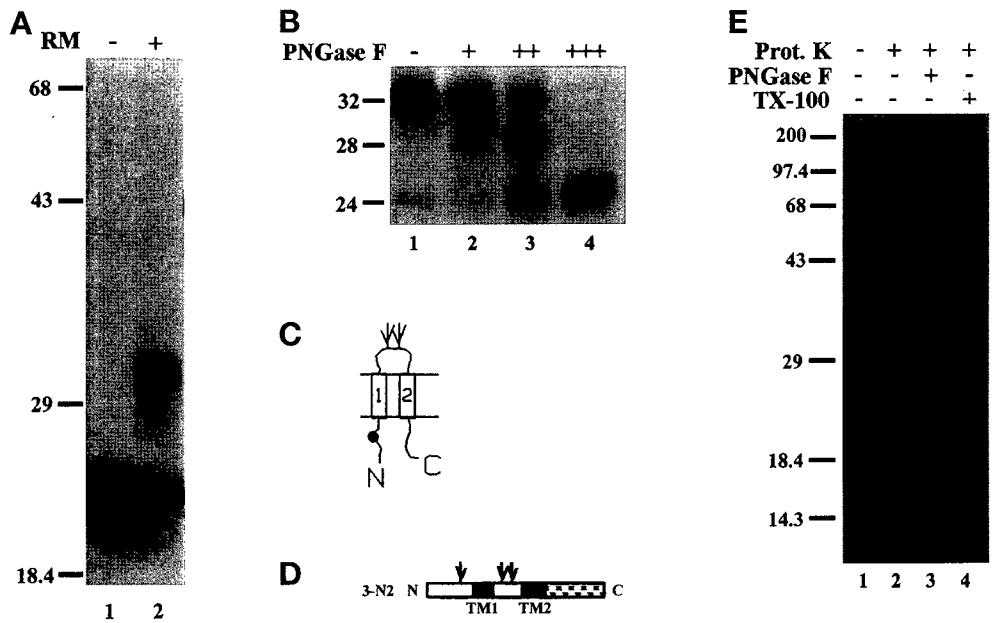


**Figure 4.** In vitro translation and post-translational treatment of 3-N2. (A) Cell-free translation. In vitro 3-N2 transcripts were used to direct translation in the absence (lane 1) or presence (lane 2) of RM. (B) Endoglycosidase PNGase F treatment. The membrane-associated proteins were treated in the absence (lane 1) or presence of increasing amounts (lanes 2–4) of PNGase F. The completely deglycosylated peptides are shown in lane 4. Intermediate products were observed when less PNGase F was used (lanes 2 and 3). (C) Topological model of 3N-2. See Figure 2D, legend, for details. (D) Schematic drawing of the 3-N2 linear structure. See Figure 2E, legend, for details. (E) Proteinase K treatment. The membrane-associated 3-N2 proteins were treated by proteinase K in the absence (lanes 2 and 3) or presence (lane 4) of Triton X-100. PNGase treatment after proteinase K digestion is shown in lane 3. The asterisk in lane 3 indicates the deglycosylated protease-resistant peptide backbone of ~10 kDa.

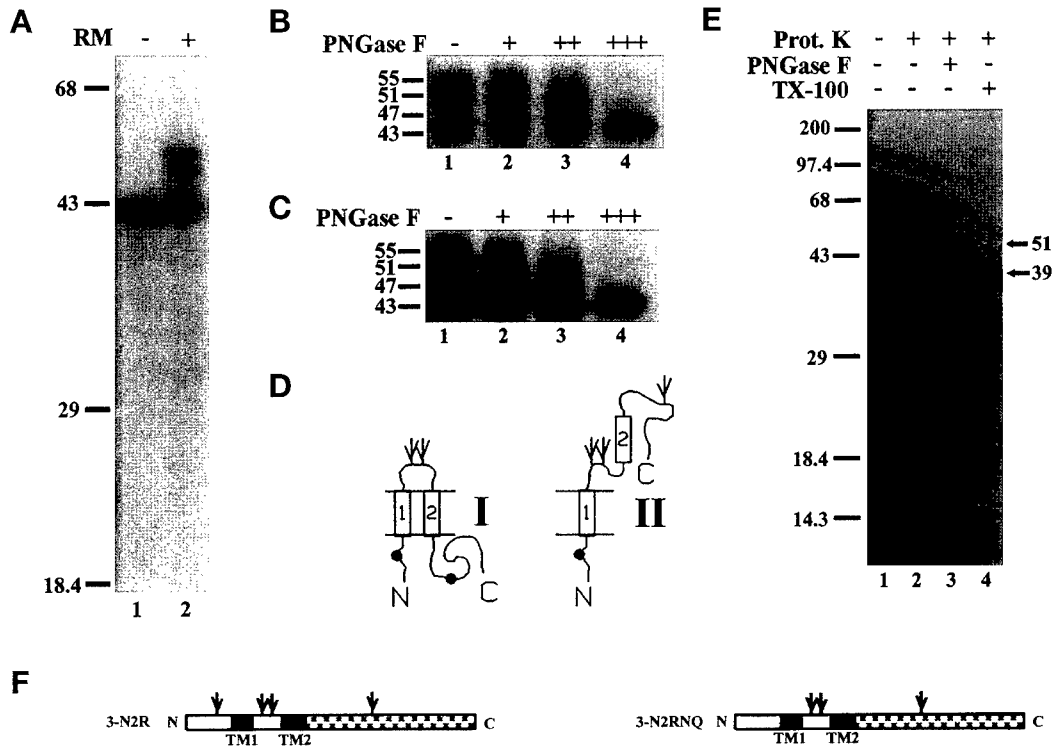


**Figure 5.** In vitro translation and post-translational treatment of 3-N2R. (A) Cell-free translation. In vitro transcripts of 3-N2R were used to direct translation in the absence (lane 1) or presence (lane 2) of RM. (B and C) Endoglycosidase PNGase F treatment. The membrane-associated wild-type 3-N2R (B) or mutant 3-N2RNQ (C) proteins were treated in the absence (lane 1) or presence of increasing amounts (lanes 2–4) of PNGase F. The completely deglycosylated peptides are shown in lane 4 of B and C. Intermediate products were observed when less PNGase F was used (lanes 2 and 3). (D) Topological model of 3-N2R. See Figure 2D, legend, for details. (E) Proteinase K treatment. The membrane-associated wild-type 3-N2R proteins were treated by proteinase K in the absence (lanes 2 and 3) or presence (lane 4) of Triton X-100. PNGase F treatment after proteinase K digestion is shown in lane 3. (F) Schematic drawing of the wild-type 3-N2R and mutant 3-N2RNQ linear structure. See Figure 2E, legend, for details.

say. If the reporter is in the RM lumen and is glycosylated (Figure 5D, model II), a protease-resistant peptide of ~52 kDa (including the three oligosaccharide chains) should be observed with proteinase K treatment of the membrane fraction. As shown in Figure 5E, lane 2, a peptide of ~18 kDa and a doublet of peptides of 49–51 kDa were produced from protease treatment. Further treatment with PNGase F reduced the 18-kDa peptide to ~10 kDa and the 49–51 kDa peptides to 39–41 kDa (Figure 5E, lane 3). The 18-kDa product presumably represents the fragment of TM1-loop-TM2 with two oligosaccharide chains, as shown in the model I structure (Figure 5E). The 49–51 kDa doublet presumably represents the fragment of TM1-loop-TM2-reporter with three oligosaccharide chains, as shown in the model II structure (Figure 5D). The size shift of the protease-resistant fragments induced by PNGase F is consistent with two and three oligosaccharide chains removed (~3 kDa/sugar chain), respectively. It is not known why more than one protected peptide band at 39–41 kDa was observed. This, possibly, is due to protease cleavage at different sites, and the 39-kDa peptide is the major one. All fragments were completely digested if the RM was permeabilized with Triton X-100 (Figure 5E, lane 4), confirming that they were protected from protease digestion by the membrane.

To ascertain that the third glycosylation was not due to the glycosylation of another potential glycosylation site at the N-terminal end, I constructed a mutant cDNA that does not have the potential glycosylation site at the N-terminal end (Figure 5F, 3-N2RNQ). Translation of the 3-N2RNQ transcript produced both the membrane-associated 51- and 55-kDa proteins (Figure 5C, lane 1). Limited endoglycosidase treatment of these peptides showed that the 51-kDa peptides contain two, whereas the 55-kDa peptides contain three, oligosaccharide chains (Figure 5C, lanes 2–4). These results exclude the possibility that the potential glycosylation site at the N-terminal end was used (see Table 1). Together, these results suggest that the efficiency of TM2 to stop the membrane translocation of the C-terminal reporter into the RM lumen is only ~40-70% (derived from the intensity of the two glycosylated products of 55 and 51 kDa, such as the gels shown in Figure 5, A and B). This event resulted

**Table 1.** Summary of glycosylations in the truncated N-terminal half proteins

| | N-Terminal end | First loop[a] | Reporter peptide |
|---|---|---|---|
| 3-N2 | − | + | N/A[b] |
| 3-N2R | − | + | + |
| 3-N3 | + | + | N/A[b] |
| 3-N3R | + | + | − |
| 3-N4R | +[c] | + | − |
| 3-N5R | − | + | + |
| 3-N6R | − | + | − |
| 1/3-N2R | − | + | + |
| 1/3-N3RTA | − | + | − |
| 1/3-N3RTA2 | − | + | − |

[a] The loop linking TM1 and TM2.

[b] The 3-N2 and 3-N3 proteins do not contain reporter peptide with the glycosylation site.

[c] Glycosylation in the N-terminal end of 3-N4R protein is much less than the 3-N3R protein.

in the translocation of the C-terminal reporter into RM lumen (Figure 5D, models I and II). However, it should be noted that the membrane-protected 39-kDa peptides seem to be less than the protected 10-kDa peptides (Figure 5E, lane 3). It is currently not known whether some of the reporter in the model II molecules (Figure 5D) was relocated to the cytoplasm after glycosylation, resulting in the model I structure but with a glycosylated reporter. Thus, only portions of the model II molecules exist after translation is completed. This has been observed with the reporter of another polytopic membrane protein (In-Inc-Inc fusion protein; Lipp *et al.*, 1989).

### *The N-Terminal End of the 3-N3R Peptide Is Translocated into the RM Lumen*

To determine the role of the TM3 in topogenesis of the human *MDR3* Pgp, I made a 3-N3R cDNA construct. This construct encodes the first three TM segments, a reporter peptide, and, in total, five potential glycosylation sites (Figure 6D). Translation of the 3-N3R transcript in RRL generated a 58-kDa peptide (Figure 6A, lane 1). In the presence of RM, additional membrane-associated proteins of 66 and 70 kDa were generated (Figure 6A, lane 2). These proteins are glycosylated versions of the proteins generated in the absence of RM, as shown by complete endoglycosidase treatment (Figure 6A, lane 5). Endoglycosidase digestion under limited conditions showed that the 66-kDa and the 70-kDa proteins contain two and three oligosaccharide chains, respectively (Figure 6A, lanes 3–4).

The 66-kDa peptide presumably represents the nascent 3-N3R protein with both N and C terminus in cytoplasm and the glycosylated loop between TM1 and TM2 in RM lumen (Figure 6C, model II). To determine whether the 70-kDa protein was generated because of glycosylation of the reporter peptide in RM lumen as predicted (Figure 6C, model I), I used a truncated 3-N3 transcript (Figure 6D) that lacks the reporter to direct translation. In the absence of RM, a 22-kDa peptide was generated (Figure 6B, lane 1). In the presence of RM, three additional membrane-associated products of 26, 30, and 34 kDa were produced (Figure 6B, lane 2). Treatment with endoglycosidase PNGase F reduced all three products to 21 kDa (Figure 6B, lane 5). Intermediate products with one and two oligosaccharide chains were observed under limited conditions of PNGase F digestion (Figure 6B, lanes 3 and 4). These results indicate that products with three oligosaccharide chains were also generated from the 3-N3 transcript. Therefore, I conclude that the third glycosylation in the 70-kDa 3-N3R translation products in Figure 6A was not due to the glycosylation of the C-terminal reporter in RM lumen, as shown in the model I structure (Figure 6C and Table 1). This was supported by the observation that no peptide fragments corresponding to the glycosylated reporter

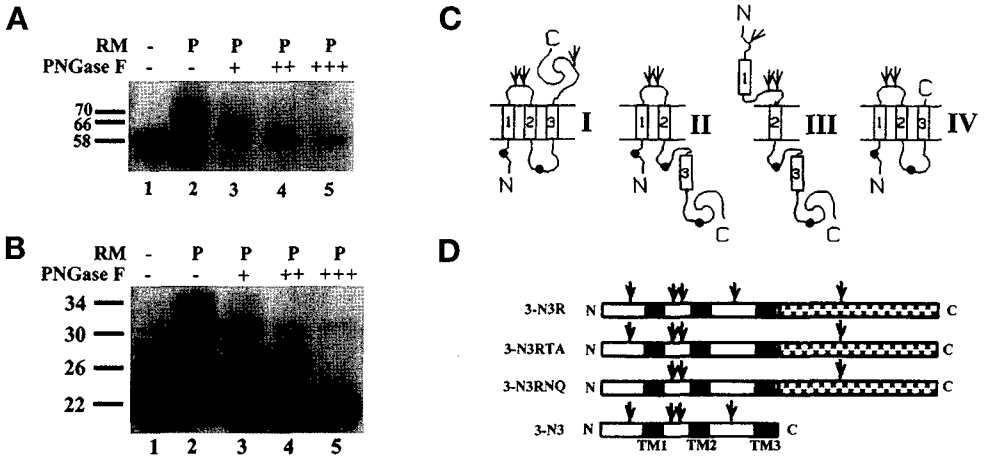


**Figure 6.** In vitro translation and post-translational treatment of 3-N3R and 3-N3. (A and B) Translation and post-translational treatment of 3-N3R and 3-N3. In vitro 3-N3R (A) and 3-N3 (B) transcripts were used to direct translation in RRL in the absence (lane 1) or presence (lane 2) of RM. Limited and complete endoglycosidase (PNGase F) digestions of membrane-associated proteins (p, pellet) are shown in lanes 3–5. (C) Topologies of 3-N3R and 3-N3. See Figure 2D, legend, for detail. (D) Schematic drawing of the wild-type 3-N3R, the mutant 3-N2RTA and 3-N2RNQ, and the truncated 3-N3 linear structure. See Figure 2E, legend, for details.

were protected from the proteinase K digestion of 3-N3R translation products. It is worth noting that the generation of the glycosylated 34 kDa 3-N3 protein is decreased, as compared with the glycosylated 70-kDa 3-N3R protein (compare the ratio of 34- to 30-kDa proteins in Figure 6B, lane 2, with that of 70- to 66-kDa proteins in Figure 6A, lane 2). The reason for this is not known. It is probably due to the truncation of the C-terminal end of the protein in 3-N3, which affects the anchorage of the TM1 and TM2 (see DISCUSSION).

To determine which of the two remaining potential glycosylation sites (one at the N-terminal end and one in the loop linking TM2 and TM3) in 3-N3R protein was used, two glycosylation-mutant 3-N3R DNAs (Figure 6D, 3-N3RTA and 3-N3RNQ) were constructed and used for in vitro transcription and translation. The yield of glycosylated peptides of 66 and 70 kDa was similar between the wild-type 3-N3R and the mutant 3-N3RTA transcript (Figure 7, lanes 1 and 2). However, the 70-kDa glycosylated protein was not produced from the mutant 3-N3RNQ transcript (Figure 7, lane 3). These results indicate that the third glycosylation in 3-N3R was likely at the N-terminal end of the protein and suggest that the N-terminal end of the 70-kDa 3-N3R proteins was translocated into the RM lumen (Figure 6C, model III, and Table 1).

### *Topogenesis of the TM4*

To determine the topogenic role of the TM4, I constructed 3-N4R DNA. This DNA encodes a peptide with four TM segments and a C-terminal reporter peptide (Figure 8C). Protein products of 61 kDa were translated from the 3-N4R in vitro transcripts in the absence of RM (Figure 8A, lane 1). An additional protein of 69 kDa was translated in the presence of RM (Figure 8A, lane 2). Complete endoglycosidase PNGase F treatment reduced the 69-kDa protein to 61 kDa (Figure 8A, lane 5), indicating that it is glycosylated. Under limited conditions of PNGase F treatment, one intermediate product was observed (Figure 8A, lanes 3–4). These results suggest that the 69-kDa protein contain two oligosaccharide chains. A minor diffused band of ~73 kDa (indicated by an arrow in Figure 8A, lane 2) was also generated in the presence of RM and was sensitive to PNGase F digestion. It may be a minor product that has three oligosaccharide chains attached (see discussion below).

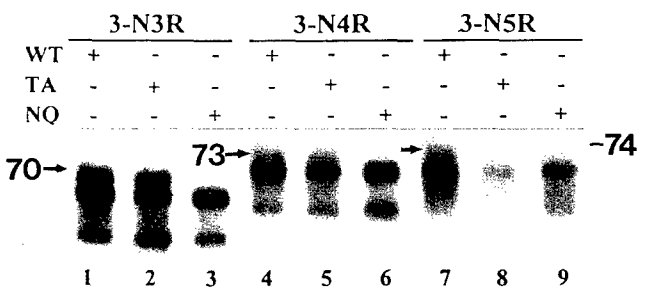


**Figure 7.** In vitro translation of wild-type and mutant 3-N3R, 3-N4R, and 3-N5R. In vitro transcripts of wild-type and mutant 3-N3R, 3-N4R, and 3-N5R were used to direct translation in RRL in the presence of RM; the membrane fractions were isolated and analyzed on SDS-PAGE. The arrows indicate the peptides with three oligosaccharide chains, and their apparent molecular weights are shown. WT, wild type; TA, single mutant; NQ, double mutant.

The 69-kDa protein with two oligosaccharides represents molecules with the model I structure (Figure 8B). To determine the origin of the third glycosylation in the minor 73-kDa protein, I made two mutant 3-N4RTA and 3-N4RNQ (Figure 8C) constructs. As shown in Figure 7, the 73-kDa product was generated from the 3-N4RTA (Figure 7, lane 5) as from the wild-type sequence (Figure 7, lane 4), but not from the 3-N4RNQ (Figure 7, lane 6). These results suggest that the minor 73-kDa 3-N4R protein, like the 70-kDa 3-N3R protein (Figure 8), has a glycosylated N-terminal end in the RM lumen (Figure 8B, model II, and Table 1).

### *Topogenesis of the TM5*

To determine the topogenic role of the TM5, I constructed 3-N5R DNA. It encodes a peptide with five TM segments and a C-terminal reporter peptide (Figure 9D). A 62-kDa protein was translated from the 3-N5R in vitro transcripts in the absence of RM (Figure 9A, lane 1). In the presence of RM, two membrane-associated proteins of 70 and 74 kDa were generated in addition to the 62-kDa protein (Figure 9A, lane 2). Endoglycosidase PNGase F treatment indicates that the 70- and the 74-kDa proteins contain two and three oligosaccharide chains, respectively (Figure 9A, lanes 3–5).

The 70-kDa protein with only two oligosaccharide chains presumably represents the model II molecules (Figure 9B). To determine the origin of the third glycosylation in the 74-kDa protein, I constructed mutant 3-N5R DNAs to make 3-N5RTA and 3-N5RNQ (Figure 9D). Unlike the mutant 3-N3R and mutant 3-N4R, neither of the mutations in 3-N5R eliminated the generation of the 74-kDa protein (Figure 7, compare lanes 7–9). Therefore, the third glycosylation in 3-N5R protein was not due to the glycosylation at the N-terminal end nor in the loop linking TM2 and TM3 of the protein. Likely, the reporter of the 3-N5R protein was translocated into the RM lumen and glycosylated (Figure 9B, model I, and Table 1). Proteinase K treatment of membrane-associated 3-N5R proteins generated 18- and 34-kDa protease-resistant fragments (Figure 9C, lane 1). Both fragments contain oligosaccharide chains, as demonstrated by their susceptibility to PNGase F treatment (Figure 9C, lane 2). The 18-kDa frag-

ment presumably represents the glycosylated loop linking TM1 and TM2, whereas the 34-kDa fragment is likely the glycosylated reporter peptide in the RM lumen, as shown in the model I structure (Figure 8E).

However, the above experiments did not exclude the possibility that the 74-kDa protein represents a molecule with its TM4 exposed to the RM lumen and TM3 and TM5 in membranes (Figure 9B, model III). In this case, the third glycosylation would be in the loop linking TM4 and TM5. If this is true, proteinase K digestion will generate a glycosylated fragment consisting of TM3-loop-TM4-loop-TM5. According to the amino acid sequence, this fragment has a calculated size of 16 kDa plus a ~3-kDa oligosaccharide chain. However, I did not observe a proteinase K-resistant 19-kDa fragment that was reduced to 16 kDa with endoglycosidase PNGase F treatment (Figure 9C, compare lanes 1 and 2). Furthermore, the glycosylation site in the loop linking TM4 and TM5 is too close to the membrane (at the N-terminal end of TM5) to be accessible to the glycosyltransferase in the RM lumen (Figure 9D). Thus, it is unlikely that the model III structure (Figure 9B) exists.

### *Effects of the N-Terminal Sequence on Membrane Anchorage of the TM1 and TM2*

The above results suggest that the proper membrane anchorage of the TM1 and TM2 of human *MDR3* Pgp was affected by their C-terminal sequence. To determine whether the N-terminal sequence is also important in topogenesis, I substituted the N terminus (amino acids 1 to 75) of the 3-N2R and 3-N3RTA proteins with the corresponding N terminus (69 amino acids) of human *MDR1* Pgp (Figure 10B). In addition to a 6-amino-acid difference in length, 39 of the 75 amino acids of these two proteins are identical (or 52% identity), and the N terminus of both proteins has a potential glycosylation site. The fusion DNAs were used to make transcripts, which, in turn, were used to direct translation in RRL in the presence of RM. As shown in Figure 10A, proteins with two and three oligosaccharide chains were generated from both the wild-type (3-N2R) and the hybrid (1/3-N2R) transcript (Figure 10A, compare lanes 1 and 2). It is possible that the reporter in both 3-N2R and 1/3-N2R protein was glycosylated in the RM lumen. It is unlikely that the N-terminal end of the 1/3-N2R protein was located in the RM lumen, causing the glycosylation of the potential site in the N-terminal end. First, it has been shown previously that the N-terminal end of human *MDR1* Pgp was located in the cytoplasm when the first TM segment was fused to a reporter and expressed in frog oocytes and RRL (Skach and Lingappa, 1993b). Second, the N-terminal end of human *MDR1* Pgp was not glycosylated when it was expressed in RRL in a construct consisting of human *MDR1* TM1–TM2 and a reporter (Skach and Lingappa, 1993b; our unpublished observation). Third, the N-terminal end of human *MDR1* Pgp was not glycosylated when engineered into the 3-N3R protein (see 1/3-N3R below). Thus, replacing the first 75 amino acids of human *MDR3* Pgp with that of the human *MDR1* Pgp may not help the membrane anchorage of the TM2 of human *MDR3* Pgp. However, replacing the first 75 amino acids (including the TM1) of human *MDR3* Pgp with that of human *MDR1* Pgp in the 3-N3RTA construct eliminated the generation of the protein with three oligosaccharide chains (Figure 10A, compare lanes 3 and 4). Therefore, the N-terminal end of the hybrid 1/3-N3RTA protein is likely in the cytoplasm and not translocated into the RM lumen. Replacing the N-terminal 59 amino acids (without the TM1) of 3-N3RTA with the corresponding sequence from the *MDR1* sequence (Figure 10B, 1/3-N3RTA2) also inhibits the generation of the 70-kDa protein with three oligosaccharide chains (Figure 10A, lane 5). Therefore, the membrane anchorage of the TM1 of the *MDR3* Pgp depends on the N-terminal amino acid sequence, whereas the TM2 does not.

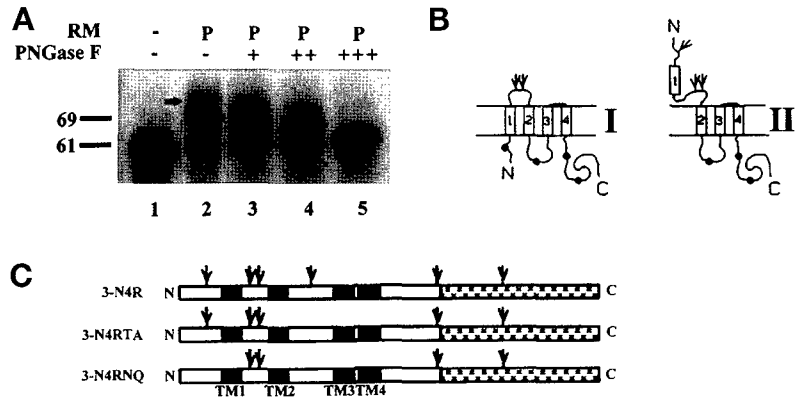


**Figure 8.** In vitro translation and post-translational treatment of 3-N4R. (A) Translation and PNGase F treatment. The translation was performed in the absence (lane 1) or presence (lane 2) of RM. The membrane-associated proteins were treated without (lane 2) or with (lanes 3–5) different amounts of PNGase F. The arrow in lane 2 indicates the minor 73-kDa protein (p, pellet). (B) Topologies of 3-N4R. See Figure 2D, legend, for details. (C) Schematic drawing of the wild-type 3-N4R, the mutant 3-N4RTA, and 3-N4RNQ linear structure. See Figure 2E, legend, for details.

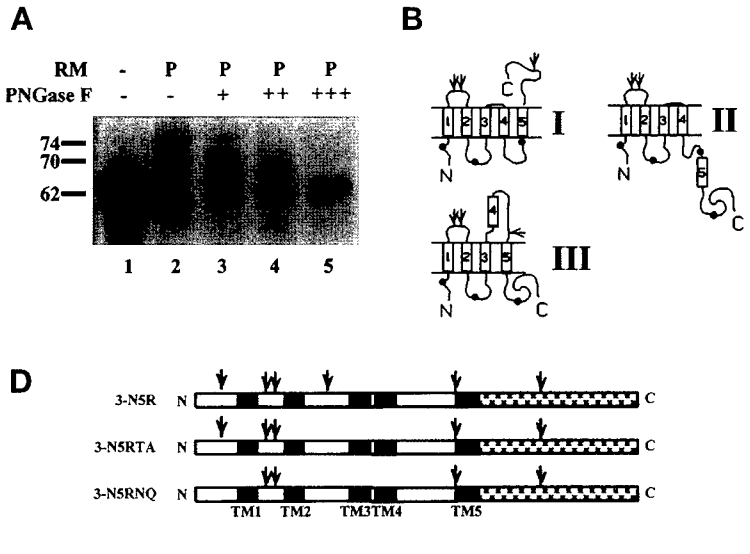


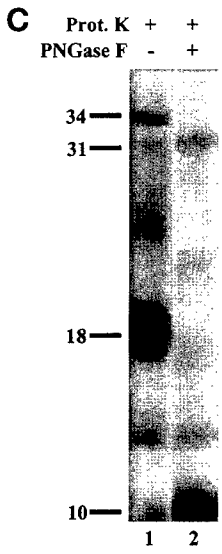


**Figure 9.** In vitro translation and post-translational treatment of 3-N5R. (A) Translation and PNGase F treatment. The translation was performed in the absence (lane 1) or presence (lane 2) of RM. The membrane-associated proteins were treated without (lane 2) or with (lanes 3–5) different amounts of PNGase F (p, pellet). (B) Topologies of 3-N5R. See Figure 2D, legend, for details. (C) Proteinase K digestion. Proteinase K digestion was performed on the membrane pellet fraction (lane 1) or followed by PNGase F digestion (lane 2). (D) Schematic drawing of the wild-type 3-N5R, the mutant 3-N5RTA, and 3-N5RNQ linear structure. See Figure 2E, legend, for details.

## DISCUSSION

In this study, I have investigated the membrane assembly process and the topogenesis of the non-MDR–causing human *MDR3* Pgp by using a cell-free system. The results suggest that all the TM segments in the N-terminal half of *MDR3* Pgp insert into membranes as expected. However, the C-terminal half molecules of *MDR3* Pgp behave differently in RM. The TM8 in the C-terminal half could not stop the membrane translocation event and was translocated into the RM lumen. These observations are similar to the study with the MDR-causing human *MDR1* Pgp (Skach *et al.*, 1993).

It has been suggested that in polytopic membrane proteins the transmembrane segments are topogenic sequences that have different functions as signal and stop–transfer sequence (Friedlander and Blobel, 1985; Audigier *et al.*, 1987; Skach and Lingappa, 1993a). Presumably, the first TM segment functions as a signal–anchor sequence, whereas the second one functions as a stop–transfer sequence (Wessels and Spiess, 1988; Hartmann *et al.*, 1989; Lipp *et al.*, 1989; Skach and Lingappa, 1993a). In this study, the TM2 of the *MDR3* Pgp was found to stop only ~40-70% of the membrane translocation event when its C-terminal end was linked to a reporter (3-N2R protein). On the other hand, the TM2 of the *MDR1* Pgp has been shown to stop the translocation event up to 90% when linked to a reporter (Skach and Lingappa, 1994). Addition of the TM3 and the linking sequences between TM2 and TM3 assists the stop–transfer activity of TM2 in the *MDR3* Pgp sequence (see results on 3-N3R and 3-N4R proteins). However, in the later context, the TM1 and the N-terminal sequence were released into the RM lumen. Only when all of the amino acid residues up to and including the TM5 were added did both TM1 and TM2 completely anchor in the membrane (see results on 3-N5R and 3-N6R). These observations suggest that the membrane assembly of the TM1 and TM2 of human *MDR3* Pgp is affected by their following amino acid sequences. Replacing the N-terminal sequence with human *MDR1* Pgp did not enhance the membrane anchorage of the TM2 in the truncated protein, suggesting that the N-terminal sequence may not be equally important to the C-terminal sequence. Further work is required to test this hypothesis. However, this replacement restored the membrane anchorage of the TM1. Apparently, the membrane insertion and anchorage of the TM1 of Pgp are affected by the N-terminal amino acid sequence. It is interesting to note that the TM8 in the C-terminal half molecule (see discussion below) did not stop the membrane translocation even in the presence of sequence up to and including the TM12. Thus, the function in membrane assembly of TM2 in the N-terminal half and TM8 in the C-terminal half is different.

It is not known why the TM3 and TM5 in *MDR3* Pgp do not initiate efficient membrane insertion event. Similar observation has been made with TM3 in the human *MDR1* Pgp (Skach and Lingappa, 1994) and with TM3 and TM5 in the CFTR protein (Chen and Zhang, 1996). There are several possible explanations for the behavior of the TM3 and TM5 in these proteins. First, the membrane insertion of TM segments in these proteins may occur by pairs. It has been shown that the TM3 in *MDR1* Pgp does not insert in the membrane unless the sequence from TM4 is present (Skach and Lingappa, 1994). It is, therefore, likely that the membrane insertion of TM3 and TM5 of *MDR3* Pgp requires the TM4 and TM6, respectively. This paired membrane insertion may be more thermodynamically favorable than insertion by a single TM segment. Sec-

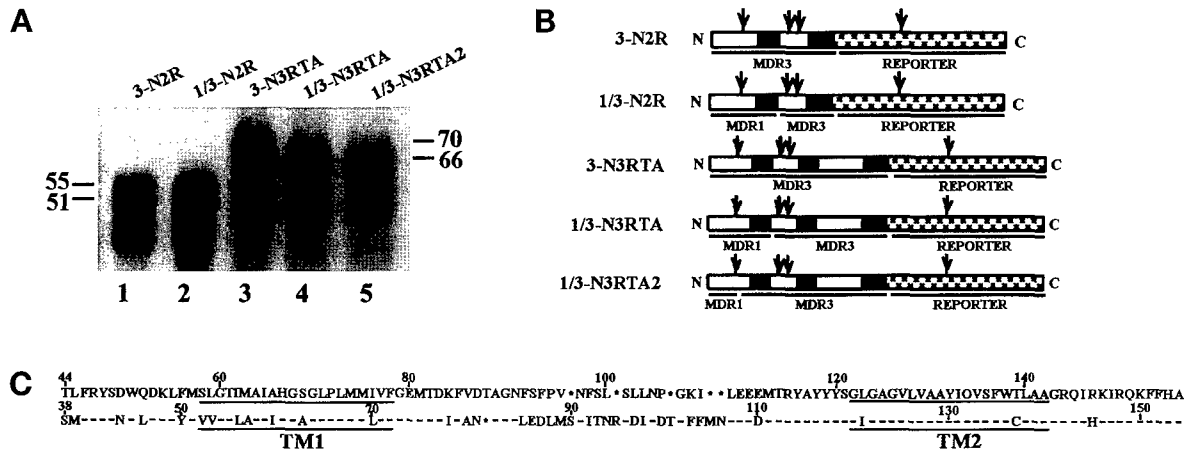


**Figure 10.** In vitro translation of 1/3-N2R and 1/3-N3RTA hybrid constructs. (A) In vitro translation of wild-type and hybrid constructs. The 3-N2R (lane 1), 1/3-N2R (lane 2), 3-N3RTA (lane 3), 1/3-N3RTA (lane 4), and 1/3-N3RTA2 (lane 5) transcripts were used to direct translation in RRL in the presence of RM; the membrane fraction was analyzed by SDS-PAGE. The glycosylated proteins were indicated by molecular weight markers. (B) Schematic linear structure of the MDR1–MDR3 fusion proteins. The first 75 amino acids in 3-N2R and 3-N3RTA were replaced at cDNA level by the corresponding amino acids from human MDR1 Pgp to generate the 1/3-N2R and 1/3-N3RTA constructs. The N-terminal 59 amino acids in 3-N3RTA were replaced by the corresponding amino acid from *MDR1* Pgp to generate the 1/3-N3RTA2 construct. The approximate positions of fusion among MDR1, MDR3, and reporter are underlined. (C) Alignment of the TM1, TM2, and their flanking amino acid sequences between human *MDR1* (bottom) and *MDR3* (top) Pgp. The amino acids are shown in single-letter code, and the TM segments are underlined. The (−) indicates the identical amino acids between the two Pgp isoforms, and an asterisk (*) denotes a gap created to align the two sequences.

ond, the nonmembrane-spanning segments may contain sequences that signal the proper membrane anchorage of the TM segments. Indeed, deletion of C-terminal sequences altered the proper membrane anchorage of TM2, although the TM1 was present to form a pair with TM2 in the 3-N2R protein. It has also been suggested that the loop in the RM lumen of an artificial polytopic membrane protein affects the membrane translocation of TM segment (Lipp *et al.*, 1989). Third, the reporter peptide used in this study may be too bulky and cannot be efficiently translocated into the RM lumen by TM3 and TM5. However, this possibility is unlikely because the similar reporter has been successfully used previously (Zhang *et al.*, 1993), and it can be translocated into RM lumen when present in the 3-N2R protein (Figure 4). Finally, the TM3 and TM5 may not be in the membrane. Their cytoplasmic location cannot be excluded from this study. Further studies are necessary to distinguish among these possibilities and help unveil the membrane insertion and assembly process of mammalian polytopic membrane proteins.

In the C-terminal half of Pgp, the TM7 presumably initiated the membrane targeting and insertion into RM. The TM8 was expected to stop the membrane translocation event to form an extracellular loop. However, in this study the TM8 did not stop the membrane translocation event and was found in the RM lumen. Similar observation has been made with other Pgp isoforms, including the human *MDR1* Pgp (Skach *et al.*, 1993) and mouse *mdr1* Pgp (Zhang and Ling, 1991). It is not known why the TM8 did not stop the membrane translocation event, but possibly there are not enough positive charges after the TM8 that can help to stop the membrane translocation event. It is also possible that the TM8 lacks information that can interact with the TM7 or components in the protein-conducting channel to stop the membrane translocation. Further work is required to resolve this issue. Another possibility is that truncation of the N-terminal half molecule causes the generation of the alternative topology of the C-terminal half molecule. However, I think that this possibility is unlikely. First, it has been shown that the TM8 of human *MDR1* Pgp (Skach *et al.*, 1993), mouse *mdr1* Pgp (Zhang and Ling, 1991), and hamster *pgp1* Pgp (Han and Zhang, unpublished observation) did not stop the membrane translocation event in the presence of their N-terminal half sequences. Second, recent studies with hamster *pgp1* Pgp indicate that addition of positive charges at the C-terminal side of TM8 may help the TM8 to anchor in the membrane, resulting in the predicted topology (Han and Zhang, unpublished observation). Third, the loop linking TM8 and TM9 were detected in Pgp expressed in MDR cells with site-specific antibodies (Zhang *et al.*, 1996).

The results in this study suggest that the membrane insertion event of the internal signal–anchor and stop–transfer sequences in mammalian polytopic membrane proteins such as Pgp and CFTR cannot be easily separated. The process of initiation of membrane translocation and membrane anchorage of a mamma-

lian polytopic membrane protein is likely more complicated than anticipated and may vary with different TM segments in different proteins. This is consistent with the conclusion derived from studies on a yeast polytopic membrane protein, *Saccharomyces cerevisiae* HMG-CoA reductase, (Sengstag *et al.*, 1990). Thus, the membrane insertion of TM segments of polytopic membrane proteins in mammalian systems may not simply follow the sequential event as suggested (Friedlander and Blobel, 1985). Future studies are being directed to investigate the molecular mechanisms underlying the membrane biogenesis of ATP-binding cassette transporters. The specific amino acid residues responsible for the variation in membrane insertion and anchorage of TM segments in mammalian ABC transporters will be identified. Further molecular dissection of the membrane insertion process and comparison between different isoforms of Pgp (e.g., *MDR1* and *MDR3* Pgp) will help understand the molecular mechanism of membrane insertion and assembly of mammalian polytopic membrane proteins.

Finally, different conclusions concerning Pgp topology have been derived from different laboratories. Although alternative topologies of Pgp were observed (Zhang and Ling, 1991; Zhang *et al.*, 1993, 1996; Skach *et al.*, 1993; Bibi and Béjà, 1994; Béjà and Bibi, 1995; this study), Loo and Clarke (1995) and Kast *et al.* (1995, 1996) believe that Pgp has only the predicted topology. The reason for this difference is not known. It may be due to the use of different expression systems or to different approaches such as truncations, addition of reporters or epitopes, and site-directed mutagenesis. It, however, should be noted that the loop linking TM4 and TM5 and the loop linking TM8 and TM9 are very sensitive to mutation. Engineering epitopes or changing amino acids in these loops often caused a nonfunctional protein (Kast *et al.*, 1995, 1996; Loo and Clarke, 1995). Although controversial views on the final Pgp topology still exist, I believe that observation of different Pgp topologies reflects only different faces of the same molecule. It has been shown that two different topological forms of colicin Ia exist in different functional states (Slatin *et al.*, 1995). Interchanges between the different topological structures of Pgp may involve the transport function of Pgp, and this hypothesis makes Pgp a very interesting model also to study the topology–function relationship.

## ACKNOWLEDGMENTS

The author thanks Drs. Guillermo Altenberg, Wanjin Hong, Javior Navarro, Thierry Pourcher, and Mr. Mingang Chen for their comments on this manuscript. This work was supported by National Institutes of Health grant CA-64539 and by a United States Army Research and Development grant.

## REFERENCES

Audigier, Y., Friedlander, M., and Blobel, G. (1987). Multiple topogenic sequences in bovine opsin. Proc. Natl. Acad. Sci. USA *84*, 5783–5787.

Béjà, O., and Bibi, E. (1995). Multidrug resistance protein (Mdr)-alkaline phosphatase hybrids in *Escherichia coli* suggest a major revision in the topology of the C-terminal half of Mdr. J. Biol. Chem. *270*, 12351–12354.

Bibi, E., and Béjà, O. (1994). Membrane topology of multidrug resistance protein expressed in *Escherichia coli*. J. Biol. Chem. *269*, 19910–19915.

Blobel, G. (1980). Intracellular protein topogenesis. Proc. Natl. Acad. Sci. USA *77*, 1496–1500.

Braell, W.A., and Lodish, H.F. (1982). The erythrocyte anion transport protein is cotranslationally inserted into microsomes. Cell *28*, 23–31.

Brown, D., and Simoni, R. (1984). Biogenesis of 3-hydroxy-3-methylglutaryl coenzyme A reductase, an integral glycoprotein of the endoplasmic reticulum. Proc. Natl. Acad. Sci. USA *81*, 1674–1678.

Chavez, R.A., and Hall, Z.W. (1991). The transmembrane topology of the amino terminus of the alpha subunit of the nicotinic acetylcholine receptor. J. Biol. Chem. *266*, 15532–15538.

Chen, C.-J., Clarke, D., Ueda, K., Pastan, I., Gottesman, M.M., and Roninson, I.B. (1990). Genomic organization of the human multidrug resistance (MDR) gene and origin of P-glycoprotein. J. Biol. Chem. *265*, 506–514.

Chen, M.A., and Zhang, J.T. (1996). Membrane insertion, processing, and topology of cystic fibrosis transmembrane conductance regulator (CFTR) in microsomal membranes. Mol. Membr. Biol. *13*, 33–40.

Friedlander, M., and Blobel, G. (1985). Bovine opsin has more than one signal sequence. Nature *318*, 338–343.

Goldman, G., and Blobel, G. (1981). In vitro biogenesis, core glycosylation, and membrane integration of opsin. J. Cell Biol. *90*, 236–242.

Hartmann, E., Rapoport, T.A., and Lodish, H.F. (1989). Predicting the orientation of eukaryotic membrane-spanning proteins. Proc. Natl. Acad. Sci. USA *86*, 5786–5790.

Helenius, A. (1994). How N-linked oligosaccharides affect glycoprotein folding in the endoplasmic reticulum. Mol. Biol. Cell *5*, 253–265.

Kast, C., Canfield, V., Levenson, R., and Gros, P. (1995). Membrane topology of P-glycoprotein as determined by epitope insertion: transmembrane organization of the N-terminal domain of *mdr3*. Biochemistry *34*, 4402–4411.

Kast, C., Canfield, V., Levenson, R., and Gros, P. (1996). Transmembrane organization of mouse P-glycoprotein determined by epitope insertion and immunofluorescence. J. Biol. Chem. *271*, 9240–9248.

Lipp, J., Flint, N., Haeuptle, M.-T., and Dobberstein, B. (1989). Structural requirements for membrane assembly of proteins spanning the membrane several times. J. Cell Biol. *109*, 2013–2022.

Loo, T.W., and Clarke, D.M. (1995). Membrane topology of a cysteine-less mutant of human P-glycoprotein. J. Biol. Chem. *270*, 843–848.

Schekman, R. (1994). Translocation gets a push. Cell *78*, 911–913.

Schinkel, A.H., Roelofs, M.E.M., and Borst, P. (1991). Characterization of the human *MDR3* P-glycoprotein and its recognition by P-glycoprotein-specific monoclonal antibodies. Cancer Res. *51*, 2628–2635.

Sengstag, C., Stirling, C., Schekman, R., and Rine, J. (1990). Genetic and biochemical evaluation of eucaryotic membrane protein topol-

ogy: multiple transmembrane domains of *Saccharomyces cerevisiae* 3-hydroxy-3-methylglutaryl coenzyme A reductase. Mol. Cell. Biol. *10*, 672–680.

Silve, S., Volland, C., Garnier, C., Jund, R., Chevallier, M., and Haguenauer-Tsapis, R. (1991). Membrane insertion of uracil permease, a polytopic yeast plasma membrane protein. Mol. Cell. Biol. *11*, 1114–1124.

Skach, W.R., Calayag, M.C., and Lingappa, V.R. (1993). Evidence for an alternate model of human P-glycoprotein structure and biogenesis. J. Biol. Chem. *268*, 6903–6908.

Skach, W.R., and Lingappa, V.R. (1993a). Intracellular trafficking of pre-(pro) proteins across RER membrane. In: Mechanisms of Intracellular Trafficking and Processing of Proproteins, ed. Y.P. Loh, Boca Raton, FL: CRC Press, 19–77.

Skach, W.R., and Lingappa, V.R. (1993b). Amino-terminal assembly of human P-glycoprotein at the endoplasmic reticulum is directed by cooperative actions of two internal sequences. J. Biol. Chem. *268*, 23552–23561.

Skach, W.R., and Lingappa, V.R. (1994). Transmembrane orientation and topogenesis of the third and fourth membrane-spanning regions of human P-glycoprotein (*MDR1*). Cancer Res. *54*, 3202–3209.

Slatin, S.L., Qiu, X.-Q., Jakes, K.S., and Finkelstein, A. (1995). Identification of a translocated protein segment in a voltage-dependent channel. Nature *371*, 158–161.

Wessels, H., and Spiess, M. (1988). Insertion of a multispanning membrane protein occurs sequentially and requires only one signal sequence. Cell *55*, 61–70.

Zhang, J.T., Duthie, M., and Ling, V. (1993). Membrane topology of the N-terminal half of the hamster P-glycoprotein molecule. J. Biol. Chem. *268*, 15101–15110.

Zhang, J.T., Lee, C.-H., Duthie, M., and Ling, V. (1995). Topological determinants of internal transmembrane segments in P-glycoprotein sequences. J. Biol. Chem. *270*, 1742–1746.

Zhang, J.T., and Ling, V. (1991). Study of membrane orientation and glycosylated extracellular loops of mouse P-glycoprotein by in vitro translation. J. Biol. Chem. *266*, 18224–18232.

Zhang, J.T., and Ling, V. (1993). Membrane orientation of transmembrane segments 11 and 12 of MDR- and non-MDR-associated P-glycoproteins. Biochim. Biophys. Acta *1153*, 191–202.

Zhang, M., Wang, G.C., Shapiro, A., and Zhang, J.T. (1996). Topological folding and proteolysis profile of P-glycoprotein in membranes of multidrug-resistant cells: implications for the drug-transport mechanism. Biochemistry *35*, 9728–9736.